WWW.CMIT-JOURNAL.RU

ISSN 2587-8999
DOI: 10.23947/2587-8999

Computational Mathematics and Information Technology

Vol. 6,

no. 1. 2023

Founder and Publisher: Don State Technical University

The certificate of registration of mass media No. ФС77-66529

Computational Mathematics and Information Technologies

Vol. 6, no. 1

Theoretical and scientific-practical journal

Published since 2017

Quarterly
January-March 2023

ISSN 2587-8999
DOI: 10.23947/2587-8999

Founder and publisher: Don State Technical University, Rostov-on-Don, Russian Federation

The scope of "Computational Mathematics and Information Technologies" is focused on fundamental and applied research according to the following scientific sections:

1. Computational Mathematics
2. Mathematical Modelling
3. Information Technologies

Computational Mathematics and Information Technologies is covered by the following services: Russian Scientific Citation Index, Crossref, Cyberleninka.

The "Computational Mathematics and Information Technologies" Electronic journal was registered by the Federal Service for Supervision in the Field of Communications, Information Technologies and Mass Communications on July 21, 2016 (Certificate of Registration — EL No. FS 77-66529 — electronic edition).

Founder, Publisher and Editorial Correspondence Address:

1, Gagarin Sq., Rostov-on-Don, 344003, Russia. Phone: +7(863) 273–85–14
E-mail: CMIT-EJ@yandex.ru https://cmit-journal.ru/

TABLE OF CONTENTS

Igor Petrov, corresponding member of the Russian Academy of Sciences, is 70 years old

Igor Petrov, Corresponding Member of the Russian Academy of Sciences, Doctor of Physical and Mathematical Sciences, Professor, Honored Professor of the Moscow Institute of Physics and Technology, turned 70 on February 8, 2023.

The scientific interests are, first of all, computer methods for solving dynamic systems of partial differential equations and numerical modeling of processes occurring in deformable media under their dynamic loading.

Scientific activity is inextricably linked with the Moscow Institute of Physics and Technology, where he entered the Aerophysics and Space Research Faculty in 1970. After graduating from the Institute, in 1976, he was assigned to the Department of Computational Mathematics at MIPT as a junior researcher. In 1983, he defended his dissertation there for the degree of Candidate of Physical and Mathematical Sciences. In 1991, at the same department, he defended his thesis for the Doctor of Physical and Mathematical Sciences degree on the topic "Numerical study of problems of dynamics of deformable media by grid-characteristic methods".

The grid-characteristic method for the numerical solution of problems of deformable solid mechanics, geophysics, biomechanics, contact problems was first applied by Igor Petrov. He developed hybrid grid-characteristic schemes for the numerical solution of this class of problem and extended them to the multidimensional case together with corresponding member of the Russian Academy of Sciences Alexander Kholodov. These schemes are based on an approach using the space of indeterminate coefficients. Igor Petrov considered a wide class of problems on high-speed collision of deformable bodies in a wide range of collision velocities using various nonlinear rheological models, including elastic-plastic, viscoelastic, and damaged media.

The professor pays great attention to solving geophysical and seismic exploration problems, problems of seismic resistance of ground structures, asteroid hazard, railway safety, as well as problems of biology and medicine in recent years. The simulation of seismic signals-responses from the main types of fractured carbonate and shale reservoirs when filled with fluid, gas and with collapsed cracks revealed the possibility to determine the change in reservoir saturation.

The scientist has achieved significant success in solving problems related to the development of the Arctic shelf of the Northern Seas of the Russian Federation. Igor Petrov is developing a promising direction related to numerical modeling of the behavior of composite elements of aircraft and spacecraft under the influence of aerodynamic loads, and with the tasks of non-destructive damage control of these elements. The development of new grid-characteristic numerical methods is conducted by the professor. Attention is also paid to solving inverse problems, including with the use of neural networks, when the results of a high-precision numerical solution of the corresponding direct problem are used to form a training sample.

Igor Petrov is one of the leading specialists in the field of computer science, applied mathematics, and computer modeling today. He is the author of 445 scientific and 24 educational works, co-author of 4 monographs and 4 textbooks, 4 scientific collections published by SPRINGER, has 4 patents, 3 copyright certificates of state registration of computer programs.

I. B. Petrov is an active teacher. For more than 40 years he has been engaged in scientific work with students and postgraduates of MIPT. Under his leadership, 26 candidate's (54 with students of students) and 5 doctoral dissertations were defended.

Igor Petrov is a member of the editorial boards of 8 scientific journals; a member of the MIPT Academic Council; Chairman of the MIPT Dissertation Councils; member of the dissertation Councils of the Institute of Applied Mathematics of the Russian Academy of Sciences, Institute of Computational Mathematics of the Russian Academy of Sciences, MSU; Chairman of the State Attestation Commissions of MSU, Baltic Federal University, Innopolis; head of grants of the RFBR, RSF; expert of the Councils of the Russian Academy of Sciences, RFBR. He is an honored worker of the Higher School of the Russian Federation, an honorary worker of science and technology. Moscow, Honored Professor of MIPT, Honorary

Professor of Innopolis University and Xi'an University (China), member of the Mathematical Sciences Section of the Coordinating Council of Fundamental Scientific Research of the Russian Federation, the National Committee for Industrial and Applied Mathematics.

For outstanding achievements, the scientist was repeatedly rewarded with awards and medals, among them medal of the Order "For Merit to the Fatherland" 2d Class and the MIPT badge "Star of Phystech".

We sincerely congratulate Igor Petrov on his anniversary. We wish him health, happiness, as well as further active scientific and educational activities.

Academician of RAS Boris N. Chetverushkin;
Dr.Sci. (Phys.-Math.) Alexander E. Chistyakov;
Dr.Sci. (Phys.-Math.) Vladimir A. Gasilov;
Corresponding Member of RAS Valentin A. Gushchin;
Dr.Sci. (Eng.) Vladimir I. Marchuk;
Dr.Sci. (Phys.-Math.) Alexander P. Ch. Petrov;
Dr.Sci. (Phys.-Math.) Sergey V. Polyakov;
Academician of RAS Aleksandr A. Shananin;
Corresponding member of RAS Alexander I. Sukhinov;
Corresponding member of RAS Vladimir F. Tishkin;
Corresponding member of RAS Vladimir V. Voevodin;
Corresponding member of RAS Mikhail V. Yakobovski.

UDC 519.63 *Review article*
https://doi.org/10.23947/2587-8999-2023-6-1-6-21

Grid-characteristic methods. 55 years of developing and solving complex dynamic problems

I. B. Petrov

Moscow Institute of Physics and Technology (National Research University), 9, Institutsky Lane, Dolgoprudny, Moscow Region, Russian Federation

petrov@mipt.ru

Abstract

The development of a computational method is not a simple matter and boils down to replacing the differential operator with a difference one. To construct it, it is necessary to correctly set a mathematical problem that is adequate to the physical one under consideration. In addition, the algorithm must meet some other requirements. Therefore, to create a numerical algorithm requires not only ingenuity and imagination, but also a deep understanding of the reasons why these requirements are caused.

Systems of partial differential equations of hyperbolic type are used to describe the unsteady behavior of continuous media. To solve these problems, characteristic methods were developed in such a way as to take into account the corresponding properties of hyperbolic equations and to be able to build a so-called characteristic irregular grid adapting to the solution of the problem. Methods of end-to-end counting have been developed that take into account the properties of systems of hyperbolic equations — inverse methods of characteristics or grid-characteristic methods.

In grid-characteristic methods, a regular computational grid is used, not a solvable initial system is approximated on it, but compatibility conditions along characteristic lines with interpolation of the desired functions at the points of intersection of characteristics with a coordinate line on which the data is already known. The obtained characteristic form of the gas dynamics equations makes it possible to understand how to set the boundary conditions correctly.

It is necessary to take into account the physical side of the problem being solved, when developing the method. When developing the method, it is necessary to take into account the physical side of the problem being solved. At the same time, the method must meet certain requirements, the understanding of which is necessary during its development.

Keywords: numerical methods, systems of hyperbolic differential equations, wave processes, numerical solutions on characteristic grids, irregular grid, grid-characteristic methods

For citation. Petrov, I. B. Grid-characteristic methods. 55 years of developing and solving complex dynamic problems / I. B. Petrov // Computational Mathematics and Information Technologies. — 2023. — Vol. 6, № 1. — P. 6–21. https://doi.org/10.23947/2587-8999-2023-6-1-6-21

Обзорная статья

Сеточно-характеристические методы. 55 лет разработки и решения сложных динамических задач

И. Б. Петров

Московский физико-технический институт (национальный исследовательский университет), Российская Федерация, Московская область, г. Долгопрудный, Институтский переулок, 9

petrov@mipt.ru

Аннотация

Введение. Разработка вычислительного метода не является делом простым и сводящимся к замене дифференциального оператора разностным. Для его построения необходимо грамотно поставить математическую задачу, адекватную рассматриваемой физической. Кроме того, алгоритм должен удовлетворять и некоторым другим требованиям. Поэтому для создания численного алгоритма нужна не только изобретательность и фантазия, но и глубокое понимание причин, которыми эти требования вызываются.

Для описания нестационарного поведения сплошных сред используются системы дифференциальных уравнений в частных производных гиперболического типа. Для решения этих проблем характеристические методы разрабатывались таким образом, чтобы учесть соответствующие свойства гипер-болических уравнений и иметь возможность строить т.н. характеристическую, адаптирующую к решению задачи, нерегулярную сетку. Разработаны методы сквозного счета, учитывающие свойства систем уравнений гиперболического типа — обратные методы характеристик или сеточно-характеристические методы.

В сеточно-характеристических методах используется регулярная расчетная сетка, на ней аппроксимируется не решаемая исходная система, а условия совместимости вдоль характеристических линий с интерполяцией искомых функций в точках пересечения характеристик с координатной линией, на которой данные уже известны. Полученная характеристическая форма уравнений газовой динамики позволяет понять, как правильно ставить граничные условия.

Построение численного метода не является простым делом и не сводится к формальной замене производных аппроксимирующими их разностными соотношениями (например, с помощью конечных разностей). При разработке метода необходимо учитывать физическую сторону решаемой задачи. При этом метод должен удовлетворять определенным требованиям, понимание которых необходимо при его разработке.

Ключевые слова: численные методы, системы дифференциальных уравнений гиперболического типа, волновые процессы, численные решения на характеристических сетках, нерегулярная сетка, сеточно-характеристические методы.

Для цитирования. Петров, И. Б. Сеточно-характеристические методы. 55 лет разработки и решения сложных динамических задач / И. Б. Петров // Computational Mathematics and Information Technologies. — 2023. — Т. 6, № 1. — С. 6–21. https://doi.org/10.23947/2587-8999-2023-6-1-6-21

Introduction. Systems of partial differential equations of hyperbolic type are usually used to describe the unsteady behavior of continuous media — gas, solid deformable body, liquid, plasma. These are Euler systems in gas dynamics, Lame systems in elasticity theory, Timoshenko systems in shell theory, Maxwell systems in magnetic hydrodynamics, Bio systems in fluid-saturated porous media, Marchuk systems in climatology and oceanology, etc. The fields of application of such systems are extensive. The corresponding numerical methods used to solve these systems originate in the 40−50s of the XX century. Their development was connected, first of all, with the need to predict the consequences of a nuclear explosion (the consequences of the tragedy of Hiroshima and Nagasaki and the further implementation of the nuclear program in the Soviet Union, which was a necessary counterweight to the nuclear threat from overseas). Soon there were problems about the flow of blunted bodies in dense layers of the atmosphere moving at hypersonic speeds (the problem of delivery). The first difference schemes for solving problems of gas dynamics were created — Lax, Lax-Wendroff, Courant-Izakson-Rice (Godunov), Landau-Meiman-Khalatnikov, Rusanov, etc. A detailed description of the history of the schemes and their overview can be found in well-known works [1−13].

Systems of hyperbolic differential equations have the most general properties:

– the equations describe wave processes, propagation of weak perturbations, or wavefront;

– in the case of linear problems on the propagation of wave fronts, the characteristics can be found independently of the solution of the equation (or system of equations) under consideration, which makes it possible to obtain exact solutions of Dalembert, Kirchhoff, as well as numerical solutions on characteristic grids;

– in the case of nonlinear partial differential equations, the intersection of characteristics is possible when discontinuities occur;

– the characteristic properties of hyperbolic equations make it possible to study the correctness of the formulation of initial boundary value problems, for example, to determine the number of boundary conditions and conditions on the interface surfaces of media.

The main feature of hyperbolic equations or systems of differential equations is the finite velocity of propagation of waves (or perturbations) in the medium, as well as the presence of characteristic surfaces (lines — in the one-dimensional case) denoting the domain of dependence of solutions. On these surfaces, the number of independent variables decreases by one. For the first time, the characteristic properties of such systems were studied in [14], where the concept of Riemann invariants was introduced. Numerical methods that take into account the characteristic properties of hyperbolic systems of equations are

described in detail in [2−12]. The important fact is also noted that using the method of characteristics, the theorems of existence, uniqueness and continuous dependence of the solution of the classical Cauchy problem on the input data were proved [1]. However, this domain is limited in the nonlinear case, because, unlike the linear one, these solutions can have, after some time, unlimited first derivatives — the so-called gradient catastrophe, i.e. discontinuities can arise from smooth initial data. In this case, they speak of a generalized solution of the equations of gas dynamics. A generalized solution, in this case, is understood as a solution that satisfies the laws of conservation of mass, momentum, energy, as well as an inequality that means an increase in entropy in a closed system. From a mathematical point of view, the requirement of increasing entropy guarantees the uniqueness of the generalized solution, as well as its stability with respect to small perturbations. It follows from what has been said that the construction of a numerical method is not a simple matter and is not reduced to the formal replacement of derivatives by approximating their difference relations (for example, using finite differences). When developing the method, it is necessary to take into account the physical side of the problem being solved. At the same time, the method must meet certain requirements, the understanding of which is necessary during its development.

Characteristic methods were developed in such a way as to take into account the corresponding properties of hyperbolic equations and to be able to build a so-called characteristic irregular grid adapting to the solution to solve these problems. These methods are called direct characterization methods [14−17]. Direct characteristic methods allow us to distinguish discontinuities, of which two types can be distinguished: in the first case, the structure of the solution and the location of the discontinuity are a priori known; in the second case, discontinuities occur over time. As for the first type of discontinuities, their isolation in the multidimensional case is a difficult task, which many researchers have been solving, for example [2, 7, 9]. In the second case, the numerical algorithm should detect gaps formed over time, after which it is possible to solve the problem of separation of the gap. The solution of such problems presents the greater difficulties, the more gaps in the field of integration. For this reason, methods of end-to-end counting have been developed that take into account the properties of systems of hyperbolic equations — inverse methods of characteristics or grid-characteristic methods (grid-characteristic method, GCM). These methods use a regular calculation grid. However, it approximates not the initial system to be solved, but the compatibility conditions along the characteristic lines with the interpolation of the desired functions at the points of intersection of the characteristics with the coordinate line on which the data is already known. In the multidimensional case — at the intersection points of the intersection lines of characteristic and coordinate planes with planes with known data. Works are devoted to the development of these methods [2, 7, 9, 18−22].

The first methods of the first order of accuracy were proposed [2, 9, 18, 23−25], then the second [25−27] and the third [27−30]. Subsequently , higher — order schemes were developed [19, 31−35, 52, 54, 57, 58].

In such approaches (through-counting methods), the approximation of derivatives through discontinuities is realized, which, when numerically solving the problem, have a so-called “blur” region, the value of which is determined by the numerical viscosity (dissipation) of the method used. The width of this zone decreases with increasing order of accuracy of the numerical method. In addition, when numerically solving problems with large gradients of the desired functions by methods having an approximation order higher than the first, numerical (non-physical) oscillations may appear. Different approaches are used to eliminate them (or reduce the amplitude). In the first of them, additional dissipative terms were used, in particular, artificial diffusion (or viscosity), both linear and quadratic, which was published in the works of Neumann and Rachtmayer [36]. Studies of the properties and modifications of such artificial solutions can be found in other works [6, 8, 36−38], etc. Generalization of such dissipative additives to the multidimensional case was considered in the review paper [39]. It is noted that artificial dissipative terms change the solution of the original problem [38], so the resulting numerical solution of the problem should be tested. In areas where large gradients are absent, methods of a higher order of accuracy (more than the first) can be used. The latter statement, as well as the monotonicity property of first-order approximation schemes, formed the basis of the idea of hybrid methods.

In the theory of difference schemes, an important concept of monotone (majorant) schemes or schemes with positive Friedrichs approximation is introduced. Such schemes preserve the monotonic character of the numerical solution (in the one-dimensional case) on any time layer, if this is the case in the exact solution of the problem. The use of non-monotonic difference schemes leads to the appearance of non-physical oscillations in the numerical solution (i. e., oscillations having a numerical origin). For a one — dimensional linear transfer equation of S. K. Godunov [42] proved the theorem that there are no explicit linear monotone schemes with an approximation order higher than the first. In [37], this theorem was extended to the case of an arbitrary template (for implicit or multilayer schemes).

To determine the monotony of the difference scheme, explicit linear two-layer schemes are presented in the following form:

$$v_m^{n+1} = \sum_i c_i(\tau, h) \cdot v_{m+i}^n, \; i = 0, \pm 1, ..,$$

where $n\tau = t^n$ (t is the time; τ is the time step; $n = 0,1...$);
$x_m = mh$ (x is the coordinate; h is the coordinate step, $m = 0,\pm 1...$);
$v^n_m = v(t^n, x^m)$ is the desired grid function.

There are several definitions of monotony [22].

1. Schemes monotonous according to Friedrichs [41], for them: $c_i \geq 0$.

2. Schemes monotonous according to Godunov [42], for which the following inequalities are fulfilled: $v_m^{n+1} - v_m^n \geq 0$, by $v_{m+1}^n - v_m^n$ that is, on all time layers, coordinate one-sided differences do not change the sign.

3. Harten monotonic schemes [43]: $\sum_m \left| v_{m+1}^n - v_m^{n+1} \right| \leq \sum_m \left| v_{m+1}^n - v_m^n \right|$, where $TV\left(u_m^n\right) = \sum_m \left| v_{m+1}^n - v_m^{n+1} \right|$ there is a complite variation of the grid function.

4. Difference schemes based on the characteristic properties of the exact solution [19, 45] for which the inequality is fu lfilled: $\left\{v_1^n, v_2^n\right\} \leq v_m^{n+1} = v \leq \max\left\{v_1^n, v_2^n\right\}$;where v_1^n, v_2^n are the values of the grid function on the time layer t^n in the two brush nodes $\left\{t^{n+1}, x_m\right\}$ closest to the one originating from the node (minimum condition). It is shown that in the linear one-dimensional case, all the above definitions of monotonicity are equivalent and are a sufficient condition for the stability of difference schemes.

In the field of smooth numerical solutions, one can use difference schemes of an order of accuracy higher than the first, i. e., in accordance with Godunov's theorem [42], which are not monotonic. However, to eliminate (or reduce the amplitude), non-physical (numerical) oscillations in areas with large gradients of solutions, it is necessary to use monotonic schemes of the first order of approximation. The combination of these two contradictory requirements was realized in the idea of constructing hybrid difference schemes, which was first proposed by Fedorenko in [28]. These schemes are nonlinear, i. e. depending on the solution, and can be locally, at various points in the integration domain, change the order of approximation. Hybrid methods make it possible to implement end-to-end counting using schemes of an increased order of accuracy in areas with smooth solutions — in areas of large gradients of the numerical solution. This makes it possible to combine various positive qualities of difference schemes with different order of approximation in one computational algorithm. To clarify the end-to-end numerical solutions near the discontinuities in [46], it was recommended to use a differential shock wave analyzer, which allows localizing the discontinuity using the results of the end-to-end calculation and further refine the numerical solution. In [28], a method was also described for switching from a first-order scheme to a second-order scheme based on the ratio of the second or third based on the ratio of the second finite difference to the first. Hybrid schemes for linear and quasi-linear transfer equations with a smooth switch from one circuit to another were given in [47]. A hybrid scheme for a system of hyperbolic equations based on a combination of Lax [23] and Lax-Wendroff schemes [25] was proposed by Harten [48].

Van Lear's works [49, 50] also described a special algorithm for monotonizing the Lax-Wendroff scheme. Colgan in [51] proposed hybridization of the Godunov scheme using several templates, as well as a limiter (limiter) minmod. The first hybrid grid-characteristic difference schemes were described in the works of Kholodov and Petrov in [20], and their

development in [11, 21, 35]. In [44], a hybrid method based on flow correction (flux corrected transport) was proposed, in which at the first stage a solution is obtained using a scheme of the first order of accuracy, at the second a term called "antidiffusion" is added, which allows increasing the order to the second.

The use of ideas of hybridity [28], correction of flows [44], limiters [49] led to the creation of TVD schemes (total variation diminishing), [43]. A review of the limiters for this class of hybrid methods is presented in [52].

Further development of TVD methods led to the emergence of new schemes: ENO [53], TVB [54], TVD2, UNO, UNO2 [54], WENO [55], WAF (TORO [56]). The emergence of these methods led to the creation of high-order accuracy schemes (high resolution schemes), see, for example, the monographs of Thoreau, Tolstykh [57, 58].

When numerically solving multidimensional dynamic problems, one often has to deal with moving boundaries, complex integration domains. For this purpose, mobile computational grids [59] and adaptive grids [60] are used. The theory and review of works on the construction of computational grids in complex integration domains are given in monographs [61, 62]. In cases where there is a dynamic expansion of parts of a continuous medium (the expansion of gas, liquid, plasma under dynamic influences, the destruction of deformable solids during explosions, impacts, etc.), the particle methods first proposed by Harlow [63], Belotserkovsky and Davydov in [64] (the method of large particles) are useful. Another approach to solving similar problems turned out to be the smooth particle method (SPH) [66, 67].

Grid-characteristic methods were further developed in [68] (method on unstructured tetrahedral grids), [69] (combined method: SPH and grid-characteristic), [34] (methods of increased order of approximation). The class of compact schemes that allow constructing schemes of an increased order of accuracy on compact templates is developed in [58, 70–72], and in [71, 72] the grid-characteristic method was used for their construction. The discontinuous Galerkin method [73, 74], combining the capabilities of the finite element method [75] and the Godunov method [2], turned out to be a promising method that allows building computational algorithms of an increased order of accuracy. For the numerical solution of dynamic problems of gas dynamics in [76], a very effective "Cabaret" scheme (the jump transfer method) was developed, which made it possible to advance in the numerical solution of problems of plasma dynamics. A review of finite volume methods (FVO) for solving systems of hyperbolic equations, which have gained considerable popularity in the last decade, is given in the monograph [77]. Numerical methods developed for solving problems of continuum mechanics have been successfully used in various applications. Thus, among the works devoted to the calculation of aerohydrodynamic properties of aircraft, the following are noted [2, 7, 8, 9, 17, 29 et al.], monographs devoted to the study of hypersonic flow around blunted bodies [78–80]. In [81], the problems of hypersonic flow around the deformable shell of an aircraft descending in dense layers of the atmosphere were considered, in [82] — the problem of supersonic flow around a system of bodies. The calculation of flows of an incompressible fluid stratified by density in the shallow water approximation is devoted to the work [83].

The problems of solar wind flow around the Earth›s magnetosphere using the equations of magnetohasodynamics were investigated in [84]; acoustic-gravitational waves arising in the atmosphere — in [85]. The motion of an asteroid in the Earth's atmosphere, its interaction with the Earth's surface, and the subsequent propagation of seismic waves in the Earth's crust were considered in [86].

Examples of numerical solutions to problems of deformable solid mechanics can be found in [59, 35, 67–69, 74, etc.]. Wave processes and fracture processes in complex composite structures were studied in [87-89]; problems of interaction of concentrated energy flows and deformable targets — in [90–92]; seismic exploration — in [93–96]; Arctic shelf — in [97–99]; railway safety — in [100]; global intraplanetary seismics — in [101]; electromagnetic wave propagation — in [102–103]; medicine — [104–107]; the intensity of street traffic in megacities (graph problems) — in [108]; large power grids [109]; information flows in computer networks [110].

Of course, these articles cannot be called a review of applied works on numerical modeling of physical processes, because there are too many of them. However, they can give a definite picture of research in the field under consideration.

Systems of partial differential equations of the first order for two independent variables *t*, *x* have the form:

$$F_i\left(t,x,\frac{\partial u}{\partial t},\frac{\partial u}{\partial x}\right)=0,\ i=1\div N. \tag{1}$$

Vector functions, $\overline{u}=\left\{u_1,...,u_N\right\}^T$, having the first continuous derivatives and satisfying the system of equations (1), are the solution of this system.

System (2) resolved with respect to the derivative of one of the independent variables (*t* or *x*),

$$\frac{\partial u_i}{\partial t}=G_i\left(t,x,u,\frac{\partial u}{\partial x}\right) \tag{2}$$

is called the normal form.

If in the system of differential equations (1) all functions F_i ($i = 1 \div N$) are linear with respect to each of the quantities $u,\frac{\partial u}{\partial t},\frac{\partial u}{\partial x}$, then such a system is linear with respect to the specified quantities.

If the system of partial differential equations of the first order (1) is quasi-linear, that it admits writing in the form:

$$\sum_{k=1}^{N}a_{ik}\frac{\partial u_k}{\partial t}+\sum_{k=1}^{N}b_{ik}\frac{\partial u_k}{\partial x}=f_i,i=1\div N, \tag{3}$$

where a_{ik}, b_{ik} depend on the independent variables *t*, *x* and solutions $\overline{u}$.

If they do not depend on *u*, the system is called semi-linear. If f_i does not depend on the solution of the system, then it is linear.

It is possible to represent system (3) in matrix form

$$D\frac{\partial u}{\partial t}+P\frac{\partial u}{\partial x}=f, \tag{4}$$

which, assuming that the matrix *D* is nonsingular, is represented as:

$$\frac{\partial u}{\partial t}+A\frac{\partial u}{\partial x}=f. \tag{5}$$

For the case, respectively, of three or four independent variables, (5) has the form:

$$\frac{\partial u}{\partial t}+A_1\frac{\partial u_1}{\partial x_1}+A_2\frac{\partial u_2}{\partial x_2}=f, \tag{6}$$

$$\frac{\partial u}{\partial t}+A_1\frac{\partial u_1}{\partial x_1}+A_2\frac{\partial u_2}{\partial x_2}+A_3\frac{\partial u_3}{\partial x_3}=f,$$

or

$$\frac{\partial u}{\partial t}+\sum_{k=1}^{K}A_k\frac{\partial u_k}{\partial x_k}=f,\ \text{where } K=2, \text{or } 3. \tag{7}$$

In the future, we will consider a system of quasi-linear partial differential equations written in normal form for the one-dimensional case:

$$\frac{\partial u}{\partial t}+A\frac{\partial u}{\partial x}=f. \tag{8}$$

Assuming that all eigenvalues of matrix *A* are real and there is a basis of eigenvectors $\{\omega_i\}$ multiply (8) by the left eigenvector and

$$\omega_i\frac{\partial u}{\partial t}+\omega_i A\frac{\partial u}{\partial x}=\omega_i f, \tag{9}$$

or

$$\omega_i\left(\frac{\partial u}{\partial t}+\lambda_i\frac{\partial u}{\partial x}\right)=\omega_i f. \tag{10}$$

When disclosing scalar products in (10), there is:

$$\sum_{i=1}^{N} \omega_i \left(\frac{\partial u_i}{\partial t} + \lambda_i \frac{\partial u_i}{\partial x} \right) = \sum \omega_i f_i. \tag{11}$$

The expression in parentheses can be written as:

$$\frac{\partial u_i}{\partial t} + \omega_i \frac{\partial u_i}{\partial x} = \left(\frac{\partial u_i}{\partial t} \right) \Bigg|_{\frac{\partial x}{\partial t} = \lambda_i}, \tag{12}$$

where $\frac{\partial u_i}{\partial t}$ is the derivative of the desired function $u_i(t, x)$ in the direction $\frac{dx}{dt} = \lambda_i$.

Thus, a linear combination of derivatives $\left(\frac{du_i}{dt} \right)$ is obtained in (10).

The direction determined by an ordinary differential equation of the form:

$$\frac{dx}{dt} = \lambda_i \tag{13}$$

is called characteristic.

In the future, the system of partial differential equations (8) will be called hyperbolic (or a system of hyperbolic type equations) in some simply connected domain L, to which the quantities t, x, u belong, if two conditions are met at any point L:

– all corresponding values $\lambda_k(t, x, u)$ of the matrix A (t, x, u) are real;

– in a linear vector space R_N there exists an orthonormal basis $\{\omega_i\}_{i=1}^{i=N}$, composed of the left eigenvectors of the matrix A and satisfying the condition:

$$\det \Omega = \det \left\{ \omega_i^k \right\} = \det \begin{Bmatrix} \omega_1^1 \omega_2^1 & \dots & \omega_N^1 \\ - & - & - \\ \omega_1^N \omega_2^N & \dots & \omega_N^N \end{Bmatrix} = 0. \tag{14}$$

Sometimes a third condition is added to the above conditions — for the smoothness of the eigenvalues of the vectors of the matrix A (for example, in Petrovsky's definition, the condition is given that λ_k and $\left\{ \omega_i^k \right\}$ must have the same smoothness as the elements of the matrix A (t, x, u).

The system of partial differential equations (8) under consideration is called hyperbolic in the narrow sense if at any point L_N the eigenvalues of the matrix are real and different. The definition of hyperbolicity of the system implies the equivalence of two systems of equations:

$$\frac{\partial u}{\partial t} + A \frac{\partial u}{\partial x} = f,$$

$$\omega^k \left(\frac{\partial u}{\partial t} + \lambda_k \frac{\partial u}{\partial x} \right) = \omega_k f_k.$$

The system (11) is called the characteristic form of the original system of equations (8).

The characteristic form of the system under consideration can also be represented as:

$$\omega^k \left(\frac{\partial u}{\partial t} \right) = f_k, \tag{15}$$

where $\left(\frac{\partial u}{\partial t} \right)_k = \frac{\partial u}{\partial t} + \lambda_k \frac{\partial u}{\partial x}$.

If the eigenvalues and eigenvectors of the matrix A are in the system of equations

$$\frac{\partial u}{\partial t} + A \frac{\partial u}{\partial x} = 0 \tag{16}$$

are constant, then the matrix A is represented as a product:

$$A = \Omega^{-1} \Lambda \Omega, \tag{17}$$

where Λ is the diagonal matrix consisting of the eigenvalues $\{\lambda_1,...,\lambda_N\}$ of matrix A, Ω — is the matrix whose rows are the left eigenvectors of A.

When multiplying (16) by Ω and entering Riemann variables $v = \Omega u$ a new system of the form is output:

$$\frac{\partial v}{\partial t} + \Lambda \frac{\partial v}{\partial x} = 0, \tag{18}$$

where $\Lambda = \text{diag}\left\{\lambda_1, ..., \lambda_N\right\}$, or in scalar form $\frac{\partial v_k}{\partial t} + \lambda_k \frac{\partial v_k}{\partial x} = 0, \;\; k = 1 \div N.$

It can be seen that the initial system decays into N separate scalar transport equations, the solutions of which will be traveling waves

$$v_k = v_k\left(x - \lambda_k t\right), \; k = 1 \div N, \tag{19}$$

each of which propagates at a speed of λ_k, while maintaining its initial shape.

The general solution of the system is a superposition of traveling waves propagating at the specified speeds:

$$\vec{v} = \sum_{i=1}^{N} \omega^k v_k\left(x - \lambda_k t\right). \tag{20}$$

Riemann invariants

If the system of eigenvectors is orthonormal, then the values can be interpreted as the amplitudes of traveling waves. The functions are called Riemann invariants, and the system with (18) is a system in invariants.

Next, the concept of Riemann invariants is considered on a simple example — an acoustic system of their two scalar partial differential equations describing the propagation of plane sound waves:

$$\begin{cases} \dfrac{\partial u}{\partial t} + \dfrac{1}{\rho_0} \cdot \dfrac{\partial p}{\partial x} = 0 & (21.1) \\ \dfrac{\partial u}{\partial t} + \rho_0 c_0^2 \cdot \dfrac{\partial u}{\partial x} = 0, & (21.2) \end{cases}$$

where u is the velocity of the continuous medium, p is the pressure in the medium; ρ_0 is the density; c_0 is the speed of sound propagation in the medium.

If both of these equations are integrated over an arbitrary domain with a boundary G in the plane $\{t, x\}$ and go to contour integrals, this will lead to integral equations:

$$\begin{cases} \oint\limits_G \rho_0 u dx - p dt = 0, \\ \oint\limits_G \dfrac{\rho_2}{c_0} u dx - \rho_0 u dt = 0, \end{cases} \tag{22}$$

representing the laws of conservation of momentum and mass. In this case, the equation of state has the form: $p = c^2_0(\rho - \rho_0)$.

When multiplying the first equation (21.1) by $\rho_0 u$, and (21.2) by $p/(\rho_0 c^2_0)$ and adding them, the identity is derived:

$$\frac{\partial}{\partial t}\left(\rho_0 \frac{u^2}{2} + \frac{p^2}{2\,\rho_0 c_0^2}\right) + \frac{\partial}{\partial x}(pu) = 0, \tag{23}$$

from which it follows that for any closed circuit the law of conservation of energy of acoustic waves is valid:

$$\oint\limits_G \left(\rho_0 \frac{u^2}{2} + \frac{p^2}{2\rho_0 c_0^2}\right) dx - pu dt = 0. \tag{24}$$

Now it is necessary to bring the system (21) to the kinetic form. To do this, the second equation is multiplied by $(\rho_0 c_0)^{-1}$, then added to the first and subtracted from it, after which it turns out:

$$\begin{cases} \dfrac{\partial}{\partial t}\left(u + \dfrac{p}{\rho_0 c_0}\right) + c_0 \dfrac{\partial}{\partial x}\left(u + \dfrac{p}{\rho_0 c_0}\right) = 0, \\ \dfrac{\partial}{\partial t}\left(u - \dfrac{p}{\rho_0 c_0}\right) - c_0 \dfrac{\partial}{\partial x}\left(u - \dfrac{p}{\rho_0 c_0}\right) = 0. \end{cases} \tag{25}$$

Notation is introduced $R^+ = u + \dfrac{p}{\rho_0 c_0}, \;\; R^- = u - \dfrac{p}{\rho_0 c_0},$ (26)

the equations in Riemann invariants ($R^{\pm}$— Riemann invariant) are obtained:

$$\frac{\partial R^+}{\partial t}+c_0\frac{\partial R^+}{\partial x}=0,\ \frac{\partial R^-}{\partial t}-c_0\frac{\partial R^-}{\partial x}=0, \tag{27}$$

allowing you to write out their general solution:

$$R^+=f\left(x-c_0t\right),\ R^-=g\left(x+c_0t\right), \tag{28}$$

where f, g are functions defined from the conditions of the problem. Knowing the Riemann invariants, the values of the desired functions are obtained from (26):

$$\begin{cases} u=\dfrac{1}{2}\left[f\left(x-c_0t\right)+g\left(x+c_0t\right)\right], \\ p=\dfrac{\rho_0c_0}{2}\left[f\left(x-c_0t\right)-g\left(x+c_0t\right)\right]. \end{cases}$$

From the relations (27) it can be seen that the values R^+, R^- remain constant along straight lines $x_0 - c_0t$ = const and $x_0 + c_0t$ = const, accordingly, their graphs move over time to the right (left) with speed c_0.

The straight lines

$$\begin{aligned} &\frac{\partial x}{\partial t}=\pm c_0 \quad \text{or} \\ &x\pm c_0t=\text{const} \end{aligned} \tag{29}$$

are called the characteristics of the system (21), which also needs to add initial conditions:

$$u\left(x,0\right)=u_0\left(x\right),\ p\left(x,0\right)=p_0\left(x\right), \tag{30}$$

from where follows:

$$u\left(x\right)=\frac{1}{2}\left[f\left(x\right)+g\left(x\right)\right],$$

$$p_0\left(x\right)=\frac{\rho_0c_0}{2}\left[f\left(x\right)-g\left(x\right)\right],$$

or

$$f\left(x\right)=u_0\left(x\right)+\frac{\rho_0(x)}{\rho_0c_0},$$

$$g\left(x\right)=u_0\left(x\right)+\frac{\rho_0(x)}{\rho_0c_0}.$$

In this case, the solution of the system (21) with the initial data (30) is represented as:

$$\begin{cases} u\left(t,x\right)=\dfrac{1}{2}\left[u_0\left(x-c_0t\right)+u_0\left(x+c_0t\right)\right]+\dfrac{1}{2\,\rho_0c_0}\left[p_0\left(x-c_0t\right)-p_0\left(x+c_0t\right)\right], \\ p\left(t,x\right)=\dfrac{1}{2}\left[p_0\left(x-c_0t\right)+p_0\left(x+c_0t\right)\right]+\dfrac{\rho_0c_0}{2}\left[u_0\left(x-c_0t\right)-u_0\left(x+c_0t\right)\right]. \end{cases} \tag{31}$$

Let, for example, the initial conditions have the following form:

$$\begin{aligned} &u_0\left(x\right)=u_1,\ p_0\left(x\right)=p_1,\ x<X, \\ &u_0\left(x\right)=u_2,\ p_0\left(x\right)=p_2,\ x>X, \end{aligned} \tag{32}$$

where u_i, $p_i (i = 1,2)$ are constants, moreover, one of the equalities is fulfilled $u_1 \neq u_2$ or $p_1 \neq p_2$, or both at the same time.

The solution to this problem, which is not difficult to obtain, is given by the following relations:

$$\begin{aligned} &u=u_1,\ p=p_1,\ x<X-c_0t, \\ &u=u_2,\ p=p_2,\ x>X+c_0t, \\ &u=\frac{u_1+u_2}{2}-\frac{p_1+p_2}{2\,\rho_0c_0}, \\ &p=\frac{p_1+p_2}{2}-\rho_0c_0\frac{u_2+u_1}{2},\ X-ct<x<X+ct. \end{aligned} \tag{33}$$

The resulting solutions $u(t, x)$, $p(t, x)$, as can be seen, have discontinuities along the lines $x + c_0t = X$ and $x - c_0t = X$ and were formed from the initial discontinuity at the point x=X. For this reason, the considered problem is called the gap

decay problem. Generally speaking, these functions cannot formally be considered a solution to this problem due to the fact that they are not continuous. For this reason, they are called the generalized solution of the gap decay problem.
It is worth noting that the concept of invariants was introduced by Riemann in 1876.

Discussion and conclusions. More complex example is given — the solution of a one-dimensional system of gas dynamics equations:

$$\begin{cases} \dfrac{\partial u}{\partial t}+u\dfrac{\partial u}{\partial x}+\dfrac{1}{\rho}\cdot\dfrac{\partial p}{\partial x}=0 & (34.1)\\ \dfrac{\partial p}{\partial t}+u\dfrac{\partial p}{\partial x}+c^2\rho\cdot\dfrac{\partial p}{\partial x}=0, & (34.2)\end{cases}$$

where u, ρ are the velocity and density of the gas; p is the pressure in the gas, c is the sound velocity of the gas, t, x are the time and coordinate.

The second equation (27) is multiplied by $(\rho c)^{-1}$ and added to the first (27). It turns out:

$$\left[\frac{\partial u}{\partial t}+(u+c)\frac{\partial u}{\partial x}\right]+\frac{1}{\rho c}\left[\frac{\partial p}{\partial t}+(u+c)\frac{\partial p}{\partial x}\right]=0 \quad (35)$$

or

$$\left(\frac{\partial u}{\partial t}\right)^{+}+\frac{1}{\rho c}\left(\frac{\partial u}{\partial t}\right)^{+}=0, \quad (36)$$

where $\left(\dfrac{\partial u}{\partial t}\right)^{+}$ is the derivative in the direction $\dfrac{\partial u}{\partial t}=(u+c)$.

Similarly, calculations are carried out with the replacement of c by $(-c)$ after which the quasi-linear system of equations is reduced to the characteristic form:

$$\begin{cases} \left(\dfrac{\partial S}{\partial t}\right)^{0}=0, \\ \left(\dfrac{\partial u}{\partial t}\right)^{+}+\dfrac{1}{\rho c}\left(\dfrac{\partial p}{\partial t}\right)^{+}=0, \\ \left(\dfrac{\partial u}{\partial t}\right)^{-}+\dfrac{1}{\rho c}\left(\dfrac{\partial p}{\partial t}\right)^{-}=0, \end{cases} \quad (37)$$

where $\left(\dfrac{\partial}{\partial t}\right)^{0}=\dfrac{\partial}{\partial t}+u\dfrac{\partial}{\partial x}$,

and the first equation (30) expresses the law of conservation of entropy along the trajectory of the particle, i. e. on the trajectory described by an ordinary equation of the form:

$$\frac{\partial X}{\partial t}=u(t,X),\ \mathrm{X}(0)=X_0,$$

where the function $X(t)$ is the trajectory of the particle.

In the case of an isentropic flow, i. e. when

$$p=A\rho^{\gamma}(\mathrm{A}=\mathrm{const}), \quad (38)$$

and, accordingly,

$$c^2=A\gamma\rho^{\gamma-1},\left(c=\sqrt{\frac{\partial p}{\partial\rho}}\right),$$

the expression $\dfrac{\partial p}{\partial c}$ becomes differential:

$$\frac{1}{\rho c}dp=\frac{2}{\gamma-1}dc.$$

Then, after adding a multiplier $(\rho c)^{-1}$ under the sign of differentiation of the obtained equations, it turns out:

$$\begin{cases} \dfrac{\partial S}{\partial t}+u\dfrac{\partial S}{\partial t}=0 \\ \dfrac{\partial R^{+}}{\partial t}+(u+c)\dfrac{\partial R^{+}}{\partial x}=0 \\ \dfrac{\partial R^{-}}{\partial t}+(u-c)\dfrac{\partial R^{-}}{\partial x}=0, \end{cases} \quad (39)$$

or

$$\begin{cases} \left(\frac{\partial S}{\partial t}\right)^0 = 0 \\ \left(\frac{\partial R^+}{\partial t}\right) = 0 \\ \left(\frac{\partial R^-}{\partial t}\right) = 0, \end{cases} \tag{40}$$

where $R^+ = u + \frac{2c}{\gamma - 1}$, $R^- = u - \frac{2c}{\gamma - 1}$ (41)

Riemann invariants for a one-dimensional quasi-linear system of gas dynamics equations that retain their values on the trajectories of the equations,

$$\frac{\partial X^+}{\partial t} = u \pm c. \tag{42}$$

It is obvious that through the values of the Riemann invariants and entropy, which are found from the solutions of ordinary differential equations, the remaining functions (u, p, ρ), describing the gas flow are calculated. However u, c are the functions of S, $R^{\pm}$, themselves, so it is impossible to find a solution to these equations in quadratures, in any case. However, the exact solution is in the special case for γ = 3 (detonation products).

Since in this case $R^{\pm} = u \pm c$, the trajectories $X^{\pm}$ (t, $X^{\pm}_0$) are families of straight lines with constant slope.

The characteristic form of the gas dynamics equations makes it possible to understand how to set the boundary conditions correctly. For example, the left boundary of the integration domain is considered. Three characteristics with slopes u, ($u + c$), ($u - c$) pass through any point of it. Those of them whose slopes are positive are called entering the integration domain. Thus, it is necessary to set as many conditions on the left border as there are characteristics included in the area; similarly, on the right border.

References

1. Rozhdestvensky, B. L. Systems of quasi-linear equations / B. L. Rozhdestvensky, N. N. Yanenko. — Moscow : Nauka: Fizmatlit, 1978. — 687 p. (In Russ.)

2. Numerical solution of multidimensional problems of gas dynamics / S. K. Godunov, A.V. Zabrodin, M. Ya. Ivanov, A. N. Krainov, T. P. Prokopov. — Moscow : Nauka : Fizmatlit, 1973. — 400 p. (In Russ.)

3. Godunov, S. K. Difference schemes. Introduction to theory / S. K. Godunov, V. S. Ryabenky. — Moscow : Nauka : Fizmatlit, 1973. — 400 p. (In Russ.)

4. Alder, B. Computational methods in hydrodynamics / B. Alder, S. Fernbach / edited by M. Rotenberg. — Moscow : Mir, 1967. — 383 p. (In Russ.)

5. Samarsky, A. A. Theory of difference schemes / A. A. Samarsky. — Moscow : Nauka : Fizmatlit, 1977. — 653 p. (In Russ.)

6. Shokin, Yu. I. Method of differential approximation. Application to gas dynamics / Yu. I. Shokin, N. N. Yanenko. — Novosibirsk : Nauka, 1985. — 364 p. (In Russ.)

7. Belotserkovsky, O. M. Numerical modeling in continuum mechanics / O. M. Belotserkovsky. — Moscow : Fizmatlit, 1994. — 442 p. (In Russ.)

8. Samarsky, A. A. Difference methods for solving problems of gas dynamics / A. A. Samarsky, Yu. P. Popov. — Moscow : USSR, 2009. — 421 p. (In Russ.)

9. Magomedov, K. M. Grid-characteristic numerical schemes / K. M. Magomedov, A. S. Kholodov. — Moscow : Nauka, 1988. — 288 p. (In Russ.)

10. Fedorenko, F. P. Introduction to computational physics / F. P. Fedorenko. — Dolgoprudny : Intellect, 2008. — 503 p. (In Russ.)

11. Kulikovsky, A. G. Mathematical solutions of hyperbolic systems of equations / A. G. Kulikovsky, N. V. Pogorelov, A. Y. Semenov. — Moscow : Fizmatlit, 2012. — 656 p. (In Russ.)

12. Petrov, I. B. Lectures on computational mathematics / I. B. Petrov, A. I. Lobanov. — Moscow : Binom, 2010 — 522 p. (In Russ.)

13. Kukudzhanov, V. N. Computational mechanics of continuous media / V. N. Kukudzhanov. — Moscow : Fizmatlit, 2008. — 320 p. (In Russ.)

14. Riemann, B. Uber die Fortpflanzug ebener Luftwellen von endlicher Schwingungsweite / B. Reinmann // Abhadl. Von der Konglichen Gesellshaft der Wissenshaften zu Gottingen Mathem, Klass. — 1860. — Vol. 8. — P. 43–45.

15. Rusanov, V. V. Method of characteristics for spatial problems. Theoretical Hydrodynamics / V. V. Rusanov / edited by L. I. Sedov // Proceedings of the Ministry of Aviation Industry of the USSR — Moscow : Oborongiz, 1953 — Issue 3, no. 11. — P. 3−62. (In Russ.)

16. Richardson, D. J. The solution of two-dimensional hydrodynamic equation by the method of characteristic. In Method of Computational Physics / D. J. Richardson. — Academic Press : New York, 1964. — P. 295–318.

17. Zhukov, A. I. Application of the method of characteristics to the numerical solution of one-dimensional problems of gas dynamics / A. I. Zhukov // Proceedings of the V. A. Steklov Mathematical Institute. — USSR Academy of Sciences, 1958. — P. 1−152. (In Russ.)

18. Courant, R. On the solution of nonlinear hyperbolic differential equation by finite differences. Comm. Pure and Appl / R. Courant, E. Isakson, M. Rees // Communications on Pure and Applied Mathematics. — 1952. — Vol. 5, no. 5. — P. 243–254.

19. Kholodov, A. S. On the construction of difference schemes of an increased order of accuracy for hyperbolic type equations / A. S. Kholodov // Journal of Computational and Mathematical Physics. — 1980. — Vol. 20, no. 6. — P. 1601−1620. (In Russ.)

20. Petrov, I. B. On regularization of discontinuous numerical solutions of hyperbolic equations / I. B. Petrov, A. S Kholodov // Journal of Computational and Mathematical Physics. — 1984. — Vol. 24, no. 8. — P. 1172−1188. (In Russ.)

21. Favorskaya, A. V. Innovation in Wave Processes Modeling and Decision Making. Grid-characteristic Method and Applications / A. V. Favorskaya, I. B. Petrov. — Springer, 2018. — 251 p.

22. Kholodov, A. S. On the monotonicity criteria of difference schemes for hyperbolic type equations / A. S. Kholodov, Ya. A. Kholodov // Journal of Computational and Mathematical Physics. — 2006. — Vol. 46, no. 9. — P. 1638–1667. (In Russ.)

23. Lax, P. D. Weak solution of nonlinear hyperbolic equation and their numerical computation / P. D. Lax // Communications on Pure and Applied Mathematics. — 1954. — Vol. 7, no. 1. — P. 159–193.

24. Landau, L. D. Numerical methods of integration of partial differential equations by the grid method / L. D. Landau, I. N. Meiman, I. M. Khalatnikov // Proceedings of the III All-Union Mathematical Congress. — Ed. of the USSR Academy of Sciences. — Vol. 3. — P. 92−100. (In Russ.)

25. Lax, P. D. System of conservation law / P. D. Lax, B. Wendroff // Communications on Applied Mathematics. — 1960. — Vol. 13, no. 2. — P. 217–237.

26. MacCormack, R.W. The effect of viscosity in hypervelocity impact cratering / R. W. MacCormack // AIAA Paper. — 1969. — No. 69. — 354 p.

27. Kutler, P. Second and third-order noncentered difference schemes for nonlinear hyperbolic equation / P. Kutler, H. Lomax, R.F. Warming // AIAA Paper. — 1973. — No. 11. — P. 189–196.

28. Fedorenko, R. P. Application of high-precision difference schemes for numerical solution of hyperbolic equations / R. P. Fedorenko // Journal of Computational Mathematics of Mathematical Physics. — 1962. — Vol. 2, no. 6. — P. 1122−1128. (In Russ.)

29. Rusanov, V. V. Difference schemes of the third order of accuracy for end-to-end counting of discontinuous solutions / V. V. Rusanov // Reports of the USSR Academy of Sciences, 180. — 1968. — No. 6. — P. 1303−1305. (In Russ.)

30. Burstein, S. Z. Third order difference method for hyperbolic equations / S. Z. Burstein, A. A. Mirin // Journal of Computational Physics. — 1970. — Vol. 5, no. 3. — P. 547–571.

31. Tolstykh, A. I. On the construction of schemes of a given order with linear combinations of operators / A. I. Tolstykh // Journal of Computational Mathematics and Mathematical Physics. — 2000. — Vol. 2, no. 6. — P. 1122−1128. (In Russ.)

32. Rogov, V. V. Monotonic bicompact schemes for a linear transfer equation / V. V. Rogov, M. N. Mikhailovskaya // Mathematical modeling. — 2011. — Vol. 23, no. 6. — P. 98−110. (In Russ.)

33. Schwartzkopff, T. A. A high-order Approach for Linear Hyperbolic Systems in 2D / T. A. Schwarzkopff, C. D. Munz and Toro // Journal of Scientific Computing. — 2002. — Vol. 17, no. 3. — P. 231–240.

34. Grid-characteristic method using high-order interpolation on tetrahedral hierarchical grids with multiple time steps / I. B. Petrov, A.V. Favorskaya, A.V. Sannikov, I. E. Kvasov // Mathematical modeling. — 2013. — Vol. 25, no. 2. — P. 42−52. (In Russ.)

35. Petrov, I. B. Modeling of 3D seismic problems on high-performance computing systems / I. B. Petrov, N. I. Khokhlov // Journal Computational Mathematics and Mathematical Physics. — 2014 — Vol. 26, no. 1. — P. 83−95. (In Russ.)

36. Van Neumann J. A method for the numerical calculation of hydrodynamic shocks / Van Neumann J., R. D. Richtmayer // Journal of Applied Physics. — 1950. — Vol. 21, no. 3. — P. 232–237.

37. Kuropatenko, V. D. Method of constructing difference schemes for numerical integration of hydrodynamic equa-tions / V. D. Kuropatenko // Izvestiya Higher educational institutions, mathematics. — 1962. — No. 3. — P. 75−83. (In Russ.)

38. Richtmyer, R. D. Difference Methods for Initial-Value Problems / R. D. Richtmyer, K. W. Morton. — Inter-science Publishers : New-York, London, Sidney, 1967. — 418 p.

39. Wilkins, M. L. Use of artificial viscosity on multidimensial fluid dynamic calculation / M. L. Wilkins // Journal of Computational Physics. — 1980. — Vol. 36, no. 3. — P. 281–303.

40. Roache, P. J. Computational Fluid Dynamics / P. J. Roache // Numerical, Albuquerque, NM. — 1976.

41. Fridrichs, K. O. Symmetric hyperbolic linear differential equations / K. O. Fridrichs. — IBID. — 1954. — No. 2. — P. 345–392.

42. Godunov, S. K. Difference method of numerical calculation of discontinuous equations of hydrodynamics / S. K. Godunov // Mathematical Collection. — 1959. —Vol. 47 (89), issue 3. — P. 271−306. (In Russ.)

43. Harten, A. High resolution schemes for hyperbolic conservation laws / A. Harten // Journal of Computational Physics. — 1983. — Vol. 49, no. 3. — P. 357–393.

44. Boris, I. P. Flux-corrected transport. I. Shasta a fluid transport algorithm that works / I. P. Boris, D. L. Book // J. Comput. Phys. — 1973. — Vol. 11, no. 1. — P. 38–69.

45. Van Leer. Forwards the Ultimate Conversation Difference Scheme / Van Leer // Journal of Computational Physics. — Vol. 14, no. 4. — P. 361–370.

46. Yanenko, N. N. Differential shock wave analyzers / N. N. Yanenko, E. V. Vorozhtsov, V. M. Fomin // Reports of the USSR Academy of Sciences. — 1976. — Vol. 227, no. 1. — P. 50-53. (In Russ.)

47. Goldin, V. Ya. Nonlinear difference schemes for hyperbolic equations / V. Ya. Goldin, N. N. Kalitkin, T. V. Shishova // Journal Computational Mathematics and Mathematical Physics. — 1965. — No. 5. — P. 938−944. (In Russ.)

48. Harten, A. Switched numerical shuman filters for shock calculation / A. Harten, G. Zwas // Journal of Engineering Mathematics. — 1972. — Vol. 6, no. 2. — P. 207–216.

49. Van Leer B. Towards the ultimate conservative difference scheme / Van Leer B. // The guest of Monotonicity. Lecture Notes in Physics. — 1973. — Vol. 18, no. 1. — P. 163–168.

50. Van Leer B. Towards the ultimate conservative difference scheme / Van Leer B. // The guest of Monotonicity. Lecture Notes in Physics. — 1973. — Vol. 14, no. 4. — P. 361–370.

51. Kolgan, V. P. Application of the principle of minimum values of derivatives to the construction of finite-difference schemes for calculating discontinuous numerical solutions of gas dynamics / V. P. Kolgan // Scientific Notes of TsAGI. — 1972. — Vol. 3, no. 6. — P. 68−77. (In Russ.)

52. Sweby, P. K. High resolution schemes using flux limiters for hyperbolic conservation laws / P. K. Sweby // Journal on Numerical Analysis. — 1984. — Vol. 21, no. 5. — P. 995–1011.

53. Harten, A. ENO schemes with subcell resolution / A. Harten // Journal of Computational Physics. — 1989. — Vol. 83, no 1. — P. 148–184.

54. Shu, C.-W. TVB uniformly high-order accurate nonoscillatory schemes. / C.-W. Shu // Journal on Numerical Analysis. — SIAM, 1987. — Vol. 24, no. 2. — P. 279–309.

55. Liu, X-D. Weighted essentially non-oscillatory schemes / X-D. Liu, S. Osher, T. Chan // Journal of Computational Physics. — 1994. — Vol. 115, no. 1. — P. 200–212.

56. Toro, E. F. A last Riemann solver with constant covolume applied to the random choice method / E. F. Toro // International Journal for Numerical Methods in Fluids. — 1989. — Vol. 9, no. 9. — P. 1145–1164.

57. Toro, E. F. Rieman Solvers and Numerical methods for Fluid Dynamics / E. F. Toro // A practical Introduction. — Berlin : Springer, 1997.

58. Tolstykh, A. I. Compact and multi-operator approximations of high accuracy for partial differential equations / A. I. Tolstykh. — Moscow : Nauka, 2015. — 349 p. (In Russ.)

59. Petrov, I. B. Numerical investigation of some dynamic problems of deformable solid mechanics by the grid-characteristic method / I. B. Petrov, A. S. Kholodov // Journal of Computational Mathematics and Mathematical Physics. — 1984. — Vol. 24, no. 5. — P. 722−739. (In Russ.)

60. Azarenok, B. N. On the application of adaptive grids for the numerical solution of nonstationary problems of gas dynamics / B. N. Azarenok, S. A. Ivanenko // Journal of Computational Mathematics and Mathematical Physics. — 2000. — Vol. 40. — P. 1386−1407. (In Russ.)

61. Liseikin, V. D. Difference grids. Theory and applications / V. D. Liseikin. — Novosibirsk : Ed. Siberian Branch of the Russian Academy of Sciences, 2014. — 253 p. (In Russ.)

62. Automated technologies of calculation grids. Nonlinear computational mechanics of strength / Yu. V. Vasilevsky, A. A. Danilov, K. N. Lipnikov, V. N. Chugunov. — Moscow : Fizmatlit, 2016. — Vol. IV. — 211 p. (In Russ.)

63. Harlow, F. H. Numerical method of "particles" in cells for problems of hydrodynamics / H. F. Harlow / edited by S. S. Grigoryan and Yu. D. Shmyglevsky. — Moscow : Mir. — 383 p. (In Russ.)

64. Belotserkovsky, O. M. Method of large particles in gas dynamics / O. M. Belotserkovsky, Yu. M. Davydov. — Moscow : Nauka, 1982. — 392 p. (In Russ.)

65. Grigoriev, Yu. N. Numerical modeling by particle-in-cell methods / Yu. N. Grigoriev, V. A. Vshivkov, M. P. Fedorchuk. — Novosibirsk : Ed. Siberian Department, 2004. — 359 p. (In Russ.)

66. Monagan, J. J. An introduction to SPH / J. J. Monagan // Computer Physics Communications — 1988. — Vol. 48. — P. 89–96.

67. Potapov, A. P. Modeling of wave processes by the method of smoothed particles / A. P. Potapov, S. I. Roiz, I. B. Petrov // Mathematical modeling. — 2009. — Vol. 21, no. 7. — P. 20−28. (In Russ.)

68. On the grid-characteristic method on unstructured grids / I. B. Petrov, A.V. Favorskaya, M. V. Muratov [et al.] // Reports of the Academy of Sciences. — 2014. — Vol. 459, no. 4. — P. 406—408. (In Russ.)

69. On a combined method for numerical solution of dynamic spatial elastoplastic problems / I. B. Petrov [et al.] // Reports of the Academy of Sciences. — 2014. — Vol. 460, no. 4. — P. 389–391. (In Russ.)

70. Rogov, B. V. High-precision monotonic compact running counting scheme for multidimensional hyperbolic equations / B. V. Rogov // Journal of Computational Mathematics and Mathematical Physics. — 2013. — Vol. 53, no. 4. — P. 94−104. (In Russ.)

71. Kholodov, A. S. Numerical methods for solving equations and systems of hyperbolic equations / A. S. Kholodov. — Moscow : Janus-K, 2008. — Vol. 8−1, part 2. — P. 141−174. (In Russ.)

72. Golubev, V. I. Compact grid-characteristic schemes of an increased order of accuracy for a three-dimensional linear transfer equation / V. I. Golubev, I. B. Petrov, N. I. Kholodov // Mathematical modeling. — 2016. — Vol. 28, no. 2. — P. 123−132. (In Russ.)

73. Local discontinuos Galerkin method for contaminant transport / V. Aizinger, C. Dawson, D. Cockburn and P. Castillo // Advances in Water Resources. — 2000. — Vol. 24. — P. 73–78.

74. Miryakha, V. A. Numerical modeling of dynamic processes in solid deformable bodies by the discontinuous Galerkin method / V. A. Miryakha, A. V. Sannikov, I. B. Petrov // Mathematical modeling. — 2015. — Vol. 27, no. 3. — P. 96−108. (In Russ.)

75. Bate, K.-Yu. Finite element methods / K.-Yu. Bate. — Moscow : Fizmatlit, 2010. — 1022 p. (In Russ.)

76. Golovizin, V. N. Some properties of the CABARET scheme /V. N. Golovizin, A. A. Samarskii // Mathematical Models. — 1998. — No. 10. — P. 101–116. (In Russ.)

77. Randall J., Leveque. Finite Volume Methods for Hyperbolic Problems / Randall J., Leveque // Cambridge texts in applied mathematics. — Cambridge University press., 2002. — 558 p.

78. Lunev, V. V. The flow of real gases with high velocities / V. V. Lunev. — M.: Fizmatlit, 2007. (In Russ.)

79. Lyubimov, A. N. Gas flow near blunt bodies / A. N. Lyubimov, V. V. Rusanov / in 2 hours. — Moscow : Nauka, 1970. (In Russ.)

80. Utyzhnikov, S. V. Hypersonic aerodynamics and heat Transfer / S. V. Utyzhnikov, Tirskiy // Begell. — New York : Connecticut. — 536 p.

81. On the numerical solution of related problems of supersonic flow around deformable shells / P. N. Korotin, I. B. Petrov, V. B. Pirogov, A. S. Kholodov // Journal of Computational Mathematics and Mathematical Physics. — 1987. — Vol. 27, no. 8. — P. 1233−1243. (In Russ.)

82. Maksimov, F. A. Supersonic flow around a system of bodies / F. A. Maksimov // Computer research and modeling. — 2013. — Vol. 5, no. 6. — P. 969−980. (In Russ.)

83. Vedernikov, A. E. Numerical investigation of two and three-layer liquids in the shallow water approximation / A. E. Vedernikov, A. S. Kholodov // Mathematical modeling. — 1990. — Vol. 2, no. 6. — P. 9−18. (In Russ.)

84. Kholodov, A. S. Computational models of the Earth's upper atmosphere and some of their applications / A. S. Kholodov, M. O. Vasiliev, E. A. Molokov / Izvestiya RAS // series "Physics of the atmosphere and ocean". — 2010. — Vol. 46, no. 6. — P. 1−21. (In Russ.)

85. Krysanov, B. Y. Modeling by MHD equations of ionospheric disturbances generated in the near-Earth layer of the atmosphere / B. Y. Krysanov, V. E. Kunitsyn, A. S. Kholodov // Journal of Computational Mathematics and Mathematical Physics. — 2011. — Vol. 51, no. 2. — P. 282−302. (In Russ.)

86. Astanin, A. V. Modeling the Influence Bow Shock Wave on the Earth`s Surface / A. V. Astanin, A. D. Dashkevich, M. N. Petrov [et al.] // Mathematical Models and Computer Simulation. — 2017. — Vol. 9, no. 2. — P. 133–141. (In Russ.)

87. Petrov, I. B. Numerical investigation of wave processes and fracture processes in multilayer barriers / I. B. Petrov, F. B. Chelnokov // Journal of Computational Mathematics and Mathematical Physics. — 2003. — No. 43 (10). — P. 1562−1579. (In Russ.)

88. Numerical modeling of dynamic processes at a low-speed impact on a composite stringer panel /. I. B. Petrov [et al.] // Mathematical modeling. — 2014. — No. 26(9). — P. 96−110. (In Russ.)

89. Modeling of experiments on the study of the strength characteristics of ice by the Galerkin discontinuous method / V. A. Miryakha, A.V. Sannikov, V. A. Biryukov, I. B. Petrov // Mathematical modeling. — 2018. — No. 2. (In Russ.)

90. Ivanov, V. D. Modeling of deformations in targets under the action of laser radiation / V. D. Ivanov, I. B. Petrov // Proceedings of the IOF of the USSR Academy of Sciences. — 1992. — Vol. 36. — P. 247−265. (In Russ.)

91. Korotin, P. N. Numerical modeling of the behavior of elastic and elastoplastic bodies under the influence of powerful energy flows / P. N. Korotin, I. B. Petrov, A. S. Kholodov // Mathematical modeling. — 1989.— No. 1 (7). — P. 1−12. (In Russ.)

92. Ostrik, A.V. Calculation of diffraction of an acoustic pulse of short duration on a hole of complex shape in a filler surrounded by an elastic shell / A.V. Ostrik, I. B. Petrov, V. P. Petrovsky. — DAN USSR, 1990. — No. 2 (8). — P. 51−59. (In Russ.)

93. Levyant, V. B. Investigation of the characteristics of longitudinal and exchange waves of the backscattering response from the fracturing zones of the collector / V. B. Levyant, I. B. Petrov, S. A. Pankratov // Technologies of seismic exploration. — 2009. — No. 6 (2). — P. 3−11. (In Russ.)

94. Muratov, M. V. Calculation of wave responses from systems of subvertical macrofractures using the grid-characteristic method / M. V. Muratov, I. B. Petrov // Mathematical modeling. — 2013. — No. 25 (3). — P. 89−104. (In Russ.)

95. Favorskaya, A.V. Grid-characteristic method on systems of nested hierarchical grids and its application for the study of seismic waves / A.V. Favorskaya, N. I. Khokhlov, I. B. Petrov // Journal of Computational Mathematics and Mathematical Physics. — 2017. — Vol. 57, no. 11. — P. 1804−1811. (In Russ.)

96. Golubev, V. I. Modeling of dynamic processes in three-dimensional layered fractured media using a grid-characteristic numerical method / V. I. Golubev [et al.] // Applied Mechanics and technical Physics. — 2017. — Vol. 58, no. 3. — P. 190−197. (In Russ.)

97. Simulation of seismic processes in geological exploration of Arctic shelf / P. V. Stognii, I. B. Petrov, N. I. Kholodov, D. I. Petrov // Russian Journal numerical analysis and mathematical modelling. — 2017. — Vol. 32, no. 6. — P. 381–392. (In Russ.)

98. Numerical modeling of earthquake on engeneering structure on Arctic shelf / V. I. Golubev, A. V. Vasyukov, K. A. Beclemisheva, I. B. Petrov // Computational Mathematics and Information Technologies. — 2017. — No. 2. — P. 1–6. (In Russ.)

99. Numerical solution of seismic exploration problems in the Arctic region by applying the grid-characteristic method / D. I. Petrov, I. B. Petrov, A. V. Favorskaya and N. I. Kholodov // Computational Mathematics and Mathematical Physics. — 2016. — Vol. 56, no. 6. — P. 1128–1141. (In Russ.)

100. Monitoring the condition of rolling stock using high-performance methods / I. B. Petrov [et al.] // Mathematical modeling. — 2014. — Vol. 26, no. 7. — P. 19−32. (In Russ.)

101. Golubev, V. I. Modeling of wave processes of the planet using a hybrid grid-characteristic method / V. I. Golubev, I. B. Petrov, N. I. Khokhlov // Mathematical modeling. — 2015. — Vol. 27, no. 2. — P. 139−148. (In Russ.)

102. Allen Taflove, Susan C. Hagness. Computation electrodynamics. The finite-difference time-domation method / Allen Taflove, Susan C. Hagness // Artech House : Boston/London, 2005. — P. 1006.

103. Numerical solution of the system of Maxwell's equations for modeling the propagation of electromagnetic waves // Proceedings of MIPT. — 2016. — Vol. 8. — P. 121–130.

104. Agapov, P. I. Numerical modeling of the consequences of mechanical impact on the human brain in traumatic brain injury / P. I. Agapov, O. M. Belotserkovsky, I. B. Petrov // Journal of Computational Mathematics and Mathematical Physics. — 2006. — Vol. 46, no. 9. — P. 1711−1720. (In Russ.)

105. Calculation of dynamic processes in the eye during laser cataract extraction / N. N. Balanovsky, A. V. Bubnov, A. S. Obukhov, I. B. Petrov // Mathematical modeling. — 2003. — Vol. 15 (11).— P. 37−44. (In Russ.)

106. Kholodov, A. S. Mathematical modeling of irrigation and aspiration technique of phacoemulsification / A. S. Kholodov, A.V. Bubnov, T. E. Marchenkova // Ophthalmosurgery. — 1991. — No. 1. — P. 11−15.

107. Kholodov, A. S. Numerical analysis of the impact of acoustic disturbances on lung function and hemodynamics of the small circulatory circle / A. S. Kholodov, S. S. Simakov // Medicine in the mirror of informatics / edited by O. M. Belotserkovsky, A. S. Kholodov. — Moscow : Nauka, 2008 — P. 45−75. (In Russ.)

108. Kholodov, A. S. Numerical study of transport flows based on hydrodynamic models / A. S. Kholodov [et al.] // Computer research and modeling. — 2011. — Vol. 3, no. 4. — P. 389−412.

109. Modeling of global energy networks / A. K. Bordonos, Ya. A. Kholodov, A. S. Kholodov, I. I. Morozov // Mathematical modeling. — 2009. — Vol. 21, no. 6. — P. 3−16. (In Russ.)

110. Severov, D. S. Comparison of packet and streaming models of IP networks / D. S. Severov, A. S. Kholodov, Ya. A. Kholodov // Mathematical modeling. — 2011. — Vol. 23, no. 12. — P. 105−116. (In Russ.)

Submitted for publication 24.01.2023.
Submitted after peer review 27.02.2023.
Accepted for publication 28.02.2023.

About the Author:

Petrov, **Igor B.,** Corresponding Member of RAS, Dr. Sci. (Phys.-Math.), Professor Moscow Institute of Physics and Technology (National Research University) (9, Institutsky Lane, Dolgoprudny, Moscow Region, 141701, Russian Federation), Math-Net.ru, MathsciNet, eLibrary.ru, ORCID, ResearchGate, petrov@mipt.ru

The Author has read and approved the final manuscript.

UDC 519.6 *Original article*

https://doi.org/10.23947/2587-8999-2023-6-1-22-26

About the analytical solution for the advertising model of two competing firms

A. I. Sukhinov

Don State Technical University, 1, Gagarin Square, Rostov-on-Don, Russian Federation

sukhinov@gmail.com

Abstract

Introduction. The criterion for the success of an advertising campaign is the maximum profit from sales, taking into account the costs of its implementation, while the sale of the same type of goods is sales occur in a competitive environment. The article examines a model for predicting mass sales of two similar products depending on the tactics of an advertising campaign. First of all, the distribution of funds between its separate types is considered: expenses for advertising paper products, banners and advertising in electronic media (EMM).

Materials and methods. The model is formulated in the form of a Cauchy problem for a system of two ordinary differential equations with nonlinear right-hand sides, taking into account: the total number of potential solvent buyers of the first and second goods; the intensity of the advertising campaign, mainly through EMM, the positive impact on sales of the interaction of those who have already bought the first or second type of goods with potential buyers, as well as informal (at the level of buyers) anti-advertising.

The results of the study. A solution is given for the case of constant coefficients determined by the above factors for the corresponding Cauchy problem in closed form.

Discussion and conclusions. The results obtained can be used to replay model situations of advertising organization in order to determine the conditions for extracting the greatest profit from sales minus advertising costs.

Keywords: sales forecasting model, Cauchy problem, advertising costs, advertising campaign, advertising main types, competing products sales.

For citation: Sukhinov, A. I. About the analytical solution for the advertising model of two competing firms / A. I. Sukhinov // Computational Mathematics and Information Technology. — 2023. — Vol. 6, no. 1. — P. 22–26. https://doi.org/10.23947/2587-8999-2023-6-1-22-26

Научная статья

Об аналитическом решении для модели рекламы двух конкурирующих фирм

А. И. Сухинов

Донской государственный технический университет, Российская Федерация, г. Ростов-на-Дону, пл. Гагарина, 1

sukhinov@gmail.com

Аннотация

Введение. Критерием успешности рекламной кампании является максимальное извлечение прибыли от продаж с учетом затрат на ее проведение, при этом реализации однотипных товаров является продажи происходят в конкурентной обстановке. В статье исследуется модель прогнозирования массовых продаж двух однотипных товаров в зависимости от тактики рекламной кампании. Рассматривается, в первую очередь, распределение средств между ее отдельными видами: расходы на рекламную бумажную продукцию, баннеры и рекламу в электронных средствах массовой информации (ЭСМИ).

Материалы и методы. Сформулирована модель в виде задачи Коши для системы из двух обыкновенных дифференциальных уравнений с нелинейными правыми частями, учитывающими: общее число потенциальных платежеспособных покупателей первого и второго товаров; интенсивность рекламной кампании, в основном, посредством ЭСМИ; положительное влияние на продажи взаимодействия уже купивших первый или второй вид товара с потенциальными покупателями, а также неформальную (на уровне покупателей) антирекламу.

Результаты исследования. Приведено решение для случая постоянных коэффициентов, определяемых указанными выше факторами для соответствующей задачи Коши в замкнутом виде.
Обсуждение и заключения. Полученные результаты могут быть использованы для «проигрывания» модельных ситуаций организации рекламы с целью определения условий извлечения наибольшей прибыли от продаж за вычетом расходов на рекламу.

Ключевые слова: модель прогнозирования продаж, задача Коши, расходы на рекламу, рекламная кампания, основные виды рекламы, продажи конкурирующих товаров.

Для цитирования. Сухинов, А. И. Об аналитическом решении для модели рекламы двух конкурирующих фирм / А. И. Сухинов // Computational Mathematics and Information Technologies. — 2023. — Vol. 6, no 1. — С. 22–26. https://doi.org/10.23947/2587-8999-2023-6-1-22-26

Introduction. The slogan "advertising is the engine of trade" is becoming more and more relevant with the development of new electronic communication technologies. The main source of advertising was printed products at the beginning of the development of advertising technologies, such as booklets and brochures, articles in newspapers and magazines, posters, etc. The possibilities of advertising have increased significantly with the advent of radio and television, and the costs of it have also increased significantly. Advertising has become an integral part of the Internet space at the present stage. It has penetrated into all social networks and, thanks to computer and multimedia technologies, has turned into an all-pervading electronic digital environment (electronic mass media). Overexpenditures for advertising could be a small fraction of the cost of goods or services before, they reach 30 percent or more of the cost of goods and services sold now. Sales forecasting is a very important issue, which is due to the tactics of the advertising campaign and the distribution of costs between its individual types. It is important to make a timely decision about the moment of termination of advertising, especially the most expensive types of advertising, for example, the demonstration of commercials on central television channels in prime-time mode. The main criterion for the success of an advertising campaign is the extraction of maximum profit from sales, taking into account the costs of its implementation. An important factor in the subsequent sale of similar, long-term used goods (for example, iPhone) is the formation of a high consumer reputation on sales of previous generations of goods. Their popularity is determined by a higher number of products sold and an informal assessment of the product or service among buyers. Sales take place in a competitive environment and this fact is also subject to accounting. A dynamic model of an advertising campaign for sales of two competing products of the same type is proposed in the form of a Cauchy problem (with initial data) for first-order differential equations with nonlinear right-hand sides that take into account the main types of advertising and the potential market capacity. The solution of this problem is obtained in a closed form with some simplifying assumptions, which was previously repeatedly considered for the sale of one type of product [1, 2] and led to solutions in the form of logistic functions. This model can be developed and applied in other fields of activity where there is a competitive information struggle, for example, elections, public opinion formation, etc. However, this aspect is not discussed here [3, 4].

Materials and methods. Differential equations describing the rate of change over time in the number of buyers who have learned about the goods and bought them have the form:

$$\frac{dN_1}{dt}=[\alpha_{11}(t)+\alpha_{12}(t)\times N_1(t)-\alpha_{22}(t)\times N_2(t)]\times(N_0-N_1-N_2), \tag{1}$$

$$\frac{dN_2}{dt}=\left[\alpha_{21}(t)+\alpha_{22}(t)\times N_2(t)-\alpha_{12}(t)\times N_1(t)\right]\times\left(N_0-N_1-N_2\right), \tag{2}$$

$$t>0,$$

$$N_1(0)=N_{10},\ N_2(0)=N_{20},\ t=0, \tag{3}$$

where t is the time elapsed since the beginning of the advertising campaign; $N_1(t)$ and $N_2(t)$ are the numbers of buyers of the first and second goods, respectively; N_0 is the total number of potential solvent buyers of the first and second goods;

$\alpha_{11}(t)$ and $\alpha_{21}(t)$ characterize the intensity of the advertising campaign (mainly through the media) of the first and second goods; $\alpha_{12}(t)$ characterizes the positive result of the interaction of those who have already bought the first product with potential buyers; the coefficient has a similar meaning $\alpha_{22}(t)$ in the equation (2), (the word of mouth effect).

Terms $\alpha_{22}(t) \times N_2$ и $\alpha_{12}(t) \times N_1$ in the equations (1) and (2), respectively, show the influence of anti-advertising on the part of buyers: in the first case — those who preferred the second product, and in the second case — those who bought the first product, and not the second. To obtain a solution in a closed (analytical) form, all coefficients included in the system (1), (2) are considered constants, i. e. α_{ij} = const; *i, j* = 1,2. For forecasts close to real ones, these coefficients should be considered time–dependent, then it is necessary to apply numerical methods for integrating the problem (1)–(3).

As a result of the addition of equations (1) and (2), it turns out:

$$\frac{d(N_1 + N_2)}{dt} = [\alpha_{11} + \alpha_{21}] \times (N_0 - (N_1 + N_2)). \tag{4}$$

The substitution of variables in equation (4) is introduced:

$$v(t) \equiv (N_0 - (N_1 t) + (N_1 t)), \tag{5}$$

then an equation with separable variables of the form is derived

$$\frac{dv}{dt} = -[\alpha_{11} + \alpha_{21}] \times v, \quad t > 0, \tag{6}$$

with an initial condition

$$v(0) \equiv N_0 - (N_{10} + N_{20} t), \; t = 0, \tag{7}$$

the solution of which will be the function

$$v(t) \equiv (N_0 - (N_{10} + N_{20})) \times \exp(-(\alpha_{11} + \alpha_{21})t), \quad t > 0. \tag{8}$$

The resulting solution allows us to obtain an ordinary differential equation (ODE) of the first order with respect to each of the functions $N_1(t)$, $N_2(t)$. Let's express $N_2(t)$ from the ratio (8), taking into account the replacement (5):

$$N_2(t) = N_0 - N_1(t) - (N_0 - (N_{10} + N_{20})) \times \exp(-(\alpha_{11} + \alpha_{21})t). \tag{9}$$

This representation for $N_2(t)$ must be substituted into equation (1) and arrive at a first-order ODE with respect to the function $N_1(t)$:

$$\frac{dN_1}{dt} = [\alpha_{11} + \alpha_{12} N_1 - \alpha_{22}(N_0 - N_1 - (N_0 - (N_{10} + N_{20}) \exp(-(\alpha_{11} + \alpha_{21})t))] \times$$
$$\times (N_0 - N_1 - (N_0 - N_1 - (N_0 - (N_{10} + N_{20})) \exp(-(\alpha_{11} + \alpha_{21})t))).$$

Let's give similar terms and transfer the terms containing the function $N_1(t)$ to the left side, linear with respect to the desired function, an ODE of the form will turn out:

$$\frac{dN_1}{dt} + (\alpha_{12} + \alpha_{22})(N_0 - (N_{10} + N_{20})) \exp(-(\alpha_{11} + \alpha_{21})t)) N_1 =$$
$$= -(\alpha_{11} + + \alpha_{22} N_0 + \alpha_{22}(N_0 - (N_{10} + N_{20})) \exp(-(\alpha_{11} + \alpha_{21})t))(N_0 - (N_{10} + N_{20})) \exp(-(\alpha_{11} + \alpha_{21})t). \tag{10}$$

The notation is introduced:

$$N_{30} = N_0 - (N_{10} + N_{20}), \; \alpha_3 = \alpha_{11} + \alpha_{21}, \; \alpha_4 = \alpha_{12} + \alpha_{22}.$$

The equation (10) takes the form:

$$\frac{dN_1}{dt} + \alpha_4 N_{30} \exp(-\alpha_3 t) N_1 = -(\alpha_{11} - \alpha_{22} N_0 + + \alpha_{22} N_{30} \exp(-\alpha_3 t)) N_{30} \exp(-\alpha_3 t). \tag{11}$$

This equation is solved by the method of variation of an arbitrary constant. It is not difficult to find a solution to a homogeneous ODE function $N_{01}(t)$:

$$\frac{dN_{01}}{dt} + \alpha_4 N_{30} \exp(-\alpha_3 t) N_{01} = 0, \quad N_{01}(t) = C \exp\left(\frac{\alpha_4}{\alpha_3} N_{30} \exp(-\alpha_3 t)\right), \tag{12}$$

where C is the time-dependent function, $C = C(t)$:

$$N_1(t) = C(t)\, N_{01}(t). \tag{13}$$

A new independent variable has been introduced for the convenience of further transformations, the new independent variable has been introduced:

$$u = \exp(-\alpha_3 t). \tag{14}$$

Then:

$$\frac{dN_1}{dt} = \frac{dN_1}{du}\frac{du}{dt} = -\alpha_3 \frac{dN_1}{du}\exp(-\alpha_3 t) = -\alpha_3 \frac{dN_1}{du}u. \tag{15}$$

The equality (12) is written taking into account the relation (14) in the form:

$$N_1(u) = C(u)\exp\left(\frac{\alpha_4}{\alpha_3}N_{30}u\right) \tag{16}$$

and the equation (11) taking into account the equalities (14)–(16) takes the form:

$$-\alpha_3 \frac{dN_1}{du} + \alpha_4 N_{30} N_1 u = \left[\alpha_{11} - \alpha_{22}N_0 + \alpha_{22}N_{30}u\right]N_{30}u.$$

If both parts of the last equality are reduced by a function $u \neq 0$ from (14), and put (16) in the resulting equation, then the ODE for $C(u)$ takes the form:

$$\frac{dC}{du} = \left[\alpha_{11} - \alpha_{22}N_0 + \alpha_{22}N_{30}u\right]N_{30}\exp\left(-\frac{\alpha_4}{\alpha_3}N_{30}u\right). \tag{17}$$

The solution of this equation with separable variables is not difficult, because $C(u)$ can be represented as a sum of easily taken integrals

$$I_1 = \int\left[\alpha_{11} - \alpha_{22}N_0\right]N_{30}\exp\left(-\frac{\alpha_4}{\alpha_3}N_{30}u\right)du = \left(\alpha_{22}N_0 - \alpha_{11}\right)\frac{\alpha_3}{\alpha_4}\exp\left(-\frac{\alpha_4}{\alpha_3}N_{30}u\right) \tag{18}$$

and the integral I_2, which is calculated by a single application of the integration formula in parts

$$I_2 = \int \alpha_{22}\left(N_{30}\right)^2 u\exp\left(-\frac{\alpha_4}{\alpha_3}N_{30}u\right)du = -\frac{\alpha_3\alpha_{22}N_{30}u}{\alpha_4}\exp\left(-\frac{\alpha_4}{\alpha_3}N_{30}u\right) - \frac{\alpha_3\alpha_{22}}{\alpha_4^2}\exp\left(-\frac{\alpha_4}{\alpha_3}N_{30}u\right). \tag{19}$$

The equation is formed by adding (18) and (19) to calculate the coefficient $C(u)$:

$$C(u) = \left((\alpha_{22}N_0 - \alpha_{11})\frac{\alpha_3}{\alpha_4} - \frac{\alpha_3\alpha_{22}N_{30}u}{\alpha_4} - \frac{\alpha_3^2\alpha_{22}}{\alpha_4^2}\right)\exp\left(-\frac{\alpha_4}{\alpha_3}N_{30}u\right). \tag{20}$$

Let's substitute expression (20) for $C(u)$ into equality (16), a general solution for the function N_1 is obtained, which after multiplying by some constant K, defined in such a way as to satisfy the initial condition $N_1(0) = N_{10}$, gives a solution for the function N_1, who which is part of the Cauchy problem:

$$N_1(u) = C(u)\exp\left(\frac{\alpha_4}{\alpha_3}N_{30}u\right),$$

$$C(u) = K\left((\alpha_{22}N_0 - \alpha_{11})\frac{\alpha_3}{\alpha_4} - \frac{\alpha_3\alpha_{22}N_{30}u}{\alpha_4} - \frac{\alpha_3^2\alpha_{22}}{\alpha_4^2}\right)\exp\left(-\frac{\alpha_4}{\alpha_3}N_{30}u\right).$$

As a result , the last two equalities will take the form:

$$N_1(u) = K\left((\alpha_{22}N_0 - \alpha_{11})\frac{\alpha_3}{\alpha_4} - \frac{\alpha_3\alpha_{22}N_{30}u}{\alpha_4} - \frac{\alpha_3^2\alpha_{22}}{\alpha_4^2}\right), \tag{21}$$

$$u = \exp(-\alpha_3 t),\ N_{30} = N_0 - (N_{10} + N_{20}),\ \alpha_3 = \alpha_{11} + \alpha_{21},\ \alpha_4 = \alpha_{12} + \alpha_{22}. \tag{22}$$

To complete the formation of the solution for the function $N_1(t)$, it is necessary to determine the constant K, based on the initial condition (3) for $N_1(0)$. Simple calculations lead to the following equality:

$$K = N_{10}/\left((\alpha_{22}N_0 - \alpha_{11})\frac{\alpha_3}{\alpha_4} - \frac{\alpha_3\alpha_{22}N_{30}}{\alpha_4} - \frac{\alpha_3^2\alpha_{22}}{\alpha_4^2}\right). \tag{23}$$

Determining the function $N_2(t)$ from equality (5), in the case of the found function $N_1(t)$ is not difficult:

$$N_2(t) = N_0 - N_1(t) - \left(N_0 - (N_{10} + N_{20})\right)\times\exp(-(\alpha_{11} + \alpha_{21})t).$$

Remark.

In the case of a non-simultaneous start of sales of goods (for example, sales of the second type do not start at the initial moment of time, but at $t = T$), it is necessary to determine $N_1(T)$, based on a known solution for the logistic model of an advertising campaign for the sale of one type of product [1], then change the right parts of the ODE (1) and (2) and initial conditions (3):

$$\frac{dN_1(t)}{dt} = [\alpha_{11}(t) + \alpha_{12}(t) \times N_1(t) - \alpha_{22}(t) \times N_2(t)] \times (N_0 - N_1(t) - N_1(T) - N_2(t)),$$

$$\frac{dN_2}{dt} = [\alpha_{21}(t) + \alpha_{22}(t) \times N_2(t) - \alpha_{12}(t) \times N_1(t)] \times (N_0 - N_1(t) - N_1(T) - N_2(t)),$$

$$t > T,$$

$$N_{10} = N_1(T),\ N_2(T) = N_{20},\ t = T.$$

Research results. The solution is given for the case of constant coefficients determined by the following factors: the total number of potential solvent buyers of the first and second goods; the intensity of the advertising campaign, mainly through EMM; the positive impact on sales of the interaction of those who have already bought the first or second type of goods with potential buyers, informal (at the level of buyers) anti-advertising, for the corresponding Cauchy problem in closed form.

Discussion and conclusions. The results obtained can be used to "replay" model situations of advertising organization in order to determine the conditions for extracting the greatest profit from sales minus advertising costs. For forecasts that are close to real, we should abandon the assumption α_{ij} = const; $i, j = 1, 2$ and consider these coefficients time-dependent. Then it is necessary to apply numerical methods of integration of the problem (1)–(3). In addition, the determination of these coefficients in predictive models is a separate task of mathematical statistics [3, 4], for which, for example, you can use survey data at the exit from places of mass sales of goods (shopping centers). In fact, this approach is close to the exit polls technology used in elections. These aspects of the study will be the subject of future work on this topic.

References

1. Samarsky, A. A. Mathematical modeling: Ideas. Methods. Examples. / A. A. Samarsky, A. P. Mikhailov. — 2nd ed., ispr. — Moscow : Fizmatlit, 2001. — 320 p. (In Russ.)

2. Petrov, A. A. Experience of mathematical modeling of the economy. / A. A. Petrov, I. G. Pospelov, A. A. Shananin. — Moscow : Energoizdat, 1996. — 544 p. (In Russ.)

3. Petukhov, A. Yu. Modeling and analysis of socio-political processes in the Republic of Belarus in autumn 2020 / A. Yu. Petukhov, D. I. Kaminchenko // Bulletin of Tomsk State University. Philosophy. Sociology. Political science. — 2021. — Vol. 64. — P. 214–223. (In Russ.) https://doi.org/10.17223/1998863X/64/20

4. Petrov, A. Modeling the Spread of a Message in a Population with Differential Receptivity // Lecture Notes in Networks and Systems (LNNS).— 2022. — Vol. 503. — P. 35–40. https://doi.org/10.1007/978-3-031-09073-8_4

Received by the editorial office 09.02.2023.
Received after reviewing 02.03.2023.
Accepted for publication 03.03.2023.

About the Author:

Sukhinov, Alexander I., Corresponding member of RAS, Dr.Sci. (Phys.-Math), Professor, Director of the Research Institute "Mathematical Modeling and Forecasting of Complex Systems", Don State Technical University (1, Gagarin Square, Rostov-on-Don, 344003, RF), MathSciNet, eLibrary.ru, ORCID, ResearcherID, ScopusID.

The Author read and approved the final version of the manuscript.

UDC 519.6 *Original article*

https://doi.org/10.23947/2587-8999-2023-6-1-27-33

Direct seismic modeling: day surface topography and shallow subsurface anisotropy

V. I. Golubev[1,2] ✉, A. V. Shevchenko[1,2], A. V. Ekimenko[3], V. Yu. Petrukhin[4]

[1]Moscow Institute of Physics and Technology, 9, Institutskii lane, Dolgoprudny, Russian Federation

[2]Institute of Computer Aided Design of RAS, 19/18, 2-nd Brestskaya street, Moscow, Russian Federation

[3]Gazprom Neft Science and Technology Centre, 75–79d, emb. river Moika, St. Petersburg, Russian Federation

[4]PAO Sberbank, 19, Vavilova street, Moscow, Russian Federation

✉ w.golubev@mail.ru

Abstract

Introduction. The article is devoted to one of the problems in the oil and gas fields development — the correct geological models construction of the subsurface space. Researchers from various scientific groups around the world have proposed various ways to improve the accuracy of the computer simulations used in this process. The purpose of this study is to assess the degree of the day surface relief and the anisotropy of the geological section upper part influence on the recorded seismic signal using a realistic model of the Orenburg field as an example.

Materials and methods. The seismogeological model describing the Orenburg geological section Lower Permian interval is considered. The elastic properties of geological formations were estimated according to well data: density and propagation velocities of longitudinal and transverse waves. There is a high contrast of P-wave velocities estimated from sonic logs. The reservoir is confined to the lower layers in this model. It is composed of sulfate-carbonate media, uniform in density and acoustic properties. Using the grid-characteristic method, zero-offset synthetic seismograms were calculated. The choice of structural curvilinear computational grids made it possible to correctly consider the relief of the day surface.

Research results. Two different models were compared in this work. The first model included the anisotropy of the section's upper part and the day surface topography. In the second model, the upper boundary of the computational domain was flat, and the entire medium was considered within the framework of an isotropic linear elastic model. The analysis of synthetic seismograms showed that the anisotropy inherent in this model does not significantly affect the recorded seismic wave field. However, considering the relief of the day surface significantly shifts the times of arrival of reflected waves.

Discussion and conclusion. The algorithm presented in the paper can be used to verify the field data processing graph, since the assessment of the anisotropy of the medium is a standard step in building a velocity model. The presented approach can be extended to 3D realistic dimensions models.

Keywords: mathematical modeling, seismic exploration, grid-characteristic numerical method, anisotropic media, day surface topography.

Funding information. The study was carried out for the grant of the Russian Science Foundation no. 19-71-10060. https://rscf.ru/project/19-71-10060/.

For citation. Direct seismic modeling: day surface topography and shallow subsurface anisotropy / V. I. Golubev, A. V. Shevchenko, A. V. Ekimenko, V. Yu. Petrukhin // Computational Mathematics and Information Technologies. — 2023. — Vol. 6, no. 1. — P. 27–33. https://doi.org/10.23947/2587-8999-2023-6-1-27-33

Научная статья

Прямое численное моделирование: топография дневной поверхности и анизотропия верхней части разреза

В. И. Голубев[1,2] ✉, А. В. Шевченко[1,2], А. В. Екименко[3], В. Ю. Петрухин[4]

[1]Московский физико-технический институт, Российская Федерация, г. Долгопрудный, Институтский переулок, 9

[2]Институт автоматизации проектирования Российской Академии Наук, Российская Федерация, г. Москва, ул. 2-я Брестская, 19/18

[3]ООО «Газпромнефть НТЦ», Российская Федерация, г. Санкт-Петербург, наб. реки Мойки, 75−79д

[4]ПАО Сбербанк, г. Москва, ул. Вавилова, 19

✉ w.golubev@mail.ru

Аннотация

Введение. Одной из проблем разработки нефтегазовых месторождений является построение корректных геологических моделей подповерхностного пространства. Исследователями из различных научных групп во всем мире предложены различные способы повышения точности компьютерного моделирования, используемого в этом процессе. Цель настоящего исследования — оценка степени влияния рельефа дневной поверхности и анизотропии верхней части геологического разреза на регистрируемый сейсмический сигнал на примере реалистичной модели Оренбургского месторождения.

Материалы и методы. Рассмотрена сейсмогеологическая модель, описывающая нижнепермский интервал Оренбургского геологического разреза. По скважинным данным оценены упругие свойства геологических пластов: плотность и скорости распространения продольных и поперечных волн. Отмечается высокий контраст скоростей продольных волн, оцененных по диаграммам акустического каротажа. Резервуар в этой модели приурочен к нижним пластам. Он сложен сульфатно-карбонатными средами, однородными по плотности и акустическим свойствам. С использованием сеточно-характеристического метода были рассчитаны синтетические сейсмограммы нулевых удалений. Выбор структурных криволинейных расчетных сеток позволил корректно провести учет рельефа дневной поверхности.

Результаты исследования. В работе было проведено сопоставление двух различных моделей. В первую модель была включена анизотропия верхней части разреза и топография дневной поверхности. Во второй модели верхняя граница расчетной области была плоской, и вся среда рассматривалась в рамках изотропной линейно упругой модели. Анализ синтетических сейсмограмм показал, что анизотропия, присущая этой модели, не оказывает существенного влияния на регистрируемое сейсмическое волновое поле. Однако учет рельефа дневной поверхности заметно сдвигает времена прихода отраженных волн.

Обсуждение и заключение. Представленный в работе алгоритм может быть использован для верификации графа обработки полевых данных, поскольку оценка анизотропии среды является стандартным шагом при построении скоростной модели. Представленный подход может быть расширен на трехмерные модели реалистичных размеров.

Ключевые слова: математическое моделирование, сейсмическая разведка, сеточно-характеристический численный метод, анизотропные среды, топография дневной поверхности

Финансирование. Исследование выполнено за счет гранта Российского научного фонда № 19-71-10060, https://rscf.ru/project/19-71-10060/.

Для цитирования. Прямое численное моделирование: топография дневной поверхности и анизотропия верхней части разреза / В. И. Голубев, А. В. Шевченко, А. В. Екименко, В. Ю. Петрухин // Computational Mathematics and Information Technologies. — 2023. — Т. 6, № 1. — С. 27–33.
https://doi.org/10.23947/2587-8999-2023-6-1-27-33

Introduction. The problem of considering the surface topography during seismic survey simulations attracts the attention of many researchers. The trivial approach is based on the stair-step approximation of the top domain boundary and finite-difference schemes [1] on rectangular grids. However, it leads to the appearance of additional source artifacts due to diffraction. The rotated staggered-grid modification was proposed to align the grid to the boundary interface. [2]. The use of finite-difference schemes on deformed grids does not allow describing very steep slopes in relief [3]. In [4], a pseudospectral method was proposed with the mapping of rectangular grids onto a curved surface, which also turned out to be unstable near strongly inclined boundaries. Apparently, an acceptable solution is to use finite element methods

on nonstructural grids [5]. The disadvantage of this approach is a significant increase in the computational complexity of the task and the required RAM. In [6] an approach based on the combination of the discontinuous Galerkin with the finite difference method was developed. It allows to cover only the thin subsurface layer with an unstructured grid, while using the rectangular one in the rest of the geological model.

In elastic media with sharp variations of physical properties the grid-characteristic method can be effectively used [7, 8]. The method of superimposed grids was combined with it, which makes it possible to correctly describe curved boundaries [9]. This study uses a different approach. A separate curved grid is used to cover each geological layer, together with the explicit statement of contact conditions between the individual layers. This method preserves the advantages of the grid-characteristic method without leading to an excessive increase in the computational complexity of the problem. The paper takes into account the thin-layering of the upper part of the geological section using the widely used vertical transverse isotropic (VTI) model of the medium [10, 11].

The purpose of this work is to assess the degree of the daytime surface relief and the anisotropy of the upper part of the geological section influence on the recorded seismic signal using the example of the Orenburg field's realistic model.

Materials and methods. A significant amount of seismic survey is related to the investigation of oil and gas basins. These territories, being composed of sedimentary rocks, are thick strata of a thin layer interbedding. The formation conditions of sedimentary rocks determine the difference in physical properties of each layer. The geological history of each region determines the current position of the formed rock strata. Therefore, a characteristic feature is the presence of layers, laterally extended, but thin related to used seismic wavelengths. It provides the possibility to describe this geological medium by the VTI model. This model was formulated due to the registration of different velocities for vertical and inclined seismic rays in 1930-th. In this work, the seismic-geological model describing the Lower Permian interval of the Orenburg geological section was considered. The physical properties were evaluated based on borehole data from the Orenburg oil and gas condensate deposit (Fig. 1 *a*). Two main parts of the model were distinguished: (1) the thin-bedded upper interval corresponded to the Kungurian stage and (2) the lower one describing the Filippovsky horizon and the Artinsk stage. The first one was represented by pure salts and the interbedding of rock salt, anhydrites, and dolomites. A high contrast was noted in compressional wave velocities estimated by acoustic logging diagrams. The typical value for rock salt was 4500 *m/s*, for anhydrites — 6300 *m/s*, and for dolomites — in the range from 4500 *m/s* to 6500 *m/s* (Fig. 1 *b*). This interval affects kinematic characteristics of the wavefield and causes the anisotropy.

Figure 2 shows the field seismic data. The alternation of dolomite, salt and anhydrite layers induces dynamically pronounced reflections. The section shows a complex geometry of the reflecting boundaries of the upper interval and halokinesis processes, accompanied by the salt penetration into the overlying terrigenous strata. It can be assumed, that in areas of the contrast subhorizotal layer location, the anisotropy parameters will be different from the ones of salt diapirs. The reservoir in this model is confined to the lower strata. It is composed of sulfate-carbonate media, homogeneous in its density and acoustic properties. The reflective boundaries in this interval have low contrast. This fact is explained by the absence of acoustically rigid boundaries. According to the well logging, the interval is relatively homogeneous (Fig. 1 *a*). Based on the above description, an elastic two-dimensional model was developed. A thin-layered interval was described by the VTI model to achieve the desired accuracy.

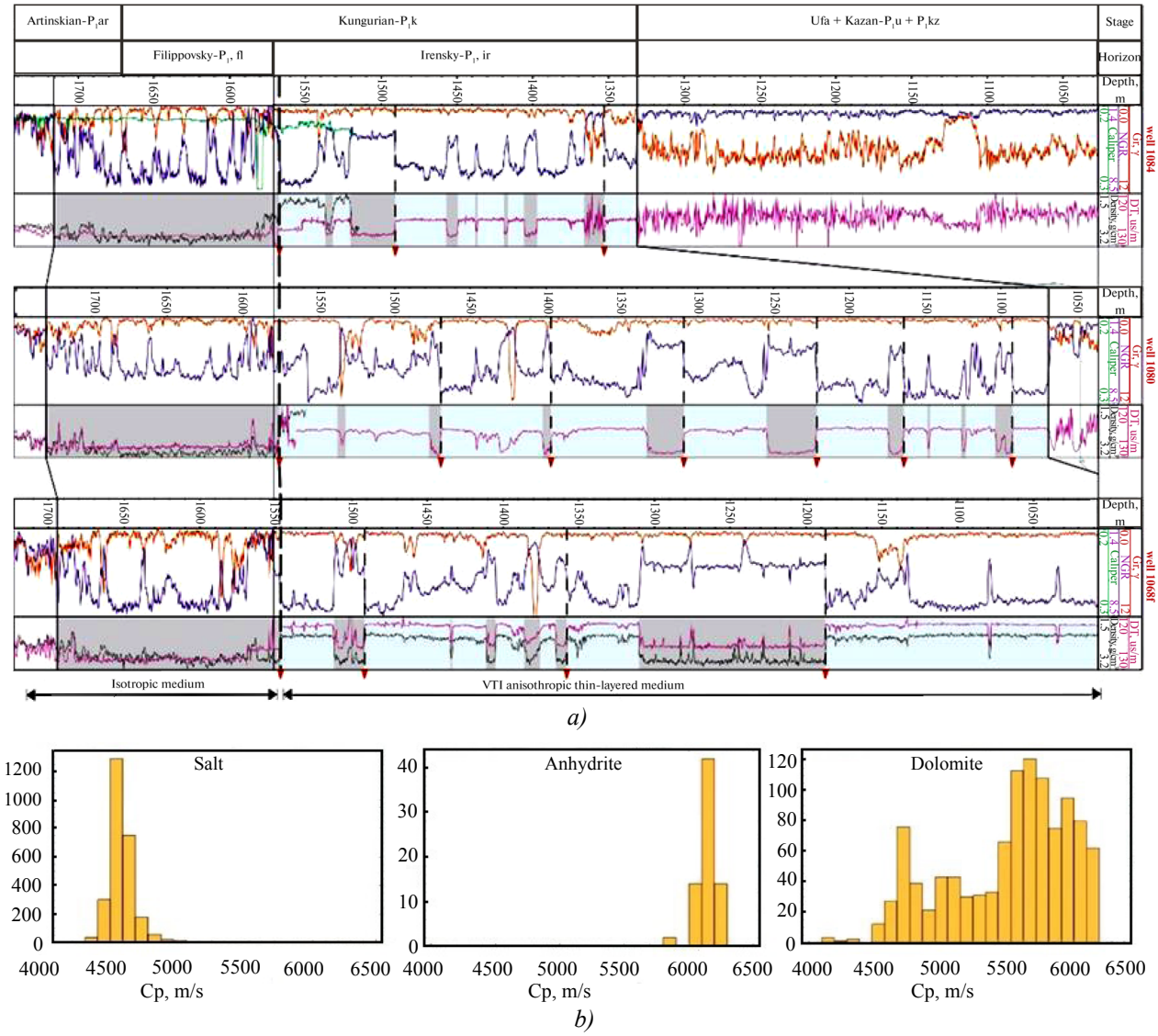

Fig. 1. The field measurements' results: *a* — Borehole data from the Orenburg oil and gas condensate deposit (by TNG-Group); *b* — P-wave velocity histograms based on sonic data

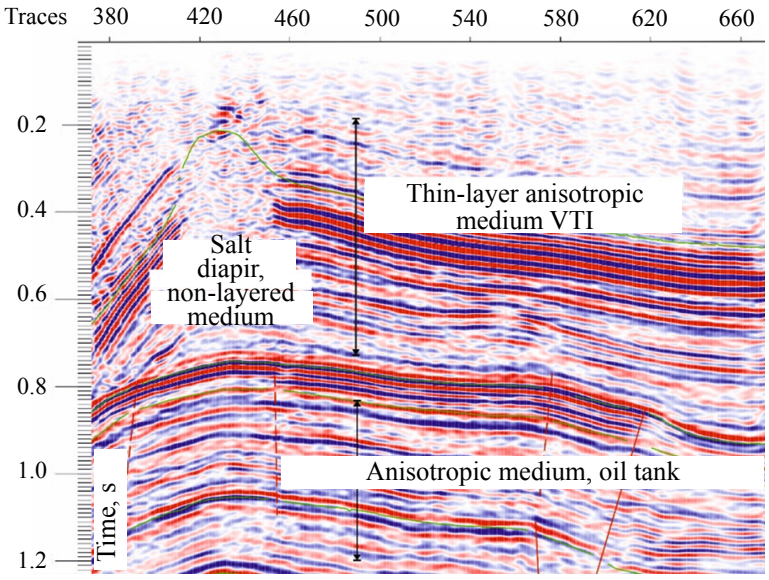

Fig. 2. The seismic section of the Orenburg deposit

The hyperbolic system of governing PDEs can be written in the canonical form:

$$\vec{q}_t + A_1\vec{q}_x + A_2\vec{q}_y = \vec{f},$$

where the vector $\vec{q}$ consists of all unknowns (velocity vector components and symmetrical stress tensor components). The space-dependent matrices A_1, A_2, are defined by the material parameters. In order to solve system (1) $\vec{q}_t + A_1\vec{q}_x = \vec{0}$, we apply the splitting technique to this 2D equation system: $\vec{q}_t + A_2\vec{q}_y = \vec{0}$ solve, firstly , secondly, solve and, finally, solve $\vec{q}_t = \vec{f}$. Thus, the multidimensional problem is reduced to a sequence of one-dimensional ones. The final step with the right-hand side can be easily and efficiently done, since it solves an ODE in each grid point. Each one-dimensional equation has the following form:

$$\vec{q}_t + A\vec{q}_\xi = \vec{0}.$$

The hyperbolicity of (1) ensures that matrix A has a full set of eigenvectors and can be represented as:

$$A = \Omega^{-1}\Lambda\Omega,$$

where matrix Λ is diagonal. The matrix A consists of eigenvectors of. Introducing the transformation to the Riemann invariants, a set of independent transport equations is obtained: $\vec{w} = \Omega\vec{q}$. The following relation is used for each equation: $\vec{w}_t + \Lambda\vec{w}_\xi = 0$., where the subscript I mark components of the vector:

$$w_i(x, t+\tau) = w_i(x - \lambda_i\tau, t),$$

After each one-dimensional step we return back to the original unknowns by: $\vec{q} = \Omega^{-1}\vec{w}$.

The critical difference between implementations of this method on rectangular grids and on structured curvilinear grids is that in the first case there are only two fixed directions along which the matrices Ω have a simple form and can be written analytically (even in case of space-dependent coefficients and matrices). In the case of the curvilinear mesh each point has a local coordinate system (ξ, η) along grid lines and matrix Ω and its inverse have to be found numerically (by an iterative procedure).

Research results. The wavefield in the described geological model was successfully simulated. The deformed grid was generated by the UNAMALLA software (Barrera et al. (2009)) and covered the region of 10 km × 5 km. The solution of one-dimensional transport equations was done by the Rusanov numerical scheme. The spatial time step was approximately 2 m. The time step was chosen to satisfy the CFL stability condition. Two different cases — with the anisotropy and topography and without both of them — were compared (Fig. 3). The careful synthetic data analysis reveals that the anisotropy inherent in this model doesn't influence the seismic wavefield significantly. On the contrary, the topography shifts noticeably arrival times of reflected waves.

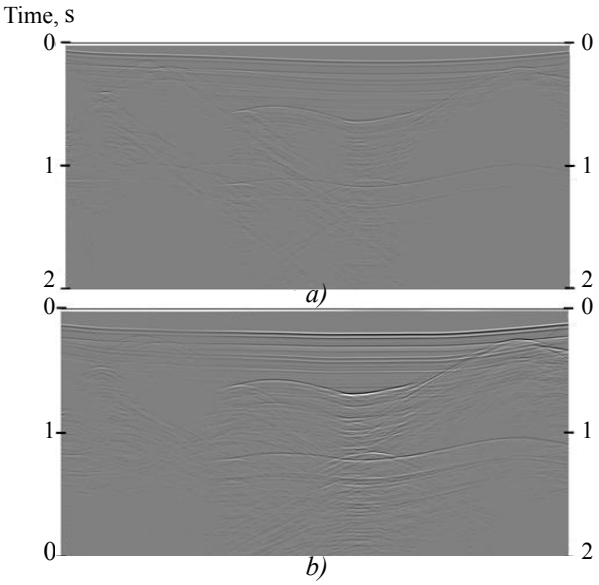

Fig. 3. Seismograms for the isotropic model with the flat day surface (*a*)
and for the VTI model with the proper topography (*b*)

Discussion and conclusions. In this work the importance of the day surface topography and the shallow subsurface anisotropy influence on seismic survey data was discussed. The real Orenburg oil and gas condensate deposit was considered for the sake of clarity. The grid-characteristic method on structured grids was successfully applied to take into account anisotropy and topography of the model. The calculated wavefields reproduce the main features of the original seismic section, which indicates the model adequacy. The numerical simulations results represent a sufficient influence of considered facts on the day surface signal.

The presented algorithm can be used for the real data processing graph verification, since the VTI anisotropy estimation is a standard step while building a depth-velocity model [13]. The presented approach can be directly extended for real-scale three-dimensional problems.

References

1. Virieux, J. P-SV wave propagation in heterogeneous media: Velocity — stress finite-difference method / J. Virieux // Geophysics. — 1986. — Vol. 51, no. 4. — P. 889–901.

2. Saenger, E. H. Finite–difference modeling of viscoelastic and anisotropic wave propagation using the rotated staggered grid / E. H. and T. B. Saenger // Geophysics. — 2004. — Vol. 69, no. 2. — P. 583–591.

3. Tarrass, I. New curvilinear scheme for elastic wave propagation in presence of curved topography / I. Tarrass, L. Giraud and P. Thore // Geophys. — 2011. — Vol. 59, no. 5. — P. 889–906.

4. Tessmer, E. Elastic wave propagation simulation in the presence of surface topography / E. Tessmer, D. and A. B. Kosloff // Geophys. — 1992. — Vol. 108, no. 2. — P. 621–632.

5. An hpadaptive discontinuous Galerkin finite-element method for 3D elastic wave modelling / V. Etienne, E. Chaljub, J. Virieux and N. Glinsky // Geophysical Journal International. — 2010. — Vol. 183.— P. 941–962.

6. Lisitsa, V. Combination of the discontinuous Galerkin method with finite differences for simulation of seismic wave propagation / V. Lisitsa, V. Tcheverda and C. Botter // Journal of Computational Physics. — 2016. — Vol. 311.— 142–157.

7. Compact Grid-Characteristic Scheme for the Acoustic System with the Piece-Wise Constant Coefficients / V. Golubev, A. Shevchenko, N. Khokhlov, I. Petrov and M. Malovichko // International Journal of Applied Mechanics. — 2022. — Vol. 14, no. 2.

8. Golubev, V. Raising convergence order of grid-characteristic schemes for 2D linear elasticity problems using operator splitting / V. Golubev, A. Shevchenko and I. Petrov // Computer Research and Modeling — 2022. — Vol. 14, no. 4. — P. 899–910.

9. Khokhlov, N. I. Overset grids approach for topography modeling in elastic-wave modeling using the grid-characteristic method / N. I. Khokhlov, V. O. Stetsyuk and I. A. Mitskovets // Computer Research and Modeling. — 2019. — Vol. 11, no. 6. — P. 1049–1059.

10. Petrov, I. B. Simulation of Seismic Waves in Anisotropic Media / I. B.Petrov, V. I. Golubev, V. Y. Petrukhin and I. S. Nikitin // Mathematics. — 2021. — Vol. 103, no. 3. — P. 146–150.

11. Golubev, V. Explicit simulation of seismic waves in fractured VTI media / V. Golubev and A. Shevchenko // 82nd EAGE Annual Conference and Exhibition. — 2021.

12. Generating Quality Structured Convex Grids on Irregular Regions / P. Barrera, F. Domınguez, G. F. Gonzalez G. and Tinoco // Electronic Transactions on Numerical Analysis. — 2009. — Vol. 34.— P. 76–89.

13. Deep Convolutional Neural Networks in Seismic Exploration Problems / A. Vasyukov, I. Nikitin, A. Stankevich and V. Golubev // Interfacial Phenomena and Heat Transfer. — 2022. — Vol. 10, no. 3. — P. 61–74.

Received by the editorial office 07.02.2023.
Received after reviewing 02.03.2023.
Accepted for publication 03.03.2023.

About the Authors:

Golubev, Vasily I., Leading Researcher, Applied Computational Geophysics Lab, Moscow Institute of Physics and Technology (National Research University), (9, Institutsky Lane, Dolgoprudny, Moscow Region, 141701, RF), Dr. (Physical and Mathematical Sciences), Associate Professor, ORCID, w.golubev@mail.ru

Shevchenko, Alexey V., postgraduate student, Moscow Institute of Physics and Technology (National Research University) (9, Institutsky Lane, Dolgoprudny, Moscow region, 141701, RF), ORCID, alexshevchenko@phystech.edu

Ekimenko, Anton V., expert of the integrated Solutions unit of Gazpromneft STC LLC (75–79d, Moika emb. river, Saint Petersburg, 190000, RF), Ph.D. (Geological and Mineralogical Sciences,), ORCID, ekimenko.av@gazpromneft-ntc.ru

Petrukhin, Vyacheslav Yu., Head of the Sberbank Direction PJSC (19, Vavilova St., Moscow, 117312, RF), ORCID, v.y.petrukhin@gmail.com

Claimed contributorship

V. I. Golubev: statement of the purpose and objectives of the study, preparation of the text, formulation of conclusions. A.V. Shevchenko: carrying out numerical calculations on an isotropic model without relief. A.V. Ekimenko: construction of a geological model, analysis of the results of numerical calculations. V. Yu. Petrukhin: carrying out calculations on an anisotropic model with relief.

Conflict of interest statement

The authors declare that there is no conflict of interest.

All authors have read and approved the final version of the manuscript.

UDC 519.6 *Original article*

https://doi.org/10.23947/2587-8999-2023-6-1-34-40

Spatial-three-dimensional wave processes' modeling in shallow water bodies taking into account the vertical turbulent exchange features

E. A. Protsenko[1], N. D. Panasenko[1], A. V. Strazhko[1]

[1]Taganrog Institute named after A. P. Chekhov (branch) of RSUE, 48, Initiative St., Taganrog, Rostov region, Russian Federation

eapros@rambler.ru

Abstract

Introduction. Reliable prediction of indicators of turbulent flows is a very difficult task, which is explained by the exceptional physical complexity of turbulence, in particular its probabilistic nature, a wide space-time spectrum and a fundamentally three-dimensional non-stationary nature. Despite conducting a wide range of studies focused on the problem under consideration, they did not fully reflect the totality of various factors and processes affecting the structure and parameters of vertical turbulent mixing. This indicates the need for a systematic analysis of the problem and modeling of such complex formalized systems. The aim of the work is to construct a scenario of changes in hydrodynamic wave processes of the coastal zone, based on an improved mathematical model of wave processes.

Materials and methods. The article is devoted to the study of spatial-three-dimensional wave processes in shallow water bodies, taking into account the features of turbulent exchange depending on the source and localization in the column of liquid, as well as the study of the influence of regular wave processes on turbulent exchange and vertically using a mathematical model of wave processes based on the system of Navier-Stokes equations, including three equations of motion in the with dynamically changing geometry of the computational domain.

The results of the study. Based on the developed software package, a scenario of changes in hydrodynamic wave processes of the coastal zone is constructed, the formation of vortex structures is predicted.

Discussion and conclusions. The separation of the wave flow into a near-surface macroturbulent layer caused by wave motion and a lower layer with background hydrodynamic turbulence is proved, the strength and intensity of turbulence changed synchronously with wave oscillations, demonstrating a pronounced asymmetry of turbulence generation throughout the water column.

Keywords: three-dimensional model of hydrodynamics, vertical turbulent exchange, numerical methods, wave processes, data filtering.

Funding information. The research was carried out at the expense of the grant of the Russian Science Foundation No. 23-21-00210, https://rscf.ru/project/23-21-00210/».

For citation. Protsenko, E. A. Modeling of spatial-three-dimensional wave processes in shallow water bodies taking into account the features of vertical turbulent exchange / E. A. Protsenko, N. D. Panasenko, A. V. Strazhko // Computational Mathematics and Information Technologies. — 2023. — Vol. 6, no. 1. — P. 34–40. https://doi.org/10.23947/2587-8999-2023-6-1-34-40

Научная статья

Моделирование пространственно-трехмерных волновых процессов в мелководных водоемах с учетом особенностей вертикального турбулентного обмена

Е. А. Проценко[1], Н. Д. Панасенко[1], А. В. Стражко[1]

[1]Таганрогский институт имени А. П. Чехова (филиал) РГЭУ (РИНХ), Российская Федерация, Ростовская область, г. Таганрог, ул. Инициативная, 48

eapros@rambler.ru

Аннотация

Введение. Достоверное предсказание показателей турбулентных потоков является весьма сложной задачей, что объясняется исключительной физической сложностью турбулентности, в частности ее вероятностной природой, широким пространственно-временным спектром и принципиально трехмерным нестационарным характером. Несмотря на проведение широкого круга исследований, ориентированных на рассматриваемую проблему, в них не была достаточно полно отражена вся совокупность разнообразных факторов и процессов, влияющих на структуру и параметры вертикального турбулентного перемешивания. Это указывает на необходимость проведения системного анализа проблемы и моделирования подобных сложно формализуемых систем. Целью работы является построение сценария изменения гидродинамических волновых процессов береговой зоны на основе усовершенствованной математической модели волновых процессов.

Материалы и методы. Исследуются пространственно-трехмерные волновые процессы в мелководных водоемах с учетом особенностей турбулентного обмена в зависимости от источника и локализации в столбе жидкости. Рассматривается влияние регулярных волновых процессов на турбулентный обмен по вертикали с помощью математической модели волновых процессов, базирующейся на системе уравнений Навье-Стокса. Модель включает в себя три уравнения движения в областях с динамически изменяемой геометрией расчетной области.

Результаты исследования. На основе разработанного комплекса программ построен сценарий изменения гидродинамических волновых процессов береговой зоны, предсказано формирование вихревых структур.

Обсуждение и заключения. Доказано разделение волнового потока на приповерхностный макротурбулентный слой, вызванный волновым движением, и нижерасположенный слой с фоновой гидродинамической турбулентностью, сила и интенсивность турбулентности изменялись синхронно с волновыми колебаниями, демонстрируя явно выраженную асимметрию генерации турбулентности по всей толще воды.

Ключевые слова: трехмерная модель гидродинамики, вертикальный турбулентный обмен, численные методы, волновые процессы, фильтрация данных.

Финансирование. Исследование выполнено за счет гранта Российского научного фонда № 23-21-00210, https://rscf.ru/project/23-21-00210/».

Для цитирования. Проценко Е. А. Моделирование пространственно-трехмерных волновых процессов в мелководных водоемах с учетом особенностей вертикального турбулентного обмена / Е. А. Проценко, Н. Д. Панасенко, А. В. Стражко // Computational Mathematics and Information Technologies — 2023. —Т. 6, № 1. — С. 34–40. https://doi.org/10.23947/2587-8999-2023-6-1-34-40

Introduction. Modern numerical models — SWAN, SWASH, FINLAB, H2Ocean and XBeach are constantly being improved due to new scientific discoveries as a result of research involving laboratory and field experiments. With the help of laboratory experiments, it is possible to obtain information about the details of the flow under controlled conditions. Flow velocities, turbulence properties and forces acting on objects can be determined and used to interpret observed phenomena, for example, erosion, and the data can be used to validate the model. At the same time, the complexity of obtaining full-scale data in the real area indicates the need to involve 3D models of hydrodynamics that take into account the specifics of coastal systems [1, 2].

Turbulence and further mixing of the aquatic environment are important mechanisms that determine the dynamics of the coastal zone, the transfer of momentum, mass and heat. Turbulence usually occurs as a result of shear or unstable stratification, while in the coastal zone, wind waves are an alternative source of turbulent mixing. In addition, turbulence can be generated as a result of bottom friction that occurs in the presence of tidal or wind currents, while baroclinic currents, nonlinear internal waves and inertial currents are important [3−5].

The task of monitoring the water surface involves the creation and verification of effective methods for clustering these objects on the surface of reservoirs, in particular, restoring the boundaries of the reservoir based on remote sensing data. Multispectral satellite images are used as sensing data. Based on the obtained images, the initial conditions for the mathematical model of hydrodynamics are determined, based on which prognostic calculations are performed.

Remote sensing data makes it possible to determine the dynamics of changes in the coastline due to a series of processed images of the same water area at different times.

Coastal areas require special attention, since interaction with bathymetry, currents, stratification, as well as vegetation, leads to complex nonlinear interactions affecting the evolution of waves.

Materials and methods

1. Spatially inhomogeneous three-dimensional wave hydrodynamics mathematical model of shallow reservoir.

Mathematical model includes [6, 7]:

$$u_t' + uu_x' + vu_y' + wu_z' = -\frac{1}{\rho}p_x' + (\mu u_x')_x' + (\mu u_y')_y' + (vu_z')_z',$$

$$v_t' + uv_x' + vv_y' + wv_z' = -\frac{1}{\rho}p_y' + (\mu v_x')_x' + (\mu v_y')_y' + (vv_z')_z', \quad (1)$$

$$w_t' + uw_x' + vw_y' + ww_z' = -\frac{1}{\rho}p_z' + (\mu w_x')_x' + (\mu w_y')_y' + (vw_z')_z' + g;$$

$$\rho_t' + (\rho u)_x' + (\rho v)_y' + (\rho w)_z' = 0, \quad (2)$$

where $V = \{u, v, w\}$ is the water flow of shallow water body velocity vector; P is the hydrodynamic pressure; ρ is the aquatic environment density; μ, n are turbulent exchange coefficients in the horizontal and vertical directions; g is the gravity acceleration.

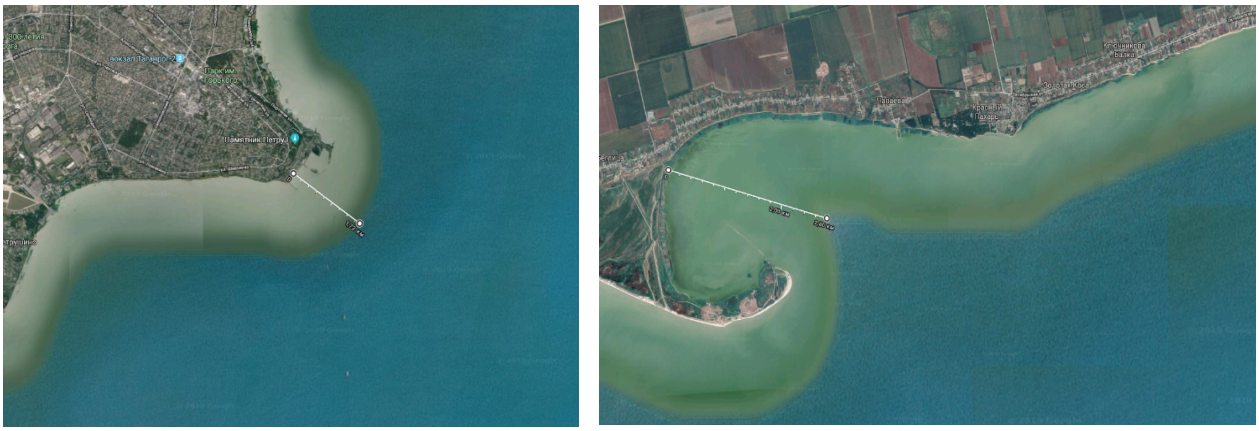

Fig. 1. Satellite images of the Azov Sea (low tide, November 22, 2019)

The raster model of the computational domain is constructed based on observations at individual points in space (Fig. 1). Discrete operational-territorial units correspond to cells of a regular grid. Figure 2 shows raster model of the computational domain.

2. Processing and parameterization of in-situ ADCP sensing data. The wave disturbance detected by the ADCP probe differs in frequency and intensity from the disturbance on the sea surface. This is due to the mutual movement of the vessel, the waves and the commensurability of their geometric dimensions. The movement of the vessel on the wave changes the frequency of the wave disturbance. If the wave scales are close to the dimensions (length, width, draft) of the vessel, then it cannot repeat its profile during its movement. The degree of impact of pitching is provided

by means of reduction coefficients, which have the form of amplitude-frequency characteristics of linear low-frequency filters [7, 8]. To represent the minimum solvable scales, it is necessary that the filter width does not exceed the step of the difference grid [9−11].

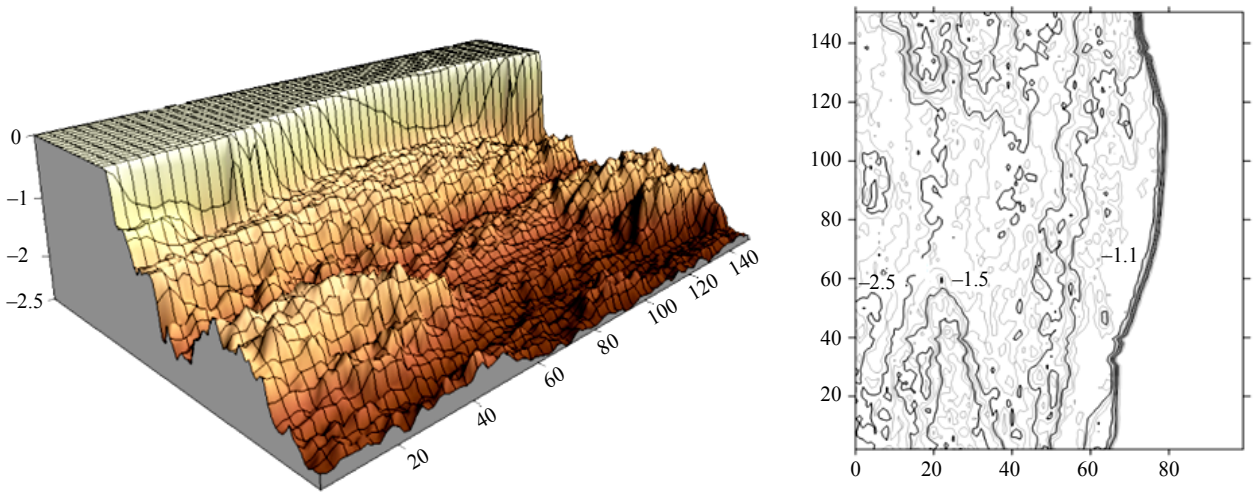

Fig. 2. Raster model of the computational domain

The initial data were obtained during the expedition in the Central-Eastern part of the Azov Sea and in the Taganrog Bay. The hydrophysical ADCP probe Workhorse Sentinel 600 was used to measure the three-dimensional velocity vector of the water medium. To process the instantaneous velocities of the water flow obtained during measurements, Gauss and Fourier filters were used at different filter widths. In these calculations, the filter scale was set based on the dimension of the hydrodynamics problem to be solved and the corresponding grid scale to this dimension.

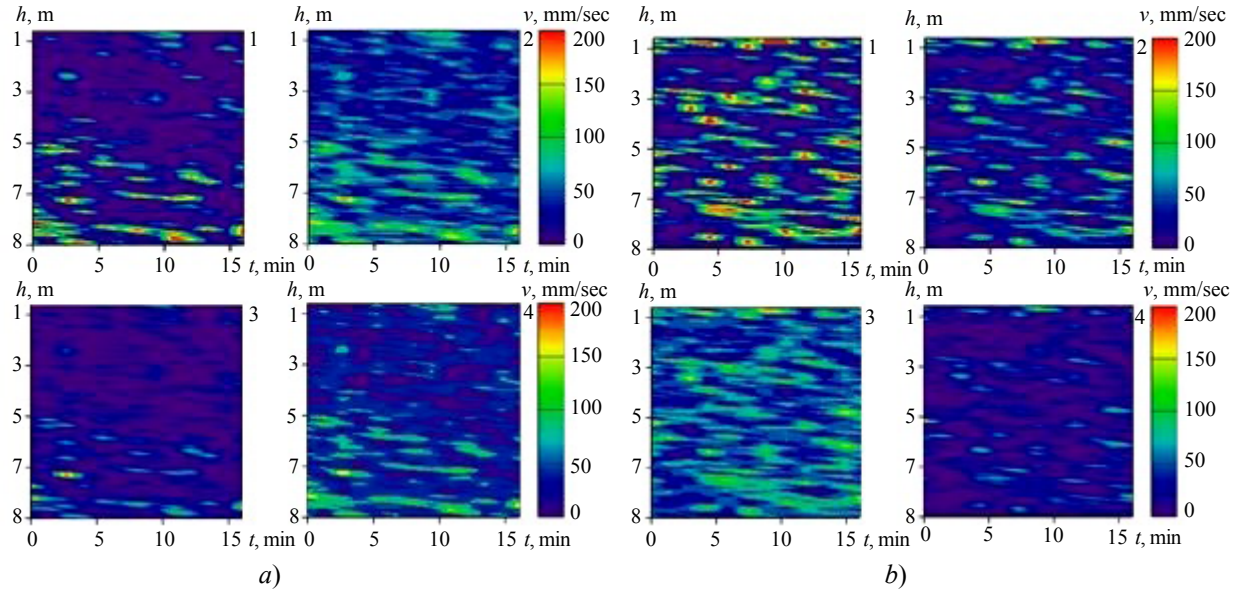

Fig. 3. Application of Gauss (a) and Fourier (b) filters: 1 — initial data, 2, 3, 4 — data obtained by filtering, with different filter widths: $\Delta_4 < \Delta_3 < \Delta_2$

Fig. 3 demonstrates the result of the software designed to eliminate the noise of expedition measurements, using the example of one of the components of the velocity vector of the water flow in the two-dimensional case. The color indicates the velocity of the water flow in mm/s in accordance with the given color scale.

Research results On the basis of numerical experiments, the distributions of the coefficients of vertical turbulent exchange are analyzed taking into account the influence of regular waves, as well as in their absence (Fig. 4); the separation of the wave flow into a near-surface macroturbulent layer caused by wave motion and a lower layer with background hydrodynamic turbulence is proved. A specific feature of the effect of regular waves on the turbulent exchange along the vertical was the increase in the coefficient of turbulent exchange in the near-surface layer and its decrease in the bottom layer compared with the distribution of coefficients obtained using the Smagorinsky parametrization.

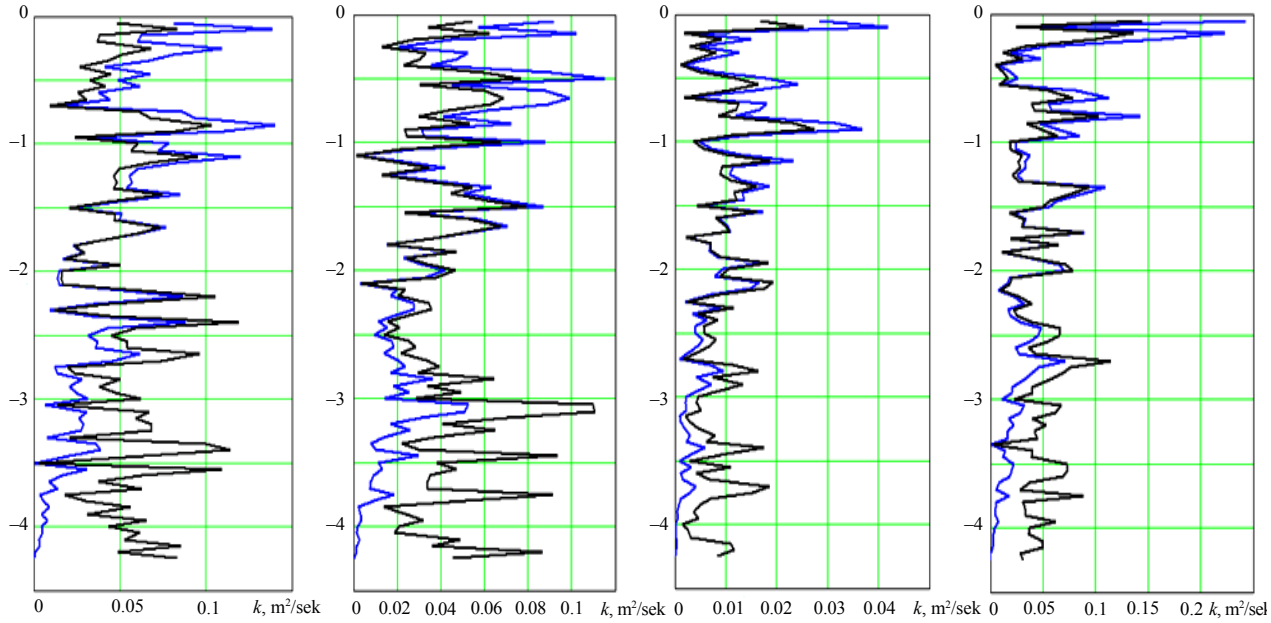

Fig. 4. Profiles of the vertical turbulent exchange coefficient (black line — excluding regular waves; blue — taking into account regular waves)

A wide range of variability of turbulent velocity pulsations is also demonstrated. The strength and intensity of turbulence changed synchronously with wave oscillations, showing a pronounced asymmetry of turbulence generation throughout the water column, including the near-surface layer, where waves amplified fluctuations in the flow velocity [12–14].

When waves break in the surf zone, turbulence can occur in several ways:

– due to fluid displacement;

– by separating the flow around the roughness elements;

– due to the injection of turbulent kinetic energy from breaking waves.

Turbulence begins to appear over a smooth seabed in the boundary layer flow when the Reynolds number (*Re*) is greater than 1.5×10^5 ($Re = Au/v$, where A is the orbital amplitude and v is the kinematic viscosity). The shift between the flow and the seabed creates microturbulent vortices such as vortex tubes and turbulent spots, which arise at the lower boundary and propagate upwards due to diffusion. The horizontal flow velocity and the turbulent kinetic energy (k) are more or less the same in phase, with k scaling with u^2. When the incoming waves are distorted, the maximum formation of k occurs under the crest of the wave.

Bottom shapes, such as wave sediments or megaripples, can appear outside and inside the surf zone, when sediments have moderate or high steepness, they often create flow separation and vortex dispersion. Turbulent vortices are formed on the leeward slope when the horizontal velocity is zero. In these coherent vortices, turbulence spreads upward due to convection, not due to diffusion. Experimental data and the Reynolds averaging method (RANS) have shown that vortex ejection increases k near the layer. For oblique, shallow waves, the generation of k is maximal when the flow reverses from the shore to the shelf.

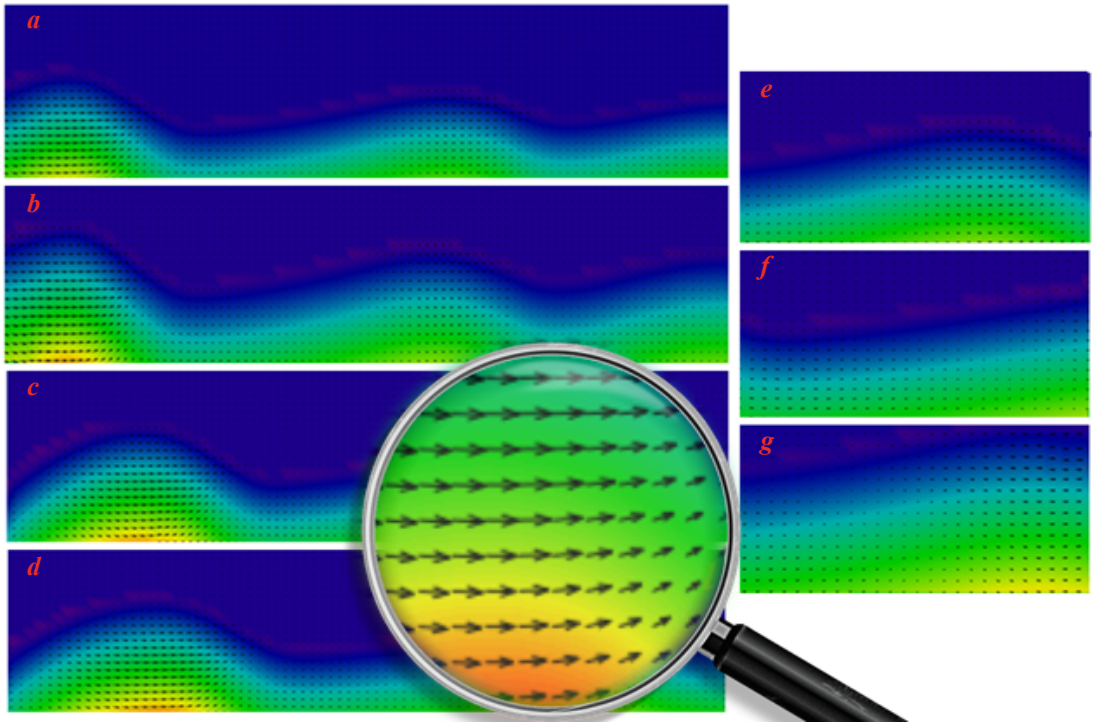

Fig. 5. Wave profiles and velocity vector fields at different time points, formation of vortex structures

The destruction of the wave is characterized by a sudden transition from a vortex-free flow to a rotational one, accompanied by a strong transformation of the wave energy into turbulence and, ultimately, into heat. Large-scale coherent vortices create strong vertical mixing, and turbulence created by surface destruction spreads downwards due to convection, however, a relatively small part of the wave energy is dissipated below the level of the trough, and most of it is between the crest of the wave and its trough. The relative height of the wave γ ($\gamma = H/h$, where H is the height of the wave, h is the depth of the water) Greek straight, Latin obliquely, higher too, did not notice is a useful parameter for characterizing or scaling the range of processes in the surf zone; for example, γ is used to predict the onset of wave destruction and the intensity of destruction. If the relative height of the wave is large enough ($\gamma > 0.4$), the turbulence of the breakers can penetrate into the boundary layer of the wave and collapse on the seabed (Fig. 5).

Although wave disruption is the main source of turbulence in the surf zone, this process is best described as stochastic. In an irregular wave field, some waves break, and some do not, so the formation (and scattering) of turbulence occurs with great frequency, and the instantaneous levels of k can be several orders of magnitude greater than the phase−averaged waves. There are different types of wave destruction, so the scale and intensity of turbulent vortices depend on the type of destruction.

When the breakers spill, turbulence spreads down to the seabed behind the crest of the wave. This process causes the appearance of obliquely descending vortices (ODES), which are pulled behind the crest of the wave. In this case, turbulence is created at the wave front and slowly spreads down to the bottom through descending vortices. Coherent turbulent structures collapse to the bottom at some distance behind the crest of the wave.

Sinking breakers create large vortices or downdraft that rotate around a horizontal axis parallel to the crest of the wave and generate vertical velocity fluctuations.

Discussion and conclusions. The paper presents the results of mathematical modeling of spatial-three-dimensional wave processes in shallow water bodies, taking into account the features of turbulent exchange. The initial conditions for the simulation were set based on the processing of remote sensing data. The process of filtering in-situ data has significantly reduced the spread of data and the amplitude of fluctuations. The separation of the wave flow into a near-surface macroturbulent layer caused by wave motion and a lower layer with background hydrodynamic turbulence is proved. A distinctive feature of the effect of regular waves on the turbulent exchange along the vertical is revealed.

References

1. Ferrer, M. A multi-region coupling scheme for compressible and incompressible flow solvers for 2-phase flow in a numerical wave tank / M. Ferrer // Computer & Fluids. — 2016. —Vol. 125. — P. 116–129.

2. Martínez-Ferrer, P. J. Improved numerical wave generation for modelling ocean and coastal engineering problems / P. J. Martínez-Ferrer, L. Qian, Z. Ma [et al.] // Ocean Engineering. — 2018. —Vol. 152. — P. 257–272.

3. John, M. H. Coastal-Trapped Waves Encyclopedia of Ocean Sciences / M. H. John // Academic Press. — 2019. — P. 598–605.

4. Numerical study on influences of breakwater layout on coastal waves, wave-induced currents, sediment transport and beach morphological evolution / J. Tang, Y. Lyu, Y. Shen [et al.] // Ocean Engineering. — 2017. — Vol. 141. — P. 375–387.

5. Experimental and numerical modelling of wave forces on coastal bridge superstructures with box girders / B. Huang, B. Zhu, S. Cui [et al.] // Ocean Engineering. — 2018. — Vol. 149. — P. 53–77.

6. Mathematical Model of Calculation of Coastal Wave Processes / A. I. Sukhinov, A. E. Chistyakov, E. F. Timofeeva, A. V. Shishenya // Mathematical Models and Computer Simulations. — 2013. — Vol. 5, no. 2. — P. 122–129.

7. Sukhinov, A. I. Mathematical Modeling of Sediment Transport in the Coastal Zone of Shallow Reservoirs / A. I. Sukhinov, A. E. Chistyakov, E. A. Protsenko // Mathematical Models and Computer Simulations. — 2014. — Vol. 6, no. 4. — P. 351–363.

8. Alekseenko, E. Nonlinear hydrodynamics in a mediterranean lagoon / E. Alekseenko, B. Roux and etc. // Nonlinear Processes in Geophysics. — 2013. — Vol. 20, no. 2. — P. 189–198.

9. Debolskaya, E. I. Vertical distribution of a pollutant in river flow: mathematical modeling / E. I. Debolskaya, E. N. Dolgopolova // Water Resources. — 2017. — Vol. 44, no. 5. — P. 731–737.

10. Optimal control of sustainable development in the biological rehabilitation of the Azov Sea / A. V. Nikitina, A. I. Sukhinov, G. A. Ugolnitsky, A. B. Usov // Mathematical Models and Computer Simulations. — 2017. — Vol. 9, no. 1. — P. 101–107.

11. Protsenko, S. Mathematical modeling of wave processes and transport of bottom materials in coastal water areas taking into account coastal structures / S. Protsenko, T. Sukhinova // MATEC Web of Conferences. — 2017. — Vol. 132. — 04002.

12. Buzalo, N. Mathematical modeling of microalgae-mineralization-human structure within the environment regeneration system for the biosphere compatible city / N. Buzalo, P. Ermachenko, T. Bock [et al.] // Procedia Engineering. — 2014. — Vol. 85. — P. 84–93.

13. Chorin, A. J. A numerical method for solving incompressible viscous flow problems / A. J. Chorin // Journal of Computational Physics. — 1967. — Vol. 2, no. 1. — P. 12–26.

14. Hirt, C. W. Volume of fluid (VOF) method for the dynamics of free boundaries / C. W. Hirt, B. D. Nichols // Journal of Computational Physics. — 1981. — Vol. 39, no. 1. — P. 201–225.

Received by the editorial office 07.02.2023.
Received after reviewing 27.02.2023.
Accepted for publication 28.02.2023.

About the Authors:

Protsenko, Elena A., PhD (Physical and Mathematical Sciences), Associate Professor of the Mathematics Department, Leading Researcher, Taganrog Institute named after A. P. Chekhov (branch) of RSUE (48, Initiative St., Taganrog, Rostov region, 347936, RF), ORCID, eapros@rambler.ru

Panasenko, Natalia D., Researcher, Taganrog Institute named after A. P. Chekhov (branch) of RSUE (48, Initiative St., Taganrog, Rostov region, 347936, RF), ORCID

Strashko, Alexander V., Researcher, Taganrog Institute named after A. P. Chekhov (branch) of RSUE, (48, Initiative St., Taganrog, Rostov region, 347936, RF), ORCID

Conflict of interest statement

The authors declare that there is no conflict of interest.

All authors have read and approved the final manuscript.

UDC 629.075, 519.5 *Original article*

https://doi.org/10.23947/2587-8999-2023-6-1-41-52

Correspondence to biophysical criteria of nonlinear effects in the occurrence of Feigenbaum bifurcation cascade in models of invasive processes

A. Yu. Perevaryukha

St. Petersburg Federal Research Center of the Russian Academy of Sciences, 39, 14-liniya St., St. Petersburg, Russian Federation

madelf@rambler.ru

Abstract

Introduction. The problem of creating a set of criteria for practically substantiated computational modeling of a number of complex staged biophysical processes with pronounced stages and critical transformations, for example, aggressive invasions, is discussed. Known models have a variety of behavior with the occurrence of bifurcations according to the same scenarios, the appearance of cycles, the coexistence of which is determined by Sharkovskii's theorem. In the limit of complication of cyclic behavior in such models, they often encounter chaotization of the trajectory, but with the existence of an infinite number of periodicity windows. The conditions for an infinite cascade of bifurcations for iterations are determined by the fulfillment of the conditions of Singer's theorem. The purpose of this work is to show that most of the nonlinear effects associated with chaotization scenarios do not have an ecological interpretation, but we will propose ways to exclude non-interpretable parametric ranges.

Materials and methods. Using methods for estimating the stability of stationary states and cyclic trajectories using Singer's theorem on the criterion for the occurrence of bifurcations for iterative models, we analyze interconnected nonlinear effects. The phenomena are considered on the example of cascades of the appearance of cycles of the period $p = 2^i + 1$, $i \to \infty$ and a cascade of cycles $p = 2^i - 1$, $i \to 0$ of "doubling" or "halfing" the period, which occur in ecological models often used to optimize fishing.

Results. It is confirmed that the coexistence of nonlinear effects turns out to be contradictory if the simulation results are interpreted in the field of biocybernetics, on the basis of model and real examples. Iterative models generate unnecessary non-linear modes of behavior, when predicting the dynamics of invasions or harvesting bioresources, taking into account the regulatory impact, for example, in the case of the well-known Feigenbaum scenario. It has been established that bifurcations connected in one scenario have no explanation in ecological reality and are not reflected in the observed biophysical systems. These mathematical artifacts are common to several biophysical models that are very different in their theoretical foundations. Chaotization in real population dynamics has somewhat different properties than can be obtained in a cascade of period doubling bifurcations. The formation of a non-attractive chaotic set in the form of a strange repeller is more consistent with the dynamics of the development of fast invasions.

Discussion and conclusions. It is shown that to describe the transformations of biosystemic processes with external influence, as the collapse of a commercial population, it is adequate to use models with the emergence of alternative attractors. These models correspond better to the transitions between the states of populations under the influence of fishing than models with the implementation of cascades of bifurcations of cycles, strange Cantor attractors and chaos regimes in the form of a continuum of unstable trajectories of all periods. The most promising are hybrid models of the life cycle with developmental stages for essential interpretation in ecology and forecasting of biosystems, as they allow to determine the parametric ranges of functioning and exclude unacceptable ranges of parameters where excessive non-linear effects occur, which have no justification for population processes. The analysis of the adequacy criteria is based on degradation scenarios for a complexly structured sturgeon population in the Volga basin, cod off the coast of Canada, outbreaks of invasive insects, and the spread of the invasive ctenophore Mnemiopsis leidy in the Caspian Sea.

Keywords: Dynamic models invasive processes; Feigenbaum bifurcation cascade; alternative attractors; complex dynamic processes, impact regulation for biosystems, hybrid computing systems, parametric ranges, theory of essential interpretation.

Acknowledgements. Gratitude towards Professor Alla Valeryevna Nikitina for friendly support.

Funding information. The work was carried out within the framework of the Russian Science Foundation Project No. 23-21-00339 “Development of methods for scenario modeling of extreme invasive processes in ecosystems, taking into account counteraction factors based on dynamically redefined computational structures”.

For citation. Perevaryukha, A. Yu. Correspondence to biophysical criteria of nonlinear effects in the occurrence of the Feigenbaum bifurcation cascade in models of invasive processes / A. Yu. Perevaryukha // Computational Mathematics and Information Technologies — 2023. — Vol. 6, no. 1. — P. 41–52. https://doi.org/10.23947/2587-8999-2023-6-1-41-52

Научная статья

Соответствие биофизическим критериям нелинейных эффектов при возникновении каскада бифуркаций Фейгенбаума в моделях инвазионных процессов

А. Ю. Переварюха

Санкт-Петербургский Федеральный исследовательский центр РАН, Российская Федерация, г. Санкт-Петербург, ул. 14-линия, 39

madelf@rambler.ru

Аннотация

Введение. Обсуждается проблема создания комплекса критериев для практически обоснованного вычислительного моделирования ряда сложных стадийных биофизических процессов с выраженной стадийностью и критическими трансформациями, например, агрессивных инвазий. Известные модели обладают разнообразным поведением с возникновением бифуркаций по одинаковым сценариям, появлением циклов, сосуществование которых определяется теоремой Шарковского. В пределе усложнения циклического поведения в таких моделях часто сталкиваются с хаотизацией траектории, но при существовании бесконечного числа окон периодичности. Условия бесконечного каскада бифуркаций для итераций определены выполнением условий теоремы Сингера. Цель работы — показать, что большинство связанных сценариями хаотизации нелинейных эффектов не имеют экологической интерпретации, но предполагаются способы исключения неинтерпретируемых параметрических диапазонов.

Материалы и методы. Методами оценки устойчивости стационарных состояний и циклических траекторий с применением теоремы Сингера о критерии возникновения бифуркаций для итерационных моделей анализируются связанные между собой нелинейные эффекты. Явления рассмотрены на примере каскадов появления циклов периода $p = 2^i + 1$, $i \to \infty$ и каскада циклов $p = 2^i - 1$, $i \to 0$ «удвоения» или «ополовинивания» периода, возникающих в часто применявшихся для оптимизации промысла экологических моделях.

Результаты исследования. На основе модельных и реальных примеров подтверждается, что сосуществование нелинейных эффектов оказывается противоречиво, если результаты моделирования интерпретируются в области биокибернетики. При прогнозировании динамики инвазий или промысла биоресурсов с учетом регулирующего воздействия итерационные модели генерируют ненужные нелинейные режимы поведения, например, в случае известного сценария Фейгенбаума. Установлено, что связанные в один сценарий бифуркации не имеют объяснений в экологической реальности и не отображаются в наблюдаемых биофизических системах. Данные математические артефакты общие для нескольких, очень разных по своим теоретическим основам, биофизическим моделям. Хаотизация в реальной популяционной динамике имеет несколько иные свойства, чем можно получить в каскаде бифуркаций удвоения периода. Более соответствует динамике развития быстрых инвазий образование непритягивающего хаотического множества в форме странного репеллера.

Обсуждение и заключения. Показано, что для описания трансформаций биосистемных процессов с внешним воздействием, как коллапса промысловой популяции, адекватно использовать модели с возникновением альтернативных аттракторов. Данные модели лучше соответствуют переходам между состояниями популяций под действием промысла, чем модели с реализацией каскадов бифуркаций циклов, странных канторовских аттракторов

и режимов хаоса в форме континуума неустойчивых траекторий всех периодов. Наиболее перспективны гибридные модели жизненного цикла со стадиями развития для сущностной интерпретации в экологии и прогнозирования биосистем, так как позволяют определять параметрические диапазоны функционирования, и исключать неприемлемые диапазоны параметров, где возникают избыточные нелинейные эффекты, которые не имеют обоснования для популяционных процессов. Анализ критериев адекватности базируется на сценариях деградации сложно структурированной популяции осетровых рыб бассейна Волги, трески у берегов Канады, вспышек численности инвазионных насекомых и распространению инвазивного гребневика *Mnemiopsis leidy* в Каспийском море.

Ключевые слова: динамические модели инвазий; каскад бифуркации Фейгенбаума; альтернативные аттракторы; сложные динамические процессы, регуляции воздействия для биосистем, гибридные вычислительные системы, параметрические диапазоны, теория сущностной интерпретации

Благодарности. Автор выражает благодарность профессору Алле Валерьевне Никитиной за дружескую поддержку.

Финансирование. Работа выполнена в рамках Проекта РНФ № 23-21-00339 «Разработка методов сценарного моделирования экстремальных инвазионных процессов в экосистемах с учетом факторов противодействия на основе динамически переопределяемых вычислительных структур».

Для цитирования. Переварюха, А. Ю. Соответствие биофизическим критериям нелинейных эффектов при возникновении каскада бифуркаций Фейгенбаума в моделях инвазионных процессов / А. Ю. Переварюха // Computational Mathematics and Information Technologies. — 2023. — Т. 6, № 1. — С. 41–52.
https://doi.org/10.23947/2587-8999-2023-6-1-41-52

Introduction. The method of organizing a basic model for analyzing the variability of scenarios, rapidly changing processes with threshold effects is consistently being developed for biological cybernetics problems [1]. Nonlinear effects can occur in a purely applied problem of forecasting the expected value of annual replenishment of populations considered from the point of view of the exploitation of biological resources. The basic computational models developed were aimed at analyzing the reproduction of the Caspian sevryuga after the overlap of spawning grounds. The models were implemented in the form of a system of equations describing the interrelated rates of population decline of the initial generation of individuals and the average growth rates of groups that form a new generation. Using auxiliary equations as a superstructure over the hybrid structure, the model managed to take into account the effect of a rapid increase in the growth rate of individuals and its further stop during the transition to maturation.

Forecasting the entry into the fishing stock of a new sequence of adjacent generations, which, according to various independent factors, may turn out to be significantly different in number, is the key task of conducting a careful fishing. The paper used a method for calculating the stages of development and adjusting the loss coefficients, which are used in the equation from the very first stage of life, where the number of the initial generation is assumed to be $N(0)$. This moment is interpreted as an event of the release of larvae of marine fish or crabs from eggs. The dynamics of a sequential decrease in the initial generation is described by a first-order differential equation, but with an overridable structure of the right part. To fix the redefinition of the calculation scheme, the event space is set on a closed time interval framed by event numbers $[0,T]$.

The phenomenon of reduction of daily loss occurs consistently at the stages of development. The structure of the basic model takes into account various key factors of mortality and a decrease in the rate of attrition during adulthood. The predicative-redefined hybrid structure of the model is written as follows:

$$\frac{dN}{dt} = \begin{cases} -(\alpha w(t)N(t) + U[x]\beta\ )N(t), \ t < \tau \\ -(\alpha_1 N(\tau)/w(\tau) + \beta\ )N(t), \ t > \tau, \quad w(t) < w_{D2}, \\ -\alpha_2 w(t)N^2(t)\ , \ w(t) < w_{D3}, \end{cases} \tag{1}$$

where, adjusted by stages of development, α is the density-determined mortality rate from depletion of vital resources; β is the coefficient of the ever-present loss from a variety of natural factors that are not related to density.

The concept of "reproductive potential" is considered abstract for ecological models of real fishing and artificial replenishment of stocks. There is reason to believe that it is reasonable to switch to a natural indicator of average fertility λ. This indicator can be estimated based on monitoring data, which was conducted on the basis of studies of fish spawning in the Volga and Don basin. Fertility will set the initial conditions for calculating the first form of the right part $N(0) = \lambda S$. The interval τ specified in (1) is the duration of the first stage with endogenous nutrition. This is an important interval for all anadromous fish. The model requires conditions for stopping calculations. An indicator is used as a conditional level of development. In the calculations of the model, when w_d is reached, the severity of mortality factors changes. The ecologically determined adjustment of parameters is interpreted by the change of habitats of juveniles in the river and the avoidance of predators during the already independent migration to the marine habitat.

The Sevryuga of the Caspian Sea was maintained artificially. When growing sturgeon fish in crowded ponds with high density (this is called the term "stocking"), instead of the value $w(\tau)$ in the denominator for the redefined form, the effect of a delay at the final stage of development was established $N(t-\zeta)$.

A dynamically redefined coefficient $U[x]$ plays an important role. The trigger, dynamically adjusted function is enabled in (1), but with a limited scope for its values. The idea of correcting the function in adjacent generations is a way to reflect the influence of extreme conditions. Often, in order to predict the success of reproduction or special states of biosystems, they encounter threshold transformations, as in the degradation scenario of a large predator population structured by spawning groups, the Kamchatka crab off the coast of the Kodiak Archipelago in the waters of Alaska.

The purpose of this article is to determine which nonlinear effects from all their diversity in the dynamics of the trajectories of biological models should be ignored when discussing the results of calculations, and which exclude descriptive possibilities when discussing environmental results. Based on the results obtained, it is possible to solve problems of adequate interpretation of the results of computational modeling of situations that arise during the development of invasive processes and collapses of biological resources. The task of modeling is to support the adoption of control decisions when regulating the impact on biosystems, for which an assessment of the state of biosystems is carried out, but where not all parameters are direct characteristics of species. The task of practical application of models is to find some narrow ranges of parameters that are not suitable for justifying decision-making.

Materials and methods. Based on the fact that the life cycle of the standard length of the organism of both fish and insects is accompanied by structural transformations, the hybrid structure presents a method for diversifying the life cycle according to a fixed set of stages and model equations for each stage.

In this study, an original version of a continuous-discrete model with a special time organization is used. The time of ontogenesis of a species is divided into frames and a hierarchy of nested continuous time segments is created, the ends of which will be discrete events of various types, which is important for analyzing the stages of species invasions.

A list of numbered events has been created within the general interval for the life cycle, where, depending on the type, an upper or lower index is used in the designation. The interval event-hybrid time divided into frames is formalized with a multiset of ordered elements combined into tuples, the number of which corresponds to generations:

$$\bigcup_n \left\{ \partial L_n, \left\{ \bigcup_i [t_0, t^i, t^{i+1}, T] \right\}_n, \partial R_n \right\},$$

where the lower indexes are the event numbers in a fixed interval of the total time interval, and the upper ones are the initial events of each frame.

B hybrid-event format, y model time with events, the number *n* indicates the frame number in the list of all generations. Recording time with event components leaves boundary slits excluded from the sequence of model frames, which have a service

purpose in numerical calculations. In modifications for invasive species in a new environment, it is advisable to specify time frames with floating boundaries that are set by growth functions.

The hybrid time model is designed to use an instrumental modeling environment with a library of numerical methods with varying integration steps. The principles of the model analysis will be the theory of the dynamics of iterations having extremes of functions with a Schwarzian of variable sign (according to the works of Singer and Sharkovsky).

In addition to using the hybrid model (1) to describe the situation of collapse of Kamchatka crab stocks, the hybrid structure was able to predict other complex stage biophysical processes — outbreaks of invasive species and the spread of new infections. A computational model has been constructed for a specific situation in the dynamics of dangerous invasive insects causing sawtooth outbreaks.

In the scenario under consideration, the rate of weight gain is indicated in inverse dependence on the average number of new generation individuals. However, it is not possible to use the inversely proportional method. For this purpose, a form of fractional dependence was chosen. This function is active until switching to active power. The increased decrease in this period of time appears due to an increase in the calorie requirement for larvae with low mobility. It should be noted that invasive species differ in their development features.

The model dynamics of the generation number for an invasive species $N(t)$ is calculated by equations combined into a system with an explicit trigger function in the interval of the event model time:

$$\begin{cases} \dfrac{dN}{dt} = -(\alpha w(t)N(t) + \Theta(S)\beta)N(t), \\ \dfrac{dw}{dt} = \dfrac{g}{\sqrt{N^k(t)} + \zeta}, \end{cases} \tag{2}$$

where S is the value of the spawning part of the fishing stock; $w(t)$ is the fixed value for the dimensional development of generation; g is the temporarily constant parameter that takes into account the limited number of available calories. ξ is the parameter that limits the rate of development regardless of $N(t)$; λ is the average fertility of the spawning part of the fishing stock, which determines the initial calculation conditions (1) as $w(0) = w_0$, $N(0) = \lambda S$; α and β are the instantaneous loss coefficients. Calculations are carried out for the time of ontogenesis, defined as the "vulnerability interval". This is a specific period of time for each species.

For aggressive invasive species, this interval depends on the environmental resistance conditions and the adaptation time of the biotic environment.

Numerically from (2) is the value of the spawning part of the commercial stock $S = N(T)$ with a small number of re-breeding individuals. Taking into account additional reproduction will lead to the formation of a vector from the components of spawning generations. Then you need to calculate the initial generation like this: $N(0) = \lambda_1 S_1 + ... + \lambda_i S_i$. For the task of modeling the invasion of insect pests, we will choose an alternative situational trigger action function: $\Theta(S) = 1 + \exp(-cS^2), \lim_{S\to\infty} \Theta(S) \to 1$. The purpose of this function is to reflect the effect of the known effect of the aggregated group, which is important for invasive processes. Alien dangerous pests that have penetrated into a new area generate a local outbreak when they pass the critical threshold of their abundance. Then high activity manifests itself in the form of repeated peaks [2]. A computational system is proposed for the model — a predicatively redefined hybrid structure of equations with a delay.

Biocybernetics develops methods of active intervention and suppression of invasive processes. Regulated resistance to an aggressively reproducing species in a biological community is produced with a delay. The situation leads to a sharp transition into the depression phase of the universe population. To stop the spread of a harmful invasive species, a special introduction of an antagonist species is carried out, but the effectiveness of this method of suppression in practice is unstable.

The model is investigated by presenting a computational scenario with a set of parameters, initial values and an algorithm for making decisions about the impact change for discrete time. Using computational experiments, it is possible to describe a real outcome scenario for a situation that leads to the collapse of the biophysical system at a controlled level of exposure. The model scenario in [3] sets the logic of managerial decision-making to change the level of external

pressure on the natural population. The simulation showed that the transition of the process to an oscillatory mode leads to the choice of a risky control mode. It was also found that the dynamics of real aquatic populations has a point of threshold reduction in the efficiency of replenishment of biological resources, which cannot be predicted based on statistical data.

Research results. The model scenario previously developed by the authors for the collapse of the Kamchatka crab of Alaska uses transformations of the phase portrait of iterations, and all of them were justified on graphs with data. In the presence of disconnected boundaries of the regions of attraction, alternative attractors and a strange chaotic repeller lead to the fact that due to chaotic regimes, uncertainty effects arise in the deterministic model.

As a result of the sequential numerical solution of the equations, a dynamic structure is determined, where the discrete component of the trajectory of a "hybrid" continuous-discrete model is studied in a computational environment as an iteration of a mapping with several extremes. Hybrid time models are designed for scenario research, taking into account the logic of making decisions regulating the impact on biosystems, which is used by experts. For the previously described behavior of the hybrid model trajectory in the form of transient randomization and changes in the boundaries of the attractor attraction areas, it was possible to choose an ecological interpretation using the example of collapses of three populations of Caspian sturgeon fish.

The properties of the described model scenario in [3] for exploited aquatic biological resources with a chaotic dynamic regime are confirmed by the author on the example of catching oceanic crustacean species. Iterative models obey the fundamental theorems of nonlinear dynamics, which is the essence of the problem of their application in the management of biosystems. It can be assumed that the nonlinear effect (bifurcation, attractor crisis or stochastic blurring for the separatrix) is hypothetically interesting for describing population processes. However, it cannot be excluded that the effect is accompanied by another metamorphosis of the phase portrait, for which it is impossible to find any biological explanation.

The methods of forecasting and assessing the state of the biosystem used by experts in the formation of the control effect require a separate analysis. In expert methods of ecology, the construction of regression models and the search for correlational relationships takes place on monitoring data. To construct dependence curves in the reproductive process of invasive species, which include values of R depending on the spawning stock S, transformations of the initial monitoring data and the construction of regression curves were proposed. In [5] to predict the dynamics of populations, the author proposed a function for evaluating the efficiency of reproduction:

$$f(S) = aS\exp(-bS). \tag{3}$$

(3) then logarithmed as follows:

$$\ln R - \ln S = \ln a - bS. \tag{4}$$

and built a curve using regression $\ln R / S$ on S for the geometric and arithmetic mean. The method cannot predict oscillations with a large amplitude, since the points would have to be grouped in a certain radius from the intersection with the bisector of the coordinate angle [6].

The motion of the trajectory points in time for a dynamic system in the dissipative case is represented by a motion in phase space to an attractor, a subset of the phase space $A \subseteq M$, invariant with respect to evolution: $\psi^{(t)}(A) = A$ for all $t \in T$. There is also a neighborhood U of the set A, in which for all $y \in U$ $\lim_{t\to\infty} \psi^{(t)}(y) = A$. is true. In the case of dynamic systems used, three topological varieties of attractors are distinguished [7].

A regular attractor for displaying the interval Ψ: $I \to I$ the state of equilibrium with the fixed point is considered x^*: $\lim_{t\to\infty} \psi^{(t)}(y) = x^*$ and a steady cycle. This mode of periodic self-oscillations can be considered expressed approximately by periodic fluctuations for biology, when the period can "float" in a certain range.

In discrete-continuous hybrid-type models, a series of tangent bifurcations is observed with the appearance of stable cycles of periods [8] $p \neq 2^i$ with sequential increase, starting from $a_1 = e^2$ In the event that the one-dimensional mapping $R_{j+1} = \psi(R_j)$ at the value of the control parameter $a = \lambda$ has a period cycle $p = 3$, then it is at the sam value of the

control parameter $a = \dot{a}$ has an infinite set of cycles of all other periods. A. N. Sharkovsky [9] proved that if the mapping $\Psi: I \to I$ has a cycle $p = n$, then $\Psi: I \to I$ also has cycles with all possible periods with the same value of the control parameters preceding the number $p = n \in \check{y}^{+}$ among the integers written out in a special order that completes the numbe 3 [10]. The cycle "three" found in the calculations means a periodic window among chaotic variants of dynamics. Hence, the appearance of a period 3 cycle is strange for a biological model.

In order to establish the properties necessary for the biological model, a functional iteration of the smoothness class C^2 the straight-line segment R^1 is selected, which is given by the function $f(x)$. This ecological function will be interpreted as a link between the spawning herd and the resulting replenishment. Let the fixed point of the display depend on the coefficients used in predicting the state of biological resources:

$$x^* = x^*(a, b), \text{ но } f'_x(x^*) = p(a), f'x \neq 0, \text{ если } x \neq c,\ f''(c) \neq 0.$$

In the above example, a differential invariant is defined for the dependence $f(x; x \neq c)$ everywhere, the sign of which is preserved for all iterations:

$$S_f = \frac{f'''(x)}{f'(x)} - \frac{3}{2}\left(\frac{f''(x)}{f'(x)}\right)^2.$$

In the case of function (1), the following properties exist:

$$\begin{aligned} f'(x) &= a\mathbf{e}^{-bx}(1-bx), \\ f''(x) &= ab\mathbf{e}^{-bx}(bx-2), \\ f'''(x) &= ab^2\mathbf{e}^{-bx}(3-bx). \end{aligned}$$

In general, the n-th derivative is expressed: $f^{(n)}(x) = a(-1)^n b^{n-1}\mathbf{e}^{-bx}(bx-n)$

The sign of the differential invariant for all iterations will look like this: $f(f(\ldots(x)\ldots)) \equiv f^n(x)$. Obviously, the property $S_f < 0$ is saved $x \in \Re$, since for $f(S) = aS\exp(-bS)$ the expression takes the form:

$$S_f = b^2\frac{-b^2x^2 + 4bx - 6}{2(1-bx)^2}$$

The position of the stationary point for function (1) depends on two parameters: $x^* = \ln a / b$, the stability criterion is a one–parameter function, and x^* loses stability:

$$f'(x^*) = -1, \text{ где критерии устойчивости}$$

$$f'(x^*) = a\mathbf{e}^{-b\frac{\ln a}{b}} - b\frac{\ln a}{b}a\mathbf{e}^{-b\frac{\ln a}{b}} = \frac{a(1-\ln a)}{\mathbf{e}^{\ln a}} = 1 - \ln a.$$

When $a = \mathbf{e}^2, f'(x^*) = -1$ for the second iteration $f^2(x)$ of the property at a stationary point losing stability x^*:

$$\frac{df^2(x^*)}{dx} = 1,$$

$$\frac{d^2f^2(x)}{dx^2} = \frac{df'(f(x))f'(x)}{dx} = f''(f(x))(f'(x))^2 + f'(f(x))f''(x),$$

$$\frac{d^2f^2(x^*)}{dx^2} = f'(x^*)f''(x^*)(f'(x^*)+1)) = 0.$$

In this case, the Schwarzman exponent y of the second iteration is always identical to the third derivative at this point:

$$S_{f^2(x^*)} = \frac{d^3f^2(x^*)}{dx^3}.$$

The cascade of bifurcations of doubling the cycle period with corresponding periodic windows is realized infinitely if the Schwarzian sign is $S_{f2} < 0$. Then $df^2(x)/dx$ at $a\mathbf{e}^2$ has the local maximum in x^* and only then a bifurcation occurs with the appearance of two new intersection points at the highest iteration. criterion for the realization of an infinite cascade of bifurcations, indicated by Mitchell Feigenbaum doubling the cycle period.

Chaotization through the Feigenbaum cascade is a consequence of the fundamental theorem from [11], where it is established that the mapping of the unimodal function with $S_f < 0$ can have no more than one stable trajectory, and this trajectory is the ω-limit set for the extremum $c: f'(c) = 0$. The problem is that for biosystems this cascade often occurs in models, but according to real data it is not justified.

The biocybernetics model (3), from a mathematical point of view, is classified as a SU-mapping. Model (1) differs from the objects studied by M. Feigenbaum and in other works on universality and renormalization theory by the presence of an inflection point $f''(x_s) = 0, x_s = 2/b$ and points where all the higher derivatives vanish. The property $\lim_{x\to\infty} f(x) \to 0$ for (1) means that the chaotic attractor can increase indefinitely, since there will be no "boundary crisis of the attractor" phenomenon.

Often in practice, a different reproduction function was used as an alternative model of the theory of the formation of generations of bioresources with the marginal biomass of the commercial reserve *K* and the degree of *b* denominators:

$$f(x) = \frac{ax}{1 + \left(\frac{x}{K}\right)^b}, \tag{5}$$

where $a > 1$ is interpreted as the reproductive potential, *K* is the value of the ecological niche and the limited limiting capacity of the medium. The degree of impact of environmental limitation on the part of the environment in (5) will be determined by *b*. The iteration of model (5) was analyzed from the point of view of the theory of bifurcations of maps on R^1. The equilibrium point for iterations (5) has the properties:

$$x^* = K\sqrt[b]{a-1},$$

$$\frac{df(x)}{dx} = \frac{(K^b + x^b)aK^b - ab(Kx)^b}{(K^b + x^b)^2},$$

$$\frac{df(x^*)}{dx} = \frac{a - ba + b}{a} > 0 \text{ when } b < 1.$$

In computational experiments based on the determination of the sign of Lyapunov exponents, the presence of chaotic properties for iterations (5) was established. In a limited range of values of parameter *a*, which can be applied to invasive populations, period doubling bifurcations occur when b changes. For $b < 1$, the function has no extremes, for $b = 2$, the function has a critical point $x = K$. The 2nd order derivative at the critical point:

$$\frac{d^2 f(x)}{dx^2} = -\frac{a}{4K},$$

So, (5) has a maximum under these conditions. In case (5), a parametric dependence is investigated for the analytical analysis of bifurcations with sufficiently flexible properties. It is possible to avoid a cascade, as well as additional nonlinear effects, internal crises of the chaotic attractor, windows of periodicity and intermittency. All these phenomena here can be carefully excluded from the modeling of biosystems, leaving only the necessary cycles.

Biophysical and commercial interpretation of nonlinear effects in these two models mutually exclude their adequacy. Having considered the change in the behavior of the model (3), we can formulate the hypothesis of "reproductive complexity". Allegedly, an increase in reproductive potential in the biosystem leads to the appearance of population fluctuations, which is expressed in the limit by fluctuations of an aperiodic nature. However, such fluctuations should have an increasing amplitude on average. Accordingly, the average minimum of chaotic fluctuations (the average value of the minimum point for the period) will tend to zero. For biosystems, this means degradation and destruction. In an alternative model, the emergence of a cascade of period cycles 2^n occurs with an increase in the degree of action of limiting environmental factors.

One of the two models will always be fundamentally inadequate. An alternative hypothesis of the essential biophysical interpretation is that the cascade of bifurcations (as well as a number of other complex nonlinear effects and the internal and boundary crisis of the chaotic attractor with the phenomenon of intermittency) for SU-maps has no biophysical interpretation.

Discussion and conclusions. It should be noted that for a number of models there are concomitant nonlinear effects that are undesirable and unnecessary for a number of reasons. Such effects are not confirmed in the analysis of observational data and they need to be excluded from the discussion.

Population cyclicity is an interesting, diverse and far from fully investigated biophysical phenomenon. Cyclicity is observed both in a laboratory aquarium with constant conditions, and in the open ocean (including climate-conditioned). The scientific problem of establishing the physical causes of long-period oscillations in many species is far from being resolved. Research in this area is continued by international teams. It is worth noting some not quite obvious aspects of the problem of describing cyclicity, interesting from the point of view of system analysis.

Population cycles (albeit not in the strictly periodic mathematical sense of a closed trajectory) can be short (weekly) in laboratory conditions. There are examples of long, even secular periods of fluctuations that do not correlate with the length of the life cycle of the species itself. Extreme, in terms of its consequences for forest ecosystems, the phenomenon occurs with the famous fluctuations in the number of the pest of the spruce leaflet *Choristoneura fumiferana* in the forests of North America from the Atlantic to the Pacific Ocean.

Since the phenomenon of population cycles in many species is well described, various mathematical methods and discrete and continuous models have been tried to model the cyclicity inherent in a number of natural populations. The possibility of obtaining cyclic behavior is evaluated for a simple model of the form $x_{n+1} = \psi(x_n; a)$ positively by many authors. However, the cycles that occur with an increase in parameter a differ not only in the period, but also in the order of traversing their constituent points, that is, the cycles of iterations with the same length (the number of points composing the cycle) period can be qualitatively different — this is one of the differences in the behavior of discrete models.

Figure 1 shows the cyclic trajectory $x_{n+1} = ax_n \exp(-bx_n)$, consisting of four points. In the calculation scenario, there were two other points of the cycle between the extreme upper and lower points of the cycle. The order of traversing the four cyclic points obtained in the computational experiment, when the trajectory passes from the upper branch to the lower one, is universal throughout the cascade. After doubling, the points appear symmetrically in the upper and lower branches until a sharp merger of all the "forked" branches of cyclic points into the Cantor attractor. The order of traversal of branches that form cyclic points is lost only with the formation of the Cantor structure after the unification of branches that were formed during the first doubling of the period.

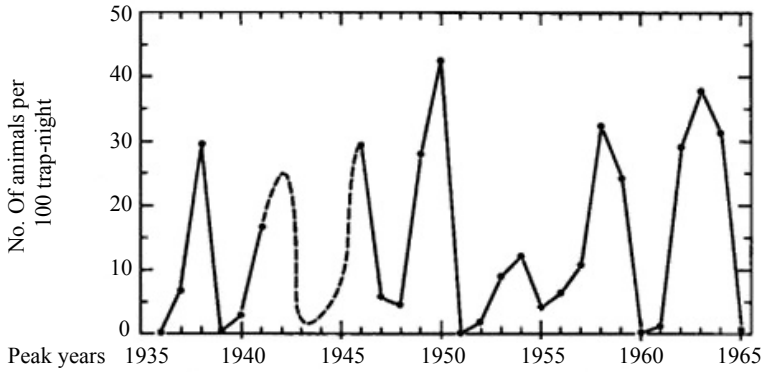

Fig. 1. Cyclical dynamics of the model (3) with a cycle period of "four" (generations (*S*) are indicated along the vertical axis, *t* — along the horizontal axis)

The establishment of the properties of the formation of cycles was perceived on the positive side of confirming the predictive capabilities of such models for populations with non-overlapping generations, and this opinion continues to be expressed, despite the proof of the universal nature of such bifurcations for unimodal functions.

Cyclic density changes are characteristic of small mammals of the Arctic islands and have often been observed in them, but the cycles do not persist and are easily destroyed by any external disturbance [12]. In addition to the length of the period p, iteration cycles $x_{n+1} = \psi(x_n)$ differ from each other by the relative location of their constituent points during traversal. Using a typical example of the dynamics of an Arctic rodent, we see that population cycles are monotonous permutations with increasing. The main peak in rodents falls at the end of the four-year period of rodent oscillations, and such cycles with a maximum at the end can be obtained in the order of the Sharkovsky theorem, but by other mathematical methods.

Using the example of longer cycles of steppe rodents in modern Kazakhstan, it is obvious that there is a stage of minimum abundance, a stage of rapid growth and peak, which is replaced by a prolonged depression with a minimal condition. For many insect pests, fading "sawtooth" series of population peaks are observed [13].

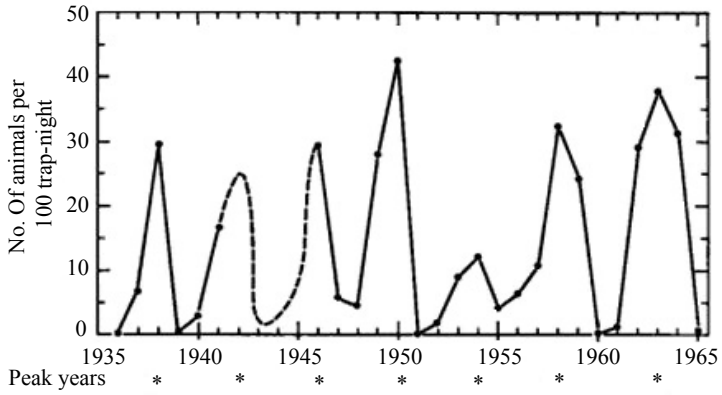

Fig. 2. Four-year cyclicity in the dynamics of the Arctic mammal population according to monitoring data [12]

A series of population outbreaks is also a form of cyclical changes, but such dynamics are not reflected by discrete iterative models. The series of oscillations were described on the basis of continuous models with a delay in operation [14].

Biophysical models in nature management that do not take into account the effect of an aggregated group (or the factor of the presence of a critically low community population) are practically beyond the scope of the possibility of interpreting the results of modeling in ecology. There are a number of other examples where the principles of ecology do not agree with the properties of the mathematical apparatus [15]. It is known that the more species there are in an ecosystem, the more stable it is [16], which means the ability to keep its state unchanged for a long time [17]. But with an increase in the dimension of the phase space of mathematical models, the possibility of trajectory behavior only becomes more complicated.

The tasks of regulating biophysical processes are only becoming more complicated due to unforeseen disturbances, therefore, the development of computational methods for analyzing the nonlinearity of situations with a description of the logic of the impact is relevant. Evolutionarily developed long-term modes of functioning of trophic chains, which include regular cycles of populations, are destroyed without maintaining species diversity [19]. Excessive exploitation of valuable populations violates the regulatory mechanisms that maintain the balance of the species ratio, which leads to the occupation of an ecological niche by harmful invaders and the spread of the invasive combworm Mnemiopsis leidy [20].

The relative position of the extremes of y functions, which are used to link the main values of the reproductive process relative to stationary points, is an important characteristic for dynamics, since it affects the nature of the boundaries of the attractor attraction areas and the occurrence of alternative cycles. For the found scenarios of transition to aperiodic dynamics and back to regular dynamics, a generalized strictly mathematical description has not yet been developed to explain the properties of the transition to chaos.

Optimization errors entail the phenomenon of structural collapse, which must be determined in a timely manner by characteristic features. Optimization for the economy of regions carries a risk, according to the theory of maximum supported withdrawal, implemented for an indefinite period of time in the practice of its application and for populations. The collapse of stocks means a long stop of fishing and depression of the economy. Regulated fishing leads to unexpected degradation of biological resources quite often. Mathematically, this is reflected by the case when an unstable equilibrium in the model is represented by a repeller point. In the ecological reality of invasive processes, this is a blurred area, not a point [21], as the result is the action of stochastic factors that cannot be taken into account directly.

The complexity of managing biosystems with the uncertainty of stochastic effects is that crisis situations are diverse in key features and are often caused by unforeseen factors of hydrology. Similar examples of models are shown in the studies of A.V. Nikitina [22] to analyze the effects of foreign invasive biota actively affecting the bottom biosystems of the Azov and Caspian Seas that have developed in long isolation [23] due to the construction of canals and active shipping.

References

1. Perevaryukha, A. Y. An iterative continuous-event model of the population outbreak of a phytophagous hemipteran/ A. Y. Perevaryukha // Biophysics. 2016. — Vol. 61, no. 2. — P. 334–341.

2. Robeva, R. The spruce budworm and forest: a qualitative comparison of ODE and Boolean models/ R. Robeva, D. Murrugarra // Letters in Biomathematics. 2016. — Vol. 3, Iss. 1. — P. 72–92.

3. Perevaryukha, A. Y. Hybrid model of the collapse of the commercial crab Paralithodes camtschaticus (Decapoda, Lithodidae) population of the kodiak archipelago / A. Y. Perevaryukha // Biophysics. — 2022. — V. 67, № 2. — P. 300–319.

4. Berezovskaya, F. S. Bifurcations of traveling waves in population models with taxis/ F. S. Berezovskaya, G. P. Karev // Successes of Physical Sciences. — 1999. — No. 9. — P. 1011–1025. (In Russ.)

5. Ricker, W. Stock and recruitment / W. Ricker // Journal Fisheries research board of Canada. — 1954. — No. 11. — C. 559–623.

6. Perevaryukha, A. Y. A model of development of a spontaneous outbreak of an insect with aperiodic dynamics/ A. Y. Perevaryukha // Entomological Review. — 2015. — Vol. 95, no. 3. — P. 397–405.

7. Guckenheimer, J. Sensitive dependence on initial conditions for one dimensional maps / J. Guckenheimer // Communications in Mathematical Physics. — 1979. — Vol. 70. — P. 133–160.

8. Feigenbaum M. J. Universal behavior in nonlinear systems / M. J. Feigenbaum // Physica D., 1983. — Vol. 7. — No. 1–3. — P. 16–39.

9. Sharkovskii, A. N. Coexistence cycles of continuous map of the line into itself / A. N. Sharkovskii // International Journal of Bifurcation & Chaos. — 1995. — Vol. 5. — P. 1263–1273.

10. Sharkovsky, A. N. On attracting and attracting sets/ A. N. Sharkovsky // Reports of the USSR Academy of Sciences. — 1965. — Vol. 160. — P. 1036–1038. (In Russ.)

11. Singer, D. Stable orbits and bifurcations of the maps on the interval / D. Singer // SIAM Journal of Applied Mathematics. — 1978. — No. 35. — P. 260–268.

12. Krebs, C. J. Population Cycles in Small Mammals/ C. J. Krebs // Advances in Ecological Research. — 1974. — Vol. 8. — P. 267–399

13. Royama, T. Analysis of spruce budworm outbreak cycles in New Brunswick, Canada, since 1952 / T. Royama, W. E. MacKinnon, E. G. Kettela, N. E. Carter, L. K. Hartling // Ecology. — 2005. — Vol. 86. — P. 1212–1224.

14. Perevaryukha, A. Y. A continuous model for oscillating outbreaks of the population of a phytophagous moth, the tent caterpillar, Malacosoma disstria (Lepidoptera, Lasiocampidae) / A. Y. Perevaryukha // Biophysics. — 2020. — Vol. 65, no. 1. — C. 118–130.

15. Courchamp, F. Allee Effects in Ecology and Conservation / F. Courchamp, B. Ludek, J. Gascoigne. — Oxford University Press : New York, 2008. — 266 p.

16. Bratus, A. S. Dynamical systems and models of biology/ A. S. Bratus, A. S. Novozhilov, A. P. Platonov. — Moscow : FIZMATLIT, 2010. — 400 p. (In Russ.)

17. Bazykin, A. D. Model of an ecosystem of three trophic levels taking into account the existence of a lower critical density of the producer population /A.D. Bazykin, E. A. Aponina // Problems of ecological monitoring and modeling of ecosystems. — 1981. — Vol. 4. — P. 186–203. (In Russ.)

18. Perevaryukha, A. Y. A continuous model of three scenarios of the infection process with delayed immune response factors / A. Y. Perevaryukha // Biophysics. — 2021. — Vol. 66, no. 2. — P. 327–348.

19. Veshchev, P. V. Efficiency of natural reproduction of sturgeons in the Lower Volga under current conditions / P. V. Veshchev, G. I. Guteneva // Russian Journal of Ecology. — 2012. — Vol. 43, no. 2. — P. 142–147

20. Perevaryukha, Y. N. Comparative immunochemical analysis of intraspecies distinctions of serum proteins of starred sturgeon Acipenser stellatus (Acipenseriformes, Acipenseridae) from the Caspian basin / Y. N. Perevaryukha, P. P. Geraskin, T. Y. Perevaryukha // Journal of Ichthyology. — 2011. — Vol. 51, no. 5. — P. 392–397.

21. Dubrovskaya, V. A. On validity criteria for the analysis of nonlinear effects in models of exploited populations / V. A. Dubrovskaya // Problems of mechanics and control: Nonlinear dynamic systems. — 2016. — No. 48. — P. 74–83. (In Russ.)

22. Nikitina, A.V. Modeling the dynamics of the number of fish populations in the waters of the Taganrog Bay / A.V. Nikitina // Proceedings of the Southern Federal University. Technical sciences. — 2009. — No. 7. — P. 169–173. (In Russ.)

23. Nikitina, A. V. Optimal control of sustainable development in the biological rehabilitation of the Azov Sea / A. V. Nikitina, A. I. Sukhinov, G. A. Ugolnitsky [et al.] // Mathematical Models and Computer Simulations. — 2017. — Vol. 9. — P. 101–107.

Received by the editorial office 10.02.2023.
Received after reviewing 02.03.2023.
Accepted for publication 03.03.2023.

About the Author:

Perevaryukha, Andrey Y., Ph.D. (Tech. Sci.), Senior Researcher at the Laboratory of Applied Informatics of St. Petersburg, FRS RAS (39, 14-line St., St. Petersburg), SPIN-code:6070-5310, SCOPUSId, ORCHID

The Author read and approved the final version of the manuscript.

UDC 519.63 *Original article*

https://doi.org/10.23947/2587-8999-2023-6-1-53-59

A family of inverse characteristics methods

I. B. Petrov ✉, D. I. Petrov

Moscow Institute of Physics and Technology (National Research University), 9, Institutsky Lane, Dolgoprudny, Moscow Region, Russian Federation

✉ petrov@mipt.ru

Abstract

Introduction. The main idea of the grid-characteristic method is to take into account the characteristic properties, systems of hyperbolic equations, and the finite velocity of propagation of perturbations in the simulated media.

Materials and methods. The simplest hyperbolic equation is a one-dimensional linear transfer equation. To increase the order of approximation of the grid-characteristic scheme to the second, you can use the Bim-Warming scheme. If we use a four-point pattern, we get a central Lax-Vendroff scheme. Difference schemes for the linear transfer equation can be obtained using the method of indefinite coefficients.

Results. The grid-characteristic scheme admits a conservative variant, which is relevant if there are discontinuities (shock waves, shock waves) inside the integration domain, while the original system of equations for a matrix with constant coefficients, in partial derivatives, should be presented in a divergent form.

Discussion and conclusions. The construction is performed similarly, when numerically solving a three-dimensional problem, in the case of upper and lower bounds, after scalar multiplication of the scheme by eigenvectors, relations approximating the compatibility conditions with the first order of accuracy are obtained.

Keywords: grid-characteristic method, hyperbolic type equations, transfer equation, Beam-Warming scheme, Lax-Wendroff scheme, method of indefinite coefficients, compatibility conditions.

Financing. The work was carried out within the framework of the Russian Science Foundation project No. 21-71-10015.

For citation. Petrov, I. B. Family of methods of inverse characteristics / I. B. Petrov, D. I. Petrov // Computational Mathematics and Information Technologies. — 2023. — Vol. 6, no. 1. — P. 53–69. https://doi.org/10.23947/2587-8999-2023-6-1-53-59

Научная статья

Семейство методов обратных характеристик

И. Б. Петров ✉, Д. И. Петров

Московский физико-технический институт (национальный исследовательский университет), Российская Федерация, Московская область, г. Долгопрудный, Институтский переулок, 9

✉ petrov@mipt.ru

Аннотация

Введение. Основной идеей сеточно-характеристического метода является учет характеристических свойств, систем уравнений гиперболического типа, конечной скорости распространения возмущений в моделируемой средах.

Материалы и методы. Простейшим уравнением гиперболического типа является одномерное линейное уравнение переноса. Для повышения порядка аппроксимации сеточно-характеристической схемы до второго, можно использовать схему Бима-Уорминга. Если использовать четырехточечный шаблон, то получим центральную схему Лакса-Вендроффа. Разностные схемы для линейного уравнения переноса можно получать, используя метод неопределенных коэффициентов.

Результаты исследования. Сеточно-характеристическая схема допускает консервативный вариант, актуальный, если внутри области интегрирования имеются разрывы (скачки уплотнения, ударные волны) при этом исходная система уравнений для матрицы с постоянными коэффициентами, в частных производных должна быть представлена в дивергентной форме.

Обсуждение и заключения. При численном решении трехмерной задачи построение производится аналогично, в случае верхней и нижней границ, после скалярного умножения схемы на собственные векторы получены соотношения аппроксимирующие с первым порядком точности условия совместимости.

Ключевые слова: сеточно-характеристический метод, уравнения гиперболического типа, уравнение переноса, схема Бима-Уорминга, схема Лакса-Вендроффа, метод неопределенных коэффициентов, условия совместимости.

Финансирование. Работа выполнена в рамках проекта Российского научного фонда № 21-71-10015.

Для цитирования. Петров, И. Б. Семейство методов обратных характеристик / И. Б. Петров, Д. И. Петров // Computational Mathematics and Information Technologies. — 2023. — Т. 6, № 1. — С. 53–69. https://doi.org/10.23947/2587-8999-2023-6-1-53-59

Introduction. The main idea of the grid-characteristic method is to take into account the characteristic properties, systems of hyperbolic equations, and the finite velocity of propagation of perturbations in the simulated media. Reviews of relevant works are given in monographs [1−4].

The simplest hyperbolic equation is a one-dimensional linear transfer equation:

$$\frac{\partial u}{\partial t} + a\frac{\partial u}{\partial x} = 0,\ a = \text{const},\ a > 0, \tag{1}$$

and the simplest difference scheme that takes into account the characteristic properties of (1) is the “corner” scheme, or the Courant-Izakson-Riess scheme:

$$u_m^{n+1} = (1-\sigma)u_m^n + \sigma u_{m-1}^n,\ \sigma = \frac{a\tau}{h}. \tag{2}$$

This scheme takes into account the direction of the characteristic of this equation and can be obtained by linear interpolation of the numerical solution from its known values at the nodes x_m, x_{m-1} calculation grid. This scheme can be represented in the following forms:

$$u_m^{n+1} = u_m^n - \sigma\begin{cases} u_{m+1}^n - u_m^n,\ a < 0, \\ u_m^n - u_{m-1}^n,\ a < 0, \end{cases}$$

(the difference is selected taking into account the slope of the characteristic):

$$u_m^{n+1} = u_m^n - \frac{\tau}{h}\left[a^+\left(u_{m+1}^n - u_m^n\right) + a^-\left(u_m^n - u_{m-1}^n\right)\right],$$

где $a^+ = 0{,}5(a+|a|)$, $a^- = 0{,}5(a-|a|)$; $u_m^{n+1} = u_m^n - \frac{\sigma}{2}\left(u_{m+1}^n - u_{m-1}^n\right) + \frac{|\sigma|}{2}\left(u_{m+1}^n - 2u_m^n + u_{m-1}^n\right)$

(a scheme with an explicit allocation of a dissipative term that ensures its stability):

$$u_m^{n+1} = u_m^n - \sigma\left(\Phi_{m+1/2}^n - \Phi_{m-1/2}^n\right),$$

where

$$\Phi_{m+1/2}^n = \frac{1}{2}\left[a\left(u_{m+1}^n - u_m^n\right) - |a|\left(u_{m+1}^n - u_m^n\right)\right]$$

(streaming form).

$$\Phi_{m-1/2}^n = \frac{1}{2}\left[a\left(u_m^n - u_{m-1}^n\right) - |a|\left(u_m^n - u_{m-1}^n\right)\right]$$

In the case of a nonlinear transfer equation:

$$\frac{\partial u}{\partial t} + \frac{\partial f}{\partial x} = 0,\ f = \frac{u^2}{2}, \tag{3}$$

the “corner” scheme, taking into account the directions of characteristics, can be presented in the following form:

$$u_m^{n+1} = u_m^n - \frac{\tau}{h}\begin{cases} f_{m+1}^n - f_m^n,\ u_m^n < 0 \\ f_m^n - f_{m-1}^n,\ u_m^n > 0. \end{cases}$$

The reduced difference scheme has the first order of approximation in time and coordinate. To increase the order of approximation of the grid-characteristic scheme to the second, you can use the Bim-Warming scheme, which can be obtained on a 4-point template $\{x_{m-2}^n, x_{m-1}^n, x_m^n\}$ by quadratic interpolation of the solution on the n-th time layer by nodes $x_{m-2}^n, x_{m-1}^n, x_m^n$:

$$u_m^{n+1} = u_m^n - \sigma\left(u_m^n - u_{m-1}^n\right) - \frac{\sigma}{2}(1-\sigma)\left(u_m^n - 2u_{m-1}^n + u_{m-2}^n\right). \tag{4}$$

If use four-point template $\left\{x_m^{n+1}, x_{m-1}^n, x_m^n, x_{m+1}^n\right\}$, can get a central Lax-Vendroff scheme:

$$u_m^{n+1} = u_m^n - \frac{\sigma}{2}\left(u_{m+1}^n - u_{m-1}^n\right) + \frac{\sigma^2}{2}\left(u_{m+1}^n - 2u_m^n + u_{m-1}^n\right). \tag{5}$$

This scheme, like the Bim-Warming scheme, has a second-order approximation in time and space O ($\tau^2 + h^2$), which is verified by decomposing grid functions $u_{m\pm1}^n$ into a Taylor series, and is stable when the Courant condition $\tau \le h/a$, is met, which can be obtained using the Neumann spectral stability feature. When adding a point x_{m-2}; to the template corresponding to the Lax-Wendroff scheme, we obtain a scheme of the 3rd order of approximation on a four-point template $\left\{x_m^{n+1}, x_{m-1}^n, x_m^n, x_{m+1}^n\right\}$:

$$\begin{aligned} u_m^{n+1} = u_m^n - \frac{\sigma}{6}\left(2u_{m+1}^n + 3u_m^n - 6u_{m-1}^n + u_{m-2}^n\right) + \frac{\sigma^2}{2}\left(u_{m+1}^n - 2u_m^n + u_{m-1}^n\right) - \\ - \frac{\sigma^3}{6}\left(u_{m+1}^n + 3u_{m-1}^n - 3u_m^n - u_{m-2}^n\right). \end{aligned} \tag{6}$$

To increase the order of accuracy of the scheme, we add a point x_{m+2} to the last template, the difference scheme of the 4th order of approximation will have the form:

$$\begin{aligned} u_m^{n+1} = u_m^n - \frac{\sigma}{12}\left(8u_{m+1}^n - 8u_{m-1}^n - u_{m+2}^n + u_{m-2}^n\right) + \frac{\sigma^2}{24}\left(16u_{m+1}^n - 30u_m^n + 16u_{m-1}^n - u_{m+2}^n - u_{m-2}^n\right) - \\ - \frac{\sigma^3}{12}\left(2u_{m-1}^n - 2u_{m+1}^n + u_{m+2}^n - u_{m-2}n\right) + \frac{\sigma^4}{24}\left(6u_m^n - 4u_{m+1}^n - 4u_{m-1}^n + u_{m+2}^n + u_{m-2}^n\right). \end{aligned} \tag{7}$$

If a linear acoustic system of equations of the form is considered

$$\begin{cases} \dfrac{\partial u}{\partial t} + \dfrac{1}{\rho}\cdot\dfrac{\partial p}{\partial x} = 0 \\ \dfrac{\partial p}{\partial t} + \rho c^2 \cdot \dfrac{\partial u}{\partial x} = 0, \end{cases} \tag{8}$$

where u, p is the local velocity of the medium and pressure, ρ is the density, c is the speed of sound, then, as noted in the second chapter, it can be reduced to the form:

$$\begin{cases} \dfrac{\partial r}{\partial t} + a\dfrac{\partial r}{\partial x} = 0 \\ \dfrac{\partial s}{\partial t} - a\dfrac{\partial s}{\partial x} = 0, \end{cases} \tag{9}$$

where $r = u + \dfrac{p}{\rho a}$, $s = u - \dfrac{p}{\rho a}$ — are Riemann invariants.

In this case, the grid-characteristic method can be presented in the following form:

$$\begin{cases} r_m^{n+1} = (1-\sigma)\cdot r_m^n + \sigma r_{m-1}^n \\ s_m^{n+1} = (1-\sigma)\cdot s_m^n + \sigma s_{m+1}^n. \end{cases} \tag{10}$$

The corresponding template has the form.

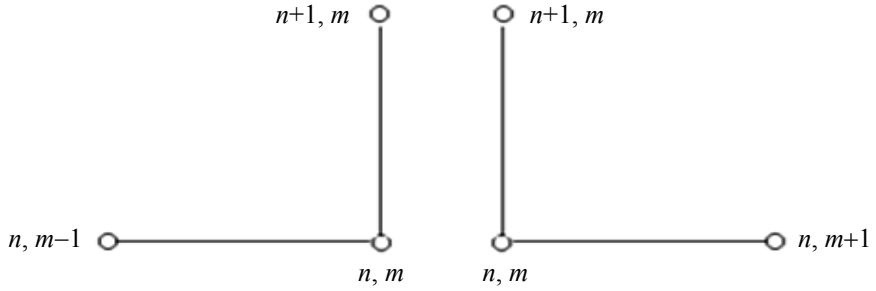

Fig. 1. Template of the grid-characteristic method for a linear acoustic system of equations

The given difference schemes can be obtained as follows.

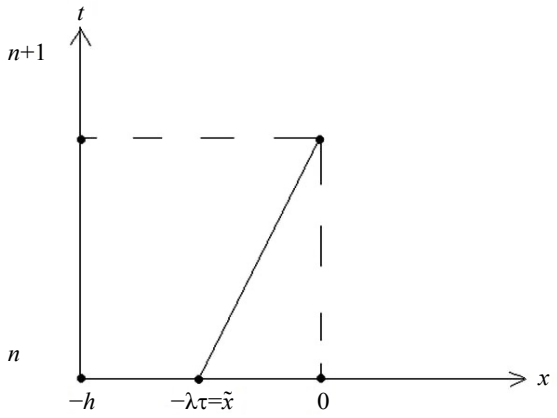

Fig. 2. Two-point template ($x_n = 0, x_m = -h$)

Figure 2 shows a two-point template ($x_n = 0, x_m = -h$), on which, in the case of a 1st-order scheme, a 1st-order polynomial is constructed $P_1(x)=a_1x + a_0$, whose coefficients are found from the conditions:

$$u_m^n = a_1 x_m + a_0,\ u_{m-1}^n = a_1 x_{m-1} + a_0:$$

$$a_1 = \left(u_m^n + u_{m-1}^n\right)/h,\quad a_0 = u_m^n.$$

Then get:

$$P(x) = \frac{u_m^n - u_{m-1}^n}{h}x + u_m^n.$$

Since $u_m^{n+1} = u(\tilde{x}) = u(-\lambda\tau)$, get the "left corner" scheme:

$$u_m^{n+1} = u_m^n - \sigma\left(u_m^n - u_{m-1}^n\right).$$

If add a point x_{m+1}^n, to this template, get a second-order polynomial: $P_2(x) = a_2x^2 + a_1x + a_0$, whose coefficients are in the same way (from the conditions for passing the polynomial $P(x)$ through the values of the function at the nodes of the template):

$$a_2 = \left(u_{m+1}^n - 2u_m^n + u_{m-1}^n\right)/2h^2,$$

$$a_1 = \left(u_{m+1}^n - u_{m-1}^n\right)/2h,$$

$$a_0 = u_m^n.$$

In this case, we get the Lax-Wendroff scheme. When adding a point x_{m-2} to this template, we get a third-order polynomial: $P_3(x) = a_3x^3 + a_2x^2 + a_1x + a_0$
with coefficients that are from the same conditions:

$$a_3 = \left(u_{m+1}^n + 3u_m^n - 3u_{m-1}^n - u_{m-2}^n\right)/6h^3,$$

$$a_2 = \left(u_{m+1}^n - 2u_m^n + u_{m-1}^n\right)/2h^2,$$

$$a_1 = \left(2u_{m+1}^n + 3u_m^n - 6u_{m-1}^n + u_{m-2}^n\right)/6h,$$

$$a_0 = u_m^n.$$

he Rusanov scheme of the third order of accuracy is obtained. If we add a point x_{m+2}, to the template, we get a polynomial of the fourth degree: $P_u(x) = a_4x^4 + a_3x^3 + a_2x^2 + a_1$
with coefficients:

$$a_4 = \left(6u_m^n - 4u_{m+1}^n - 4u_{m-1}^n + u_{m-2}^n\right)/24h^4,$$

$$a_3 = \left(2u_{m-1}^n - 2u_{m+1}^n + u_{m+2}^n + u_{m-2}^n\right)/12h^3,$$

$$a_2 = \left(16u_{m+1}^n - 30u_m^n + 16u_{m-1}^n - u_{m+2}^n - u_{m-2}^n\right)/24h^2,$$

$$a_1 = \left(8u_{m+1}^n - 8u_{m-1}^n - u_{m+2}^n + u_{m-2}^n\right)/12h,$$

$$a_0 = u_m^n,$$

and, accordingly, a scheme of the fourth order of approximation.

Difference schemes for the linear transfer equation can also be obtained using the method of indefinite coefficients. For example, on the template

$$\left\{\left(t^n, x_{m+1}\right), \left(t^n, x_m\right), \left(t^n, x_{m-1}\right), \left(t^n, x_{m-2}\right), \left(t^n, x_{m-2}\right)\right\}$$

can represent all linear schemes with undefined coefficients $\left\{\alpha_j^0; j = -2, -1, 0, 1\right\}$ in the following form:

$$u_m^{n+1} = \alpha_{-2}^0 u_{m-2}^n + \alpha_{-1}^0 u_{m-1}^n + \alpha_0^0 u_m^n + \alpha_1^0 u_{m+1}^n.$$

After decomposing the grid functions into a Taylor series:

$$u_m^{n+1} = u_m^n + \tau\left(u_t'\right)_m^n + \frac{\tau^2}{2}\left(u_t''\right)_m^n + \frac{\tau^3}{6}\left(u_t'''\right)_m^n + O'(\tau)^4,$$

$$u_{m+1}^n = u_m^n + h\left(u_x'\right)_m^n + \frac{h^2}{2}\left(u_x''\right)_m^n + \frac{h^3}{6}\left(u_t'''\right)_m^n + O'\left(h^4\right),$$

$$u_{m+1}^n = u_m^n + h\left(u_x'\right)_m^n + \frac{h^2}{2}\left(u_x''\right)_m^n + \frac{h^3}{6}\left(u_t'''\right)_m^n + O'\left(h^4\right),$$

$$u_{m-2}^n = u_m^n + 2h\left(u_x'\right)_m^n + 2h\left(u_{xx}''\right)_m^n - \frac{4h^3}{3}\left(u_x'''\right)_m^n + O'\left(h^4\right),$$

taking into account the consequences of the linear transfer equation:

$$u_t' = -\lambda u_x', \quad u_{tt}'' = \lambda^2 u_{xx}'', \quad u_t''' = -\lambda^3 u_x'',$$

$$u_{tx}'' = -\lambda u_{xx}, \quad u_{ttx}'' = \lambda^2 u_{xx}''', \quad u_{txx}''' = -\lambda u_x'''$$

and by equating the coefficients in the left and right sides of equation (10), we obtain the approximation conditions:

$$\begin{cases} \lambda_{-2}^0 + \lambda_{-1}^0 + \lambda_0^0 + \lambda_1^0 = 1, \\ 2\lambda_{-2}^0 + \lambda_{-1}^0 - \lambda_1^0 = \sigma, \end{cases} \tag{11}$$

for a first-order scheme:

$$\begin{cases} \lambda_{-2}^0 + \lambda_{-1}^0 + \lambda_0^0 + \lambda_1^0 = 1, \\ 2\lambda_{-2}^0 + \lambda_{-1}^0 - \lambda_1^0 = \sigma, \\ 4\lambda_{-2}^0 + \lambda_{-1}^0 + \lambda_1^0 = \sigma^2, \end{cases} \tag{12}$$

for a second-order scheme:

$$\begin{cases} \lambda_{-2}^0 + \lambda_{-1}^0 + \lambda_0^0 + \lambda_1^0 = 1, \\ 2\lambda_{-2}^0 + \lambda_{-1}^0 - \lambda_1^0 = \sigma, \\ 4\lambda_{-2}^0 + \lambda_{-1}^0 + \lambda_1^0 = \sigma^2, \\ 8\lambda_{-2}^0 + \lambda_{-1}^0 - \lambda_1^0 = \sigma^3, \end{cases} \tag{13}$$

for a fourth-order precision scheme.

If we find all the undefined coefficients from (13) and substitute them into (10), then we can find the first differential approximation of the scheme:

$$u_t' + \lambda u_x' = \frac{u_x^{IV}}{24}\lambda\left(\lambda^4\tau^3 + 2\lambda^2\tau h + \lambda^2 h^2 - 2h^3\right), \tag{14}$$

that is, on the considered template, it is possible to build difference schemes no higher than the third order of approximation: O (τ³ + *h*³).

In the case of a template of the general form of sets of difference schemes can be represented in the following form:

$$u_m^{n+1} = \sum \lambda_j^i(\sigma) u_{m+j}^{n+i}; \quad i = 1, 0, -1, \ldots; \; j = 0, \pm 1, \pm 2, \ldots \tag{15}$$

The conditions of approximation of the first order in this case can be written as:

$$\sum_{i,j} \alpha_j^i = 1, \quad \sum_{i,j} (j - i\sigma) \cdot \alpha_j^i(\sigma) = -\sigma.$$

The conditions of approximation of the second and higher orders will have the form:

$$\sum (j - i\sigma)^p \cdot \alpha_j^i = (-\sigma)^p;\ p = 2,3,...$$

So, for a 4-point template and a two-layer explicit difference scheme:

$$\left\{t^{n+1}, x_m; t^n, x_{m-2}; t^n; x_{m-1}; t^n; x_m; t^n; x_{m+1}\right\}$$

can represent the entire family of linear difference schemes with undefined coefficients

$$L_j^0, (j = -2,-1,0,1)$$

in the following form:

$$u_m^{n+1} = L_{-2}^0 \cdot u_{m-2}^n + L_{-1}^0 \cdot u_{m-1}^n + L_0^0 \cdot u_m^n + L_1^0 \cdot u_{m+1}^n. \quad (16)$$

The approximation conditions of the first, second and third order on the solutions of the problem are linear with respect to indefinite coefficients of equality:

$$\begin{cases} \alpha_{-2}^0 + \alpha_{-1}^0 + \alpha_0^0 + \alpha_1^0 = 1, \\ 2\alpha_{-2}^0 + \alpha_{-1}^0 - \alpha_1^0 = \sigma, \\ 4\alpha_{-2}^0 + \alpha_{-1}^0 + \alpha_1^0 = \sigma^2, \\ 8\alpha_{-2}^0 + \alpha_{-1}^0 - \alpha_1^0 = \sigma^3. \end{cases}$$

These conditions can be easily obtained if we decompose all the projection values of the exact solution of the problem when substituting into the Taylor series relative to any point of our grid pattern, for example, (t^n, x_m):

$$\begin{cases} u_m^{n+1} = u_m^n + \tau (u_t)_m^n + \frac{\tau^2}{2}(u_{tt})_m^n + \frac{\tau^3}{6}(u_{ttt})_m^n + O(\tau^4), \\ \alpha_1^0 u_{m+1}^n = \alpha_1^0 \left(u_m^n + h(u_x)_m^n + \frac{h^2}{2}(u_x)_m^n + \frac{h^3}{6}(u_{xxx})_m^n + O(h^4) \right), \\ \alpha_0^0 u_m^n = \alpha_0^0 u_m^n, \\ \alpha_{-1}^0 u_{m-1}^n = \alpha_{-1}^0 \left(u_m^n - h(u_x)_m^n + \frac{h^2}{2}(u_x)_m^n + \frac{h^3}{6}(u_{xxx})_m^n + O(h^4) \right). \\ \alpha_{-2}^0 u_{m-2}^n = \alpha_{-2}^0 \left(u_m^n - 2h(u_x)_m^n + 2h^2(u_x)_m^n - \frac{4h^3}{3}(u_{xxx})_m^n + O(h^4) \right) \end{cases}$$

The consequences of the equation should be used:

$$u_t = -\lambda u_t, u_{tt} = \lambda^2 u_{xx}, u_{tx} = -2\lambda u_{xx},$$

$$u_{ttt} = -\lambda^3 u_{xxx}, u_{ttx} = \lambda^2 u_{xxx}, u_{txx} = -\lambda u_{xxx}.$$

Using these expressions, you can get rid of partial derivatives in time by expressing them in terms of spatial derivatives:

$$u_m^{n+1} = u_m^n - \lambda\tau (u_x)_m^n + \frac{\lambda^2\tau^2}{2}(u_{xx})_m^n - \frac{\lambda^3\tau^3}{6}(u_{xxx})_m^n + O(\tau^4).$$

By equating the values u^n_m, $(u_x)^n_m$, $(u_{xx})^n_m$, $(u_{xxx})^n_m$ in the left and right parts, we obtain the approximation conditions.

In this case, $\alpha_{-2}^i = 0$ we get a difference Lax-Wendroff scheme $a\alpha_{-2}^i = \frac{\sigma}{2}(\sigma - 1)$, Bim-Warming scheme at $\alpha_{-2}^0 = \frac{\sigma}{6}(\sigma^2 - 1)$ and a third-order approximation scheme (Rusanov), the only one on the template under consideration.

Research results. Consider the case of a linear system of transfer equations of the form:

$$\frac{\partial u}{\partial t} + A\frac{\partial u}{\partial x} = 0, \quad (17)$$

where $A(n \times m)$ is a matrix with constant elements and real eigenvalues λ, i = 1,..., n. Then this matrix is represented as:

$$A = \Omega^{-1}\Lambda\Omega,$$

where Λ is a diagonal matrix consisting of eigenvalues: $\Lambda = \text{diag}\ \{\lambda_1\lambda_2, ..., \lambda_n\} = \text{diag}\{\lambda_i\}$; i =1, which are determined from the equation: det $(A - \lambda E) = 0$,

where E is a unit matrix; Ω is a matrix, whose rows are the left eigenvectors of the matrix A p to their length from a system of linear homogeneous equations

$$\omega_i \left(A - \lambda_i E\right) = 0;\ i = \ 1,...,n.$$

In this case (17) we write in the form:

$$\frac{\partial u}{\partial t} + \Omega^{-1}\Lambda\Omega \frac{\partial u}{\partial x} = 0,$$

then we multiply this system by Ω:

$$\Omega \frac{\partial u}{\partial t} + \Lambda\Omega \frac{\partial u}{\partial x} = 0. \tag{18}$$

By introducing the Riemann variables $w = \Omega u$ present the last equation as:

$$\frac{\partial w}{\partial t} + \Lambda \frac{\partial w}{\partial x} = 0, \tag{19}$$

from where it can be seen that the system decays into separate equations, the exact solutions of which are traveling waves:

$$w_i = w_i \left(x - \lambda_i t\right);\ i = 1,..,n.$$

The functions w_i are called Riemann invariants of the system (17); λ_i are the propagation velocities of perturbations in the medium. The general solution of the system of partial differential equations under consideration is the sum of n traveling waves, each of which propagates with its own characteristic velocity λ_i:

$$U = \sum_{i=1}^{n} b_i^2 w_i \left(x - \lambda_i t\right).$$

Note that if the vectors b_i are normalized, i.e. $| b_i | = 1$, the values w_i can be interpreted as the amplitudes of the corresponding traveling waves.

Let's represent (18) in scalar form:

$$\omega_i \frac{\partial u_i}{\partial t} + \lambda_i \omega_i \frac{\partial u_i}{\partial x} = 0,\ i = 1,..,n. \tag{20}$$

Next, we introduce a difference grid in the integration domain $\{t \ge 0, 0 \le x \le X\}$ the difference grid

$$\left\{t^n = n\tau; n = 0,1,...; x_i = \left(m-1\right)h; m = 1,..,M; X = \left(M-1\right)h\right\}$$

and carry out the approximation (20) using finite difference relations taking into account the slope of the characteristics:

$$\frac{\partial x}{\partial t} = \lambda_i$$

(or taking into account the sign λ_i):

$$\omega_i \frac{u_m^{n+1} - u_m^n}{\tau} \mp \lambda_i \omega_i \frac{u_{m\mp1}^n - u_m^n}{h} + \omega_i f = 0,\ i = \ 1,...,n. \tag{21}$$

The latter relation can be represented in matrix form if put:

$$|\Lambda| = \left\{|\lambda_i|\right\},\ \Lambda^+ = \frac{1}{2}\left(\Lambda + |\Lambda|\right),\ \Lambda^- = \frac{1}{2}\left(\Lambda - |\Lambda|\right): \tag{22}$$

$$\Omega\left(u_m^{n+1} - u_m^n\right) - \sigma\Lambda^+\Omega\left(u_{m-1}^n - u_m^n\right) + \sigma\Lambda^-\Omega\left(u_{m+1}^n - u_m^n\right) + \tau\Omega f = 0.$$

Since the matrix Ω is not degenerate, the resulting difference scheme can be represented as follows:

$$u_m^{n+1} = u_m^n - \sigma A\left(u_{m+1/2}^n - u_{m-1/2}^n\right) - \tau f + \frac{\sigma}{2}\Omega^{-1}|\Lambda|\Omega\left(u_{m-1}^n - 2u_m^n + u_{m+1}^n\right), \tag{23}$$

$$u_{m\pm1/2}^n = \frac{1}{2}\left(u_{m\pm1}^n + u_m^n\right).$$

In this scheme, the summand is clearly highlighted:

$$\frac{\sigma}{2}\Omega^{-1}|\Lambda|\Omega\left(u_{m-1}^n - 2u_m^n + u_{m+1}^n\right),$$

which ensures its stability when the CFL condition (Courant — Friedrichs— Levy) is met:

$$\sigma \le \frac{1}{\max|\lambda_i|}.$$

An additional "dissipative" term is introduced into the initial system, which ensures the monotony of the obtained scheme of the first order of approximation, but is also a non-physical source having a difference origin (approximation viscosity).

This difference scheme, when generalized to the multidimensional case, belongs to the class of Friedrichs positive-definite schemes, as can be seen from the following representation of it:

$$u_m^{n+1} = \left(E - \sigma\Omega^{-1}\left|\Lambda\right|\Omega\right)u_m^n + \sigma\Omega^{-1}\Lambda^{+}\Omega u_{m-1}^n - \sigma\Omega^{-1}\Lambda u_{m-1}^n - \tau f.$$

The numerical method under consideration can also be presented in the following form:

$$u_m^{n+1} = u_m^n - \sigma\left(\Omega^{-1}\Lambda\Omega\right)\Delta u + \sigma^{\beta}\left(\Omega^{-1}\left|\Lambda\right|^{\beta}\Omega\right)\Delta^2 u,$$

where

$$\Delta u = \frac{1}{2}\left(u_m^{n+1} - u_{m-1}^n\right)/2;\ \Delta^2 u = \frac{1}{2}\left(u_{m+1}^n - 2u_m^n + u_{m-1}^n\right).$$

This scheme has the first order of approximation at $\beta = 1$ and the second at $\beta = 2$.

Let's imagine this scheme as a scheme with a weighting factor α ($0 \le \alpha \le 1$):

$$u_m^{n+1} = u_m^n - \sigma\left(\Omega^{-1}\Lambda\Omega\right)\Delta u + 2\sigma\left(\Omega^{-1}\left|\Lambda\right|^{\beta}\Omega\right)\Delta^2 u + \left(1-\alpha\right)\sigma^2\left(\Omega^{-1}\Lambda\Omega\right)\Delta^2 u.$$

At $\alpha = 1$ get a scheme of the first order of approximation, at $\alpha = 0$ — the second. At $0 < \alpha < 1$ obtain a scheme having a formal first order, but with proper choice of value α, it will improve the description of numerical solutions with large gradients by reducing the approximation of viscosity [7].

The grid-characteristic scheme also admits a conservative variant, relevant if there are discontinuities (shock waves, shock waves) inside the integration domain, while the original system of equations for a matrix with constant coefficients, in partial derivatives, should be presented in a divergent form:

$$\frac{\partial u}{\partial t} + \Lambda\frac{\partial \Phi}{\partial x} = \frac{\partial u}{\partial t} + \frac{\partial u}{\partial x}\left(Au\right) = \frac{\partial u}{\partial t} + A\frac{\partial u}{\partial x} = 0, \tag{24}$$

where $A = \dfrac{\partial \Phi}{\partial u};\ \Phi = Au;$ since the system in question is hyperbolic, then: $A = \Omega^{-1}\Lambda\Omega$.

In this case, the difference scheme, which has the property of conservativeness, i.e. ensuring the implementation of conservation laws, can be presented in the following form:

$$u_m^{n+1} = u_m^n - \sigma\left(\Phi_{m+1/2}^n - \Phi_{m-1/2}^n\right) + \sigma\left[D_{m+1/2}\left(u_{m+1}^n - u_m^n\right)/h - D_{m-1/2}\left(u_m^n - u_{m-2}^n\right)/h\right], \tag{25}$$

where $\Phi_{m\pm1/2}^n = \dfrac{1}{2}\left(\Phi_{m\pm1}^n + \Phi_m^n\right)$.

It is clear that in the resulting difference scheme, in addition to physical flows through the cell boundaries there are also flows of difference origin:

$$Du''_{xx}, \text{where } D = \frac{h}{2}\Omega^{-1}\left|\Lambda\right|\Omega.$$

However, for neighboring cells on their common border, they are equal and opposite in sign: therefore, in general, inside the integration area, the scheme is conservative, which is checked by their addition over the entire area.

Note that among the schemes of the first order of approximation, this scheme has a minimum approximation viscosity. In the case of three independent variables $\{t, x, y\}$ conservative and non-conservative schemes will have, respectively, the following form:

$$\begin{aligned}
u_{ml}^{n+1} &= u_{ml}^n - \frac{\tau}{h_1}\left(\Phi_{m\pm1/2,l}^n - \Phi_{m-1/2,l}^n\right) - \frac{\tau}{h_2}\left(G_{m,l+1/2}^n - G_{m,l-1/2}^n\right) - \frac{\tau}{h_1}\cdot \\
&\cdot\left[D_{m+1/2,l}^1\left(u_{m+1,l}^n - u_{ml}^n\right)/h_1 - D_{m-1/2,l}^1\left(u_{ml}^n - u_{m-1,l}^n\right)/h_1\right] + \\
&+ \frac{\tau}{h_2}\left[D_{m,l+1/2}^2\left(u_{m,l+1}^n - u_{ml}^n\right)/h_2 - D_{m,l-1/2}^2\left(u_{m,l}^n - u_{m,l-1}^n\right)/h\right], \\
u_{m,l}^{n+1} &= u_{m,l}^n + \frac{\tau}{h_1}\left[\Omega_1^{-1}\Lambda_1^{+}\Omega_1\left(u_{m-1,l}^n - u_{ml}^n\right) - \Omega_1^{-1}\Lambda_1^{-}\Omega_1\left(u_{m+1,l}^n - u_{ml}^n\right)\right] + \\
&+ \frac{\tau}{h_2}\left[\Omega_2^{-1}\Lambda_2^{+}\Omega_2\left(u_{m,l-1}^n - u_{ml}^n\right) - \Omega_2^{-1}\Lambda_2^{-}\Omega_2\left(u_{m,l+1}^n - u_{ml}^n\right)\right],
\end{aligned} \tag{26}$$

where $D^k = \frac{h_k}{2}\Omega_k^{-1}|\Lambda_k|\Omega_k;\ k=1,2;$

the matrices Λ_k, $\Lambda^{\pm}_k$, Ω_k, as in the one-dimensional case, consist of eigenvalues and eigenvectors of matrices A_k; in the integration domain $\{t \ge 0;\ x \le x \le X,\ 0 \le y \le Y\}$ difference grid is introduced:

$$\left\{t^n = n\tau,\ n=0,1,...;\ x_n = (m-1)h_1;\ m=1,...,M;\ y_e = (l-1)h_1; l=1,..,L;\ X=(M-1)h_1,\ Y=(L-1)h_2\right\}.$$

Difference schemes for three variables are constructed similarly.

Let's return to the relation (18), which can be represented in scalar form:

$$\omega_i \frac{\partial u}{\partial t} + \lambda_i \omega_i \frac{\partial u}{\partial x} = \omega_i \left(\frac{\partial u}{\partial t} + \lambda_i \frac{\partial u}{\partial x} \right) = 0,\ i=1,..,n, \tag{27}$$

where each component of the vector:

$$\frac{\partial u}{\partial t} + \lambda_i \frac{\partial u}{\partial x} \tag{28}$$

is the transfer equation for the corresponding component of the vector u:

$$\frac{\partial u_j}{\partial t} + \lambda_i \frac{\partial u_j}{\partial x} = 0;\ j=1,..,n.$$

moreover, for each of these equations, it is possible to construct an already known scheme:

$$u_{j,m}^{n+1} = \sum_{\mu,\nu} \alpha_\mu^\gamma(\tau, h, \lambda_i) u_{j,m+\mu}^{n+\gamma} = \sum_{\mu,\nu} \alpha_\mu^\gamma(\sigma_i) u_{j,m+\mu}^{n+\gamma}. \tag{29}$$

Next, we replace the vector (28) with its difference approximation:

$$\omega_i \left(\frac{\partial u}{\partial t} + \lambda_i \frac{\partial u}{\partial x} \right) = \left[\omega_i u_m^{n+1} - \sum_{\mu,\nu} \alpha_\mu^\nu(\sigma_i) \omega_i u_{m+\mu}^{n+\gamma} \right],\ i=1,..,n, \tag{30}$$

and note that each equation in (30) is the i-th component of the vector:

so

$$\Omega \frac{\partial u}{\partial t} + \Lambda\Omega \frac{\partial u}{\partial x} = 0;$$

$$\Omega \frac{\partial u}{\partial t} + \Lambda\Omega \frac{\partial u}{\partial x} = \begin{cases} \omega_i u_m^{n+1} - \sum_{\mu,\nu} \alpha_\mu^\nu(\sigma_1)\omega_i \cdot u_{m+\mu}^{n+\gamma} \\ ---------- \\ \omega_n u_m^{n+1} - \sum \alpha_\mu^\gamma(\sigma_n)\omega_n \cdot u_{m+\mu}^{n+\gamma} \end{cases}. \tag{31}$$

Multiplying the obtained ratio by the matrix Ω^{-1}, obtain a general view of the difference scheme for the numerical solution of a system of hyperbolic equations (17):

$$u_m^{n+1} = \sum_{\mu,\gamma} \Omega^{-1} B_\mu^\gamma \Omega u_{m+\mu}^{n+\gamma}, \tag{32}$$

where $B_\mu^\gamma = \mathrm{diag}\left\{\alpha_\mu^\gamma(\sigma_i)\right\}$ is a diagonal matrix with components that are coefficients α_μ^γ, defining a specific type of scheme.

For example, in the case of considering a difference grid-characteristic scheme earlier, we obtain (see (22), (23), (24)):

$$u_m^{n+1} = \left(\Omega^{-1} E \Omega\right) u_m^n + \frac{\sigma}{2}\left(\Omega^{-1}\Lambda^+\Omega\right)\left(u_{m-1}^n - u_m^n\right) - \sigma\left(\Omega^{-1}\Lambda^+\Omega\right)\left(u_{m+1}^n - u_m^n\right); \tag{33}$$

or, in another form:

For the Lax-Wendroff scheme (5) obtained earlier for the scalar equation, have:

$$u_m^{n+1} = u_m^n + \frac{\sigma}{2}\left(\Phi_{m-1}^n - \Phi_{m+1}^n\right) + \frac{\sigma^2}{2}\left(\Omega^{-1}|\Lambda|\Omega\right)\left(u_{m-1}^n - 2u_m^n + u_{m+1}^n\right). \tag{34}$$

Grid-characteristic parametric schemes of higher approximation orders can be presented in the following form:

$$u_m^{n+1} = u_m^n + \frac{\sigma}{2}\left(\Phi_{m-1}^n - \Phi_{m+1}^n\right) + \frac{\sigma^2}{2}\left(\Omega^{-1}\Lambda^2\Omega\right)\left(u_{m-1}^n - 2u_m^n + u_{m+1}^n\right) +$$

$$+ \frac{\sigma}{2}\left(\Omega^{-1} G \Lambda \Omega\right)\left(u_{m-2}^n - 2u_{m-1}^n + u_{m+1}^n - u_{m+2}^n\right) + \frac{\sigma}{2}\left(\Omega^{-1} G |\Lambda| \Omega\right)\left(u_{m-2}^n - 4u_{m-1}^n + 6u_{m+1}^n + u_{m+2}^n\right), \tag{35}$$

where $G = \mathrm{diag}\ \{g_1(\sigma_1)\}$, $i = 1, ..., n$ is a diagonal parametric matrix.

This scheme can also be represented as a "predictor-corrector" scheme:

$$\tilde{u}_m^n = u_m^n + \frac{\sigma}{2}\left(\Phi_{m-1}^n - \Phi_{m+1}^n\right) + \frac{\sigma}{2}\left(\Omega^{-1}|\Lambda|\Omega\right)\left(u_{m-1}^n - 2u_m^n + u_{m+1}^n\right),$$

$$u_m^{n+1} = u_m^n + \Omega^{-1}\left(\frac{\sigma^2}{2}\Lambda^2 - \frac{\sigma}{2}|\Lambda|\right)\Omega\left(u_{m-1}^n - 2u_m^n + u_{m+1}^n\right) +$$

$$+ \Omega^{-1} G\Omega\left[\left(\tilde{u}_m^n - 2\tilde{u}_m^n + \tilde{u}_{m-1}^n\right) - \left(u_{m-1}^n - 2u_m^n + u_{m+1}^n\right)\right].$$

So, at

$$g_i = \frac{\sigma_i^2 - 1}{6}$$

get a scheme of the 3rd order of accuracy (analogous to the Rusanov scheme).

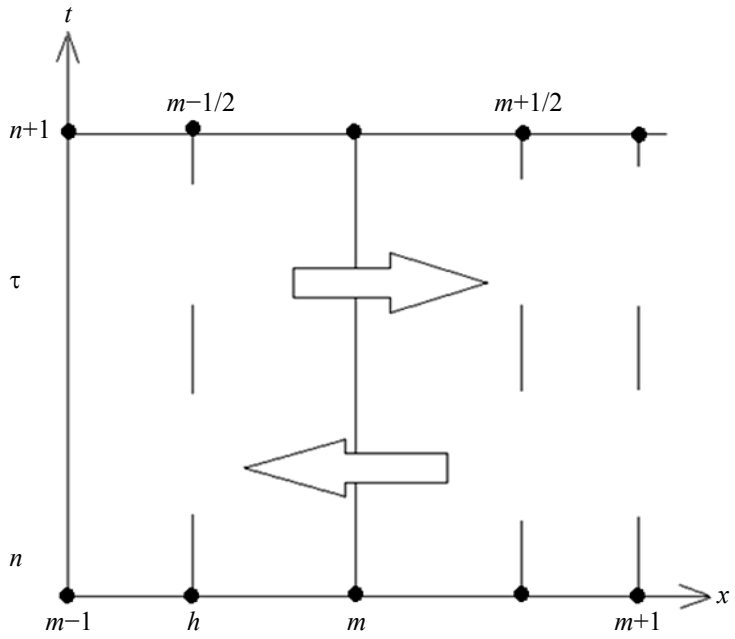

Fig. 2. Predictor-corrector scheme

The grid-characteristic method can also be represented as a flow method, or as an integro-interpolation method, if equation (23) is written in integral form:

$$\iint_s \left(\frac{\partial u}{\partial t} + \frac{\partial \Phi}{\partial x}\right) dt \cdot dx = \int_\Gamma \left(u dx - \Phi dt\right) = 0, \tag{36}$$

and then the last integral will be approximated:

$$\int_{x-1/2}^{x+1/2} u^{n+1} dx + \int_{t_n}^{t_{n+1}} \Phi_{m+1/2}^{n+1/2} dt - \int_{x_{m-1/2}}^{x_{m+1/2}} u^n dx - \int_{t_n}^{t_{m+1}} \Phi_{m-1/2dt}^{n+1/2} = 0.$$

It follows from the last equality, if the approximation of integrals is carried out by the method of averages, get:

$$u_m^{n+1} h - \Phi_{m+1/2}^{n+1/2} - u_m^n h - \Phi_{m-1/2}^{n+1/2} \tau = 0 \tag{37}$$

(integro-interpolation method),
or:

$$u_m^{n+1} = u_m^n - \sigma\left(\Phi_{m+1/2}^{n+1/2} - \Phi_{m-1/2}^{n+1/2}\right) \tag{38}$$

(flow method).

Note that in the foreign literature these methods are called finite volume methods. It is clear that (40) is a family of numerical methods whose properties depend on the method of calculating flows $\Phi_{m\pm1/2}^{n+1/2}$; for example, the linear transfer equation (1) flows can be calculated as follows, but with a half-integer upper index):

$$\Phi_{m+1/2}^{n+1/2} = \frac{1}{2}\left\{\frac{1}{2}\left[a\left(u_{m+1/2}^n - u_m^n\right) - |a|\left(u_{m+1}^n - u_m^n\right)\right] + \frac{1}{2}\left[a\left(u_{m+1/2}^{n+1} - u_m^{n+1}\right) - |a|\left(u_{m+1}^{n+1} - u_m^{n+1}\right)\right]\right\},$$

$$\Phi_{m-1/2}^{n+1/2} = \frac{1}{2}\left\{\frac{1}{2}\left[a\left(u_m^n - u_{m-1}^n\right) - |a|\left(u_m^n - u_{m-1}^n\right)\right] + \frac{1}{2}\left[a\left(u_m^{n+1} - u_{m-1}^{n+1}\right) - |a|\left(u_m^{n+1} - u_{m-1}^{n+1}\right)\right]\right\}. \tag{39}$$

Similarly, methods (33), (34), etc. can be presented in streaming form.

In the two-dimensional case, the first-order grid-based approximation method can be presented in the following form [2]:

$$u_{ml}^{n+1} = u_{ml}^{n} + b_{1ml}^{n} + b_{2ml}^{n} + \tau f_{ml}, \tag{40}$$

where

$$b_{1ml}^{n} = \sigma_1\left[\left(\Omega_1^{-1}\Lambda_1^{+}\Omega_1\right)_{ml}^{n}\left(u_{m-1,l} - u_{ml}\right)^{n} - \left(\Omega_1^{-1}\Lambda_1^{-}\Omega_1\right)_{ml}^{n}\left(u_{m+1,l} - u_{ml}\right)^{n}\right],$$
$$b_{2ml}^{n} = \sigma_2\left[\left(\Omega_2^{-1}\Lambda_2^{+}\Omega_2\right)_{ml}^{n}\left(u_{m-1,l} - u_{ml}\right)^{n} - \left(\Omega_2^{-1}\Lambda_2^{-}\Omega_2\right)_{ml}^{n}\left(u_{m+1,l} - u_{ml}\right)^{n}\right];$$
$$\Lambda_k^{+} = \frac{1}{2}\left(\Lambda_k + |\Lambda_k|\right),\ \Lambda_k^{-} = \frac{1}{2}\left(\Lambda_k - |\Lambda_k|\right),\ |\Lambda_k| = \left\{|\lambda_i^k|\right\},\ \Lambda_k = \left\{\lambda_i^k\right\},$$

$i = 1,..., N$ are the diagonal matrix; λ^k_i are the eigenvalues; $\Omega_k = \{\omega^k_{ij}\}$ are the nonsingular matrices whose rows are linearly independent eigenvalues ω^k_i of the matrix A_k.

For matrices $A_k = \{a^k_{ij}\}$, in the case of a system of equations of mechanics of a deformable solid, we have: $\lambda^k_i = \tilde{v}_k + y^k_i$, $i = 1, ..., 7$, $k = 1,2$.

Using the usual kinematic relations for the components of the symmetric strain rate tensor [8] in a spatially fixed curvilinear orthogonal coordinate system x_1 and x_2, x_3.

$$e_{mn} = \frac{1}{2}\left(\frac{1}{H_n}\frac{\partial \upsilon_m}{\partial x_n} + \frac{1}{H_m}\frac{\partial \upsilon_n}{\partial x_m}\right) + \frac{1}{H_n}\left[\delta_{mn}\left(\sum_{s=1}^{3}\frac{\upsilon_S}{H_S}\frac{\partial H_m}{\partial x_S}\right) - \frac{1}{2H_n}\left(\upsilon_m\frac{\partial H_m}{\partial x_n} + \frac{\partial H_m}{\partial x_m}\right)\right],$$

$m, n = 1, 2, 3.$

and choosing the defining relations in the form:

$$\frac{d\sigma_{ij}}{d\tilde{t}} = \frac{d\sigma_{ij}}{dt} + \frac{\upsilon_1}{H_1}\frac{d\sigma_{ij}}{dx_1} + \frac{\upsilon_2}{H_2}\frac{d\sigma_{ij}}{dx_2} + \frac{\upsilon_3}{H_3}\frac{d\sigma_{ij}}{dx_3} = \sum_{m,n=1}^{3} q_{ijmn} emn, ij = 1,2,3,$$

write a closed system of two-dimensional unsteady equations in the form:

$$\frac{\partial u}{\partial t} + A_1\frac{\partial u}{\partial x_1} + A_2\frac{\partial u}{\partial x_2} = f.$$

Strictly speaking, instead of a substantial derivative $d\sigma_{ij} / dt$ the so-called Yaumann derivative should be used for the deviator components of a stress tensor of the type:

$$\frac{\tilde{d}S}{dt} = \frac{dS}{dt} - \sum_{k=1}^{3}\left(S_{ik}\omega_{jk} + S_{jk}\omega_{ik}\right),$$
$$\omega_{ij} = \frac{1}{2}\left(\frac{\partial v_i}{\partial x_j} - \frac{\partial v_j}{\partial x_i}\right), \quad S_{ij} = \sigma_{ij} - \delta_{ij}\frac{1}{3}\sum_{k=1}^{3}\sigma_{kk},$$

which ensures zero rate of change of the stressed state of the particle during its rotation as a rigid whole.

Here the symbol $u = \{v_1, v_2, \sigma_{11}, \sigma_{22}, \sigma_{33}, T\}$ is a vector of the desired variables, including the components of the velocity vector v_1 and v_2 (along the axes — x_1, x_2 respectively), nonzero components σ_{ij} of the symmetric stress tensor and temperature T; $f(t, x_1, x_2, u) = \{f_1, f_2, f_{11}, f_{12}, f_{22}, f_{33}, f_T\}$ is the vector of the right parts with the following components in a curved orthogonal coordinate system x_1, x_2, x_3:

$$f_1 = F_1 + \frac{1}{\rho}\left[\frac{\left(\sigma_{11} - \sigma_{22}\right)}{H_1H_2}\frac{\partial H_2}{\partial x_1} + \frac{\left(\sigma_{11} - \sigma_{33}\right)}{H_1H_3}\frac{\partial H_{12}}{H_2}\left(\frac{2}{H_1}\frac{\partial H_1}{\partial x_2} + \frac{1}{H_3}\frac{\partial H_3}{\partial x_2}\right)\right] - \frac{v_2}{H_1H_2}\left(v_1\frac{\partial H_1}{\partial x_2} + v_2\frac{\partial H_2}{\partial x_1}\right),$$
$$f_2 = F_2 + \frac{1}{\rho}\left[\frac{\left(\sigma_{22} - \sigma_{33}\right)}{H_2H_3}\frac{\partial H_3}{\partial x_2} + \frac{\left(\sigma_{22} - \sigma_{11}\right)}{H_2H_1}\frac{\partial H_{12}}{H_1}\left(\frac{2}{H_2}\frac{\partial H_2}{\partial x_1} + \frac{1}{H_3}\frac{\partial H_3}{\partial x_1}\right)\right] - \frac{v_1}{H_2H_1}\left(v_2\frac{\partial H_2}{\partial x_1} + v_1\frac{\partial H_1}{\partial x_2}\right),$$
$$f_{ij} = \frac{q_{ij11}v_2}{H_1H_2}\frac{\partial H_2}{\partial x_2} - \frac{\left(q_{ij12} - q_{ij21}\right)}{2H_1H_2}\left(v_1\frac{\partial H_1}{\partial x_2} + v_2\frac{\partial H_2}{\partial x_1} + \right) + \frac{q_{ij22}v_2}{H_1H_2}\frac{\partial H_2}{\partial x_1} + \frac{q_{ij33}}{H_3}\left(\frac{v_1}{H_1}\frac{\partial H_3}{\partial x_1} + \frac{v_2}{H_2}\frac{\partial H_3}{\partial x_2}\right) - \frac{\sigma_{ij}\gamma Q}{\rho c},$$
$$f_T = \frac{1}{\rho c}\left[\frac{\sigma_{11}v_2}{H_1H_2}\frac{\partial H_1}{\partial x_2} - \frac{\sigma_{22}}{H_1H_2} + \left(v_1\frac{\partial H_1}{\partial x_2} + v_2\frac{\partial H_2}{\partial x_1}\right) + \frac{\sigma_{ij22}v_2}{H_1H_2}\frac{\partial H_2}{\partial x_1} + \frac{\sigma_{33}}{H_3}\left(\frac{v_1}{H_1}\frac{\partial H_3}{\partial x_1} + \frac{v_2}{H_2}\frac{\partial H_3}{\partial x_2}\right) + Q\right].$$

Here $F1$, $F2$ are the components of the vector of mass forces, T s the internal energy for a thermoelastic medium, c is the specific heat capacity of the material, T is the temperature, Q is the volumetric density of heat sources, H_i, i =1, 2, 3 are the Lamb coefficients characterizing the selected orthogonal curved coordinate system, ρ is the density, defined by the equation of state of a solid, for example:

$$\ln\frac{\rho}{\rho_0} = -\left(3K\right)^{-1}\sum_{i=1}^{3}\sigma_{ii} - 3\alpha T,$$

ρ_0 is the density of the material in the undeformable state, K is the volume compression ratio. In accordance with the two-dimensionality of the deformable state assumed here, there are no displacements of material points in the x_3 direction and $\sigma_{13} = \sigma_{23} = v_3 = 0$, $\partial / \partial x_3 = 0$. Matrices $A_k = \left\{a_{ij}^k\right\}, k = 1,2,\ i = 1,...,7,$ at the same time have the form:

$$A_1 = \frac{1}{H_1}\begin{vmatrix} v_1 & 0 & -1/\rho & 0 & 0 & 0 & 0 \\ 0 & v_1 & 0 & -1/\rho & 0 & 0 & 0 \\ -q_{1111} & -\left(q_{1112}+q_{1121}\right)/2 & v_1 & 0 & 0 & 0 & 0 \\ q_{1211} & -\left(q_{1212}+q_{1221}\right)/2 & 0 & v_1 & 0 & 0 & 0 \\ q_{2211} & -\left(q_{2211}+q_{2221}\right)/2 & 0 & 0 & v_1 & 0 & 0 \\ q_{3311} & -\left(q_{3312}+q_{3321}\right)/2 & 0 & 0 & 0 & v_1 & 0 \\ -\sigma_{11}/\rho_1 & -\sigma_{11}/\rho_1 & 0 & 0 & 0 & 0 & v_1 \end{vmatrix},$$

$$A_2 = \frac{1}{H_2}\begin{vmatrix} v_2 & 0 & -1/\rho & 0 & 0 & 0 & 0 \\ 0 & v_2 & 0 & -1/\rho & 0 & 0 & 0 \\ -\left(q_{1112}+q_{1121}\right)/2 & -q_{1111} & v_2 & 0 & 0 & 0 & 0 \\ -\left(q_{1212}+q_{1221}\right)/2 & -q_{1211} & 0 & v_2 & 0 & 0 & 0 \\ -\left(q_{2211}+q_{2221}\right)/2 & -q_{2211} & 0 & 0 & v_2 & 0 & 0 \\ q_{3311} & -\left(q_{3312}+q_{3321}\right)/2 & 0 & 0 & 0 & v_2 & 0 \\ -\sigma_{12}/\rho_2 & -\sigma_{22}/\rho_2 & 0 & 0 & 0 & 0 & v_2 \end{vmatrix}.$$

For the Prandtl-Reiss model adopted in this paper, the components of the fourth-rank qiikl tensor q_{iikl} of an elastic-plastic material have the form [8]:

$$q_{ijkl} = \lambda\delta_{ij}\delta_{kl} - \frac{\gamma\sigma_{ij}\delta_{ij}}{\rho c} + \mu\left(\delta_{ik}\delta_{jl} - \delta_{jk}\delta_{il}\right) - \frac{I\mu\mu_{ij}S_{kl}}{k},$$

where λ, μ are the Lyame parameters, k is the shear yield strength, δ_{mn} are Kronecker symbols, stress tensor deviator:

$$S_{mn} = \sigma_{mn} - \delta_{mn}\frac{1}{3}\sum_{S=1}^{3}\sigma_{ss},$$

$\gamma = (3\lambda + 2\mu)\,\alpha$ (α is the coefficient of linear expansion of the material during heating).

I is determined from the Mises plasticity condition:

$$I = \begin{cases} 0 \text{ at } & S = S_{11}^2 + S_{22}^2 + S_{33}^2 + S_{12}^2 < 2k^2, \\ 1 \text{ at } & S \geq 2k^2. \end{cases}$$

The defining relations at $I = 0$ are the usual "Hooke's law" for elastic isotropic materials. For $y = 0$, $Q = 0$, the first 6 equations do not include temperature and they can be solved independently of the energy equation.

$$y_1^k = -y_7^k = \left[a_k + \left(a_k^2 - 4d_k\right)^{1/2}\right]^{1/2},\quad y_2^k = -y_6^k = \left[a_k - \left(a_k^2 - 4d_k\right)^{1/2}\right]^{1/2},\quad y_3^k = -y_4^k = y_5^k = 0.$$

$$a_k = a_{13}^k a_{31}^k + a_{14}^k a_{41}^k + a_{24}^k a_{42}^k + a_{25}^k a_{52}^k,$$

$$d_k = a_{13}^k a_{24}^k\left(\left(a_{31}^k a_{42}^k - a_{32}^k a_{41}^k\right)\right) + a_{14}^k a_{25}^k \times \left(\left(a_{41}^k a_{32}^k - a_{42}^k a_{31}^k\right)\right) + a_{13}^k a_{25}^k\left(\left(a_{31}^k a_{32}^k - a_{32}^k a_{31}^k\right)\right),$$

$k = 1,2,$

$$\Omega_1=\begin{Vmatrix}\omega_1^1\\ \omega_2^1\\ \omega_3^1\\ \omega_4^1\\ \omega_5^1\\ \omega_6^1\\ \omega_7^1\end{Vmatrix}=\begin{Vmatrix}1 & \omega_{12}^1 & \omega_{13}^1 & \omega_{14}^1 & \omega_{15}^1 & 0 & 0\\ \omega_{21}^1 & 1 & \omega_{23}^1 & \omega_{24}^1 & \omega_{25}^1 & 0 & 0\\ 0 & 0 & \omega_{32}^1 & \omega_{34}^1 & 1 & 0 & 0\\ 0 & 0 & \omega_{43}^1 & \omega_{44}^1 & 0 & 1 & 0\\ 0 & 0 & \omega_{53}^1 & \omega_{54}^1 & 0 & 0 & 1\\ \omega_{21}^1 & 1 & -\omega_{23}^1 & -\omega_{24}^1 & -\omega_{25}^1 & 0 & 0\\ 1 & \omega_{12}^1 & -\omega_{13}^1 & -\omega_{14}^1 & -\omega_{15}^1 & 0 & 0\end{Vmatrix},$$

$$\Omega_2=\begin{Vmatrix}\omega_{11}^2 & 1 & \omega_{13}^2 & \omega_{14}^2 & \omega_{15}^2 & 0 & 0\\ 1 & \omega_{22}^2 & \omega_{23}^2 & \omega_{24}^{21} & \omega_{25}^2 & 0 & 0\\ 0 & 0 & 1 & \omega_{34}^2 & \omega_{35}^2 & 0 & 0\\ 0 & 0 & 0 & \omega_{44}^2 & \omega_{45}^2 & 1 & 0\\ 0 & 0 & 0 & \omega_{54}^2 & \omega_{55}^2 & 0 & 1\\ 1 & \omega_{22}^2 & -\omega_{23}^2 & -\omega_{24}^2 & -\omega_{25}^2 & 0 & 0\\ \omega_{11}^2 & 1 & -\omega_{13}^2 & -\omega_{14}^2 & -\omega_{15}^2 & 0 & 0\end{Vmatrix}.$$

Here:

$$\omega_{12}^1=\frac{\left(y_1^1-\alpha_1^1\right)}{\alpha_2^1},\qquad \omega_{21}^1=\frac{\alpha_2^1}{\left(y_2^1\right)^2-\alpha_1^1},$$

$$\omega_{11}^1=\frac{\alpha_2^2}{\left(y_1^2\right)^2-\alpha_1^2},\quad \omega_{12}^1=\frac{\left(y_2^2\right)-\alpha_1^2}{\alpha_2^2},$$

$$\alpha_i^k=a_{13}^k a_{31}^k+a_{14}^k a_{41}^k,\qquad \alpha_2^k=a_{24}^k a_{41}^k+a_{25}^k a_{51}^k, k=1,2,$$

$$\omega_{i3}^1=\frac{a_{13}^k\omega_{i1}^k}{y_i^k},\qquad \omega_{i4}^1=\frac{a_{14}^k\omega_{i1}^k+a_{24}^k\omega_{i2}^k}{y_i^k},$$

$$\omega_{i5}^k=\frac{a_{25}^k\omega_{12}^k}{y_i^k}, i=1,2,$$

$$\omega_{i3}^k=\frac{a_{42}^k\beta_{i1}^1-a_{41}^1\beta_{i2}^1}{a_{32}^1\beta_{i2}^1-a_{41}^1\beta_{i2}^1},\quad \omega_{i4}^k=\frac{a_{32}^k\beta_{i1}^1-a_{31}^1\beta_{i2}^1}{a_{31}^1\beta_{42}^1-a_{32}^1\beta_{41}^1},$$

$$\omega_{i4}^2=\frac{a_{52}^2\beta_{i1}^2-a_{51}^2\beta_{i2}^2}{a_{51}^2\beta_{i2}^2-a_{52}^1\beta_{41}^2},\quad \omega_{i5}^k=\frac{a_{42}^2\beta_{i1}^2-a_{41}^2\beta_{i2}^2}{a_{52}^2\beta_{i1}^2-a_{51}^1\beta_{42}^2},$$

$$\beta_{ij}^1=a_{5j}^1\omega_{i5}^1+a_{6j}^1\omega_{i6}^1+a_{7j}^1\omega_{i7}^1,$$

$$\beta_{ij}^2=a_{3j}^2\omega_{i3}^2+a_{6j}^2\omega_{i6}^2+a_{7j}^2\omega_{i7}^2,\ j=1,2,\ i=3,4,5,$$

$$\Omega_k^{-1}=\left\{p_{ij}^k\right\}.$$

in this case, for inverse matrices have:

$$\Omega^{-1}{}_k=\begin{Vmatrix}p_{11}^k & p_{12}^k & 0 & 0 & 0 & p_{12}^k & p_{11}^k\\ p_{21}^k & p_{22}^k & 0 & 0 & 0 & p_{22}^k & p_{21}^k\\ p_{31}^k & p_{32}^k & p_{33}^k & 0 & 0 & -p_{32}^k & -p_{31}^k\\ p_{41}^k & p_{42}^k & p_{43}^k & 0 & 0 & -p_{42}^k & -p_{41}^k\\ p_{51}^k & p_{52}^k & p_{53}^k & 0 & 0 & -p_{52}^k & -p_{51}^k\\ p_{61}^k & p_{62}^k & p_{63}^k & 1 & 0 & -p_{62}^k & -p_{61}^k\\ p_{71}^k & p_{72}^k & p_{73}^k & 0 & 1 & -p_{72}^k & -p_{71}^k\end{Vmatrix},$$

where

$$p_{11}^1=p_{22}^1=\frac{(\Delta_2^1)}{2},\qquad p_{12}^1=-\frac{\omega_{12}^1}{2\Delta_2^1},\qquad p_{21}^1=-\frac{\omega_{21}^1}{2\Delta_2^1},\qquad \Delta_2^1=1-\omega_{12}^1\omega_{21}^1.$$

$$p_{31}^1=\frac{\omega_{25}^1\omega_{34}^1-\omega_{14}^1\omega_{25}^1}{2\Delta_1^1},\qquad p_{32}^1=\frac{\omega_{14}^1-\omega_{15}^1\omega_{34}^1}{2\Delta_1^1},$$

$$p_{33}^1=\frac{\omega_{15}^1\omega_{24}^1-\omega_{14}^1\omega_{25}^1}{2\Delta_1^1},\qquad p_{41}^1=\frac{\omega_{23}^1-\omega_{25}^1\omega_{33}^1}{2\Delta_1^1},$$

$$p^1_{42} = \frac{\omega^1_{15}\omega^1_{33} - \omega^1_{13}}{2\Delta^1_1}, \qquad p^1_{43} = \frac{\omega^1_{25}\omega^1_{13} - \omega^1_{15}\omega^1_{23}}{\Delta^1_1},$$

$$p^1_{51} = \frac{\omega^1_{24}\omega^1_{33} - \omega^1_{23}\omega^1_{34}}{2\Delta^1_1}, \quad p^1_{52} = \frac{\omega^1_{13}\omega^1_{24} - \omega^1_{14}\omega^1_{33}}{2\Delta^1_1},$$

$$p^1_{53} = \frac{\omega^1_{14}\omega^1_{23} - \omega^1_{13}\omega^1_{24}}{\Delta^1_1},$$

$$p^1_{i1} = \left[\omega^1_{i-2,3}\left(\omega^1_{24} - \omega^1_{25}\omega^1_{34}\right) - \omega^1_{i-2,4}\left(\omega^1_{23} - \omega^1_{25}\omega^1_{33}\right)\right]\left(2\Delta^1_1\right)^{-1},$$

$$p^1_{i2} = \left[\omega^1_{i-2,4}\left(\omega^1_{13} - \omega^1_{15}\omega^1_{33}\right) - \omega^1_{i-2,3}\left(\omega^1_{14} - \omega^1_{15}\omega^1_{34}\right)\right]\left(2\Delta^1_1\right)^{-1},$$

$$p^1_{i3} = \left[\omega^1_{i-2,3}\left(\omega^1_{14}\omega^1_{25} - \omega^1_{15}\omega^1_{24}\right) - \omega^1_{i-2,4}\left(\omega^1_{13}\omega^1_{25} - \omega^1_{15}\omega^1_{23}\right)\right]\left(\Delta^1_1\right)^{-1},$$

$$\Delta^1_1 = \omega^1_{15}\left(\omega^1_{24}\omega^1_{33} - \omega^1_{23}\omega^1_{34}\right) + \omega^1_{25}\left(\omega^1_{13}\omega^1_{34} - \omega^1_{14}\omega^1_{33}\right) + \left(\omega^1_{14}\omega^1_{23} - \omega^1_{13}\omega^1_{24}\right).$$

And, similarly:

$$p^2_{43} = \frac{\omega^2_{23}\omega^2_{23} - \omega^2_{13}\omega^2_{25}}{\Delta^2_1}, \quad p^1_{54} = \frac{\omega^2_{23}\omega^2_{34} - \omega^2_{24}}{2\Delta^2_1},$$

$$p^2_{52} = \frac{\omega^2_{14} - \omega^2_{13}\omega^2_{34}}{2\Delta^2_1}, \quad p^1_{53} = \frac{\omega^2_{13}\omega^2_{24} - \omega^2_{23}\omega^2_{14}}{\Delta^2_1},$$

$$p^2_{i1} = \left[\omega^2_{i-2,3}\left(\omega^2_{24} - \omega^2_{25}\omega^2_{34}\right) - \omega^2_{i-2,4}\left(\omega^2_{25} - \omega^2_{23}\omega^2_{35}\right)\right]\left(2\Delta^2_1\right)^{-1},$$

$$p^2_{i2} = \left[\omega^2_{i-2,4}\left(\omega^2_{15} - \omega^2_{13}\omega^2_{35}\right) - \omega^2_{i-2,5}\left(\omega^2_{14} - \omega^2_{13}\omega^2_{34}\right)\right]\left(2\Delta^1_2\right)^{-1},$$

$$p^1_{i3} = \left[\omega^2_{i-2,4}\left(\omega^2_{13}\omega^2_{25} - \omega^2_{15}\omega^2_{23}\right) - \omega^2_{i-2,5}\left(\omega^2_{14}\omega^2_{23} - \omega^2_{13}\omega^2_{24}\right)\right]\left(\Delta^2_1\right)^{-1},$$

$$i = 6, 7,$$

$$\Delta^2_1 = \omega^2_{13}\left(\omega^2_{24}\omega^2_{35} - \omega^2_{25}\omega^2_{34}\right) + \omega^2_{23}\left(\omega^2_{15}\omega^2_{34} - \omega^2_{14}\omega^2_{35}\right) + \left(\omega^2_{14}\omega^2_{25} - \omega^2_{15}\omega^2_{24}\right).$$

When constructing calculation formulas on the boundaries of a rectangular (in coordinates t, x_1, x_2) integration domain, we limit ourselves to considering only the upper ($x_2 = 0$) and lower ($x_2 = 1$) boundaries, bearing in mind that the remaining boundaries ($x_1 = 0, x_{1*}$) are often the plane (or axis) of symmetry or periodicity of the solution, or are chosen in such a way that perturbations do not reach these boundaries during the time under consideration $t \le t_1$. Generalization to the case of more complex conditions at the borders $x_1 = 0$ does not present fundamental difficulties and is similar to the one discussed below.

Multiplying scalar by eigenvectors $(\omega^2_i)^n_{ml}$, obtain the relations:

$$\left(\omega^2_i\right)^n_{ml} u^{n+1}_{ml} = B^2_i = \left(\omega^2_i\right)^n_{ml}\left(u^n_{ml} + \tau f^n_{ml}\right) \pm$$

$$\pm \frac{\tau}{h_2}\left(\lambda^2_i\right)^n_{ml}\left(\omega^2_i\right)^n_{ml}\left(u_{m,l\mp1} + u^n_{ml}\right), i = 1,...,7,$$

compatibility conditions approximating with the first order of accuracy along the intersection lines of the characteristic surfaces of the system and the coordinate plane $x_1 = x_{1m}$ (with equations $dx_2 = \lambda^2_i\, dt$):

$$\omega^2_i u_t + \lambda^2_i \omega^2 u_{x2} = \omega^2_i\,(f - A_1 u_{x2}),\ i = 1,.., 7.$$

As is known, the number of boundary conditions for a hyperbolic system of equations of the type is determined by the number of negative (positive) eigenvalues of the matrix Au at the upper (respectively, lower) boundary of the integration domain. In the problems considered below, there is a situation $\lambda^2_7 < \lambda^2_6 < 0$, at the upper boundary $x_1 = 0$, and at the lower boundary $x_2 = 0$ respectively $\lambda^2_1 > \lambda^2_1 > 0$ therefore, two boundary conditions are required at each of these boundaries, which look like

$$\Phi_i(t, x_1, u_1,..., u_7) = 0,\ i = 1, 2 \text{ при } x_2 = 0,$$
$$\Phi_i(t, x_1, u_1,..., u_7) = 0,\ i = 167 \text{ при } x_2 = 1,$$

причем необходимо, чтобы $\det \Omega_- \ne 0$, $\det \Omega_+ \ne 0$,

where, respectively, $\Omega_- = \left\| \overline{\omega}_1 \overline{\omega}_2 \omega_3 ... \omega_7 \right\|^T$, $\Omega_+ = \left\| \omega_1 ... \omega_5 \overline{\omega}_6 \overline{\omega}_7 \right\|^T$.

Where $\overline{\omega}_i = \{\partial \phi_i / \partial u_1, ..., \partial \varphi_i / \partial u_7\}, i = 1,2,6,7$, a $i = 1,...7$ are the eigenvectors of the A_2 matrix. For the problems considered below, the boundary conditions were chosen semi-linear and after their approximation had the form:

$$\phi_i = \overline{\omega}_i \left(t^{n+1}, x_{1m} \right) u_{ml}^{n+1} - g_i \left(t^{n+1}, x_{1m} \right) = 0,$$

$i = 1,2$ при $x_2 = 0$, $i = 6,7$ при $x_2 = 1$.

Consider a possible splitting scheme for the case of two variables:

$$\frac{\partial u}{\partial t} + A \frac{\partial u}{\partial x} + B \frac{\partial u}{\partial y} = 0:$$

$$\beta_1 \left(\frac{\partial u}{\partial t} + \beta_1^{-1} A \frac{\partial u}{\partial x} \right) + \beta_2 \left(\frac{\partial u}{\partial t} + \beta_2^{-1} B \frac{\partial u}{\partial y} \right) = 0,$$

$$\beta_1 + \beta_2 = 1, \ \beta \geq 0, \ \beta_2 \geq 0; \ u_{ml}^{n+1} = \beta_1 u_{1ml}^{n+1} + \beta_2 u_{2ml}^{n+1},$$

where u_{1ml}^{n+1} and u_{2ml}^{n+1} are from the numerical solution of two one-dimensional systems of equations:

$$\frac{\partial u}{\partial t} + \beta_1^{-1} A \frac{\partial u}{\partial x} = 0 \text{ и } \frac{\partial u}{\partial t} + \beta_2^{-1} A \frac{\partial u}{\partial y} = 0.$$

In the case of a spatial dynamic problem: $\frac{\partial u}{\partial t} + \sum_{k=1}^{3} A_k \frac{\partial u_k}{\partial x_k} = 0$

the matrices have the form: $r_{ijkl} = \frac{1}{2} \left(q_{ijkl} + q_{ijkl} \right), l \neq k;$

$u = \{v_1, v_2, v_3, \sigma_{11}, \sigma_{12}, \sigma_{13}, \sigma_{22}, \sigma_{23}, \sigma_{33}, U\}$ is the vector column of the desired values.

$$A_1 = \begin{vmatrix} v_1 & 0 & 0 & -1/\rho & 0 & 0 & 0 & 0 & 0 & 0 \\ 0 & v_1 & 0 & 0 & -1/\rho & 0 & 0 & 0 & 0 & 0 \\ 0 & 0 & v_1 & 0 & 0 & -1/\rho & 0 & 0 & 0 & 0 \\ -q_{1111} & -r_{1112} & 0 & v_1 & 0 & 0 & 0 & 0 & 0 & 0 \\ -q_{1211} & -r_{1212} & 0 & 0 & v_1 & 0 & 0 & 0 & 0 & 0 \\ -q_{1311} & -r_{2212} & 0 & 0 & 0 & v_1 & 0 & 0 & 0 & 0 \\ -q_{2211} & -r_{1312} & 0 & 0 & 0 & 0 & v_1 & 0 & 0 & 0 \\ -q_{2311} & -r_{3212} & 0 & 0 & 0 & 0 & 0 & v_1 & 0 & 0 \\ -q_{3311} & -r_{3312} & 0 & 0 & 0 & 0 & 0 & 0 & v_1 & 0 \\ -\sigma_{11}/\rho & -\sigma_{12}/\rho & 0 & 0 & 0 & 0 & 0 & 0 & 0 & v_1 \end{vmatrix},$$

$$A_2 = \begin{vmatrix} v_2 & 0 & 0 & -1/\rho & 0 & 0 & 0 & 0 & 0 & 0 \\ 0 & v_2 & 0 & 0 & -1/\rho & 0 & 0 & 0 & 0 & 0 \\ 0 & 0 & v_2 & 0 & 0 & -1/\rho & 0 & 0 & 0 & 0 \\ -r_{1112} & -q_{1122} & 0 & v_2 & 0 & 0 & 0 & 0 & 0 & 0 \\ -r_{1212} & -q_{1232} & 0 & 0 & v_2 & 0 & 0 & 0 & 0 & 0 \\ -r_{1312} & -q_{1322} & 0 & 0 & 0 & v_2 & 0 & 0 & 0 & 0 \\ -r_{1222} & -q_{2222} & 0 & 0 & 0 & 0 & v_2 & 0 & 0 & 0 \\ -r_{2312} & -q_{2322} & 0 & 0 & 0 & 0 & 0 & v_2 & 0 & 0 \\ -r_{3312} & -q_{3322} & 0 & 0 & 0 & 0 & 0 & 0 & v_2 & 0 \\ -\sigma_{12}/\rho & -\sigma_{22}/\rho & 0 & 0 & 0 & 0 & 0 & 0 & 0 & v_2 \end{vmatrix},$$

$$A_2 = \begin{vmatrix} v_3 & 0 & 0 & -1/\rho & 0 & 0 & 0 & 0 & 0 & 0 \\ 0 & v_3 & 0 & 0 & -1/\rho & 0 & 0 & 0 & 0 & 0 \\ 0 & 0 & v_3 & 0 & 0 & -1/\rho & 0 & 0 & 0 & 0 \\ -r_{1113} & -r_{1123} & -q_{1133} & v_3 & 0 & 0 & 0 & 0 & 0 & 0 \\ -r_{1213} & -r_{1223} & -q_{1233} & 0 & v_3 & 0 & 0 & 0 & 0 & 0 \\ -r_{1313} & -r_{1323} & -q_{1333} & 0 & 0 & v_3 & 0 & 0 & 0 & 0 \\ -r_{2213} & -r_{2223} & -q_{2233} & 0 & 0 & 0 & v_3 & 0 & 0 & 0 \\ -r_{2313} & -r_{2323} & -q_{2333} & 0 & 0 & 0 & 0 & v_3 & 0 & 0 \\ -r_{3313} & -r_{3323} & -q_{3333} & 0 & 0 & 0 & 0 & 0 & v_3 & 0 \\ -\sigma_{13}/\rho & -\sigma_{23}/\rho & -\sigma_{33}/\rho & 0 & 0 & 0 & 0 & 0 & 0 & v_3 \end{vmatrix}.$$

One of the possible grid-characteristic schemes for the numerical solution of the reduced system can be represented as:

$$u_{mlp}^{n+1} = u_{mlp}^{n+1} - \sigma_1 \Omega_1^{-1} \Lambda_1 \Delta_m u + \sigma_1^{\gamma} \Omega_1 \left|\Lambda_1\right|^{\gamma} \Omega_1 \Delta_m^2 u - \sigma_2 \Omega_2^{-1} \Lambda_1 \Delta_l u +$$
$$+\sigma_2^{\gamma} \Omega_2 \left|\Lambda_2\right|^{\gamma} \Omega_2 \Delta_l^2 u - \sigma_3 \Omega_3^{-1} \Lambda_1 \Delta_p u + \sigma_3^{\gamma} \Omega_3 \left|\Lambda_3\right|^{\gamma} \Omega_2 \Delta_p^2 u,$$
$$u_m = 0,5\left(u_{m+1,l,p}^{n} - u_{m-1,l,p}^{n}\right),$$
$$u_l = 0,5\left(u_{m,l,p+1}^{n} - u_{m,l,p-1}^{n}\right),$$
$$u_m^2 = 0,5\left(u_{m+1,l,p}^{n} - 2u_{mlp}^{n} + u_{m-1,l,p}^{n}\right),$$
$$u_l^2 = 0,5\left(u_{m,l+1,p}^{n} - 2u_{mlp}^{n} + u_{m,l-1,p}^{n}\right),$$
$$u_p^2 = 0,5\left(u_{m,l,p+1}^{n} - 2u_{mlp}^{n} + u_{m,l,p-1}^{n}\right),$$

h_k (τh_k — шаги пare the steps by time and three coordinates; k = 1,2,3), or

$$u_{mlp}^{n+1} = u_{mlp}^{n} + \sigma_1 \left[\left(\Omega_1^{-1}\Lambda_1^{+}\Delta_m\right)_{mlp} \Delta_m^{-} u - \left(\Omega_1^{-1}\Lambda_1^{+}\Omega_1\right)_{mlp} \Delta_m^{+} u\right]^n +$$
$$+ \sigma_2 \left[\left(\Omega_2^{-1}\Lambda_2^{+}\Delta_m\right)_{mlp} \Delta_m^{-} u - \left(\Omega_2^{-1}\Lambda_2^{+}\Omega_2\right)_{mlp} \Delta_m^{+} u\right]^n + \sigma_3 \left[\left(\Omega_3^{-1}\Lambda_3^{+}\Delta_m\right)_{mlp} \Delta_m^{-} u - \left(\Omega_3^{-1}\Lambda_3^{+}\Omega_3\right)_{mlp} \Delta_m^{+} u\right]^n,$$
$$\Delta_l^{\pm} = u_{m,l\pm1,p} - u_{mlp},$$
$$\Delta_p^{\pm} = u_{m,l,p\pm1} - u_{mlp}.$$

The scheme has the first order of accuracy at $\gamma = 1$ which was implemented in the work), the second at $\gamma = 2$; the "damping" (viscous) term is clearly highlighted, which gives the scheme stability and positive (according to Friedrichs [5]) certainty (or monotony — in the one-dimensional case); when implemented, there is no need to find matrices $\Lambda_k^{\pm}$; the scheme is easy to hybridize (i. e., for example, to assume $\gamma = 1$ in areas with large gradients of flow parameters and $\gamma = 2$ in "smooth" areas). The advantage of recording a grid-characteristic scheme is to reduce the number of arithmetic operations.

Discussion and conclusions. The construction of a numerical algorithm at boundary points is described in detail in [8] for the two-dimensional case. When numerically solving a three-dimensional problem, the construction is performed similarly; for example, in the case of upper and lower bounds, after scalar multiplication of the scheme by eigenvectors $(\omega^3{}_i)^n{}_{mlp}$ obtain the following relations:

$$\left(\omega_i^3\right)_{mlp}^{n} u_{mlp}^{n+1} = \left(\omega_i^3\right)_{mlp}^{n} u_{mlp}^{n} + \sigma_1 \left\{\left[\left(\Omega_1^{-1}\Lambda_1^{+}\Omega_1\right)_{mlp} \Delta_m^{-} u - \left(\Omega_2^{-1}\Lambda_2^{+}\Omega_2\right)_{mlp} \Delta_m^{+} u\right]^n +\right.$$
$$\left. + \sigma_2 \left[\left(\Omega_2^{-1}\Lambda_2^{+}\Omega_2\right)_{mlp} \Delta_l^{-} u - \left(\Omega_2^{-1}\Lambda_2^{-}\Omega_2\right)_{mlp} \Delta_l^{+} u\right]^n\right\} \pm \sigma_3 \left(\lambda_i^3\right)_{mlp}^{n} \left(\omega_i^3\right)_{mlp}^{n} \Delta_l^{\pm} u; \quad i = 1,\ldots,I,$$

compatibility conditions approximating with the first order of accuracy

$$\omega_i^3 u_t + \lambda_i^3 \omega_i^3 u'_{\eta_3} = -\omega_i^3 \left(A_1 u'_{\eta_1} + A_2 u'_{\eta_2}\right).$$

In the case of a one-dimensional system of gas dynamics equations:

$$\frac{\partial u}{\partial t} + A \frac{\partial u}{\partial x} = 0$$

the vector of the desired functions and the matrix A have the following form [2]:

$$u = \begin{Bmatrix} \rho \\ u \\ \varepsilon \end{Bmatrix}, \; A = \begin{Bmatrix} u & p & 0 \\ \rho^{-1} \dfrac{\partial p}{\partial s} & u & \rho^{-1} \dfrac{\partial p}{\partial \varepsilon} \\ 0 & p/\rho & u \end{Bmatrix},$$

where ρ is the density, u is the velocity, ε is the density of the internal energy of the gas.

The actual values of the matrix have the form:

$$\lambda_1 = u + c; \; \lambda_2 = u; \; \lambda_3 = u - c,$$

where c is the speed of sound in a gas, the matrices from the eigenvectors, in fact, will be:

$$\Omega = \begin{Bmatrix} \omega_1 \\ \omega_2 \\ \omega_3 \end{Bmatrix} = \begin{Bmatrix} \dfrac{\partial p}{\partial \rho} & \rho c & \dfrac{\partial p}{\partial \varepsilon} \\ p & 0 & -\rho^2 \\ p & -\rho e & \dfrac{\partial p}{\partial \rho} \end{Bmatrix}.$$

References

1. Rozhdestvensky, B. L. Systems of quasi-linear equations and their applications to gas dynamics / B. L. Rozhdestvensky, N. N. Yanenko. — Moscow : Nauka, 1968. — 546 p.

2. Magomedov, K. M. Grid-characteristic methods / K. M. Magomedov, A. S. Kholodov / 2nd ed. — Moscow : Yurayt, 2017. — 312 p.

3. Kulikovsky, A. G. Mathematical problems of numerical solution of hyperbolic systems of equations / A. G. Kulikovsky, N. A. Pogorelov, A. Y. Semenov. — Moscow : Fizmatlit, 2012. — 656 p.

4. Favorskaya, Alena V. Innovation in Wavt Processes Modeling and Decision Making Grid-Charakteristic Method and Applications / Alena V. Favorskaya, Igor B. Petrov (Ed.). — Springer, 2018. — 270 p.

5. Fridrichs, K. O. Symmetrics hyperbolic linear differential equation / K. O. Fridrichs // Communs Pure and Appl. Math. — 1954. — V. 7, no. 2. — P. 345—392.

6. Godunov, S. K. Difference method for numerical calculation of discontinuous solutions of hydrodynamic equations. Mathematical Collection. — 1959. — Vol. 47 (89), issue 3. — P. 271–306.

7. Petrov, I. B. On the use of hybridized grid-characteristic son of three-dimensional problems of dynamics of a deformable solid / I. B. Petrov, A. G. Tarasov, A. S. Kholodov // Journal of Computational Mathematics and Mathematical Physics. — 1990. — Vol. 30, no. 8. — P. 1237–1244.

8. Petrov, I. B. Numerical investigation of some dynamic problems of deformable solid mechanics by the grid-characteristic method / I. B. Petrov, A. S. Kholodov // Journal of Computational Mathematics and Mathematical Physics. 1990. — Vol. 30, no. 8. — P. 1237–1244.

Submitted for publication 02.02.2023.
Submitted after peer review 01.03.2023.
Accepted for publication 02.03.2023.

About the Authors:

Petrov, **Igor B.,** Corresponding Member of RAS, Dr.Sci. (Phys.-Math.), Professor Moscow Institute of Physics and Technology (National Research University) (9, Institutsky Lane, Dolgoprudny, Moscow Region, 141701, RF), Math-Net.ru, MathsciNet, eLibrary.ru, ORCID, ResearchGate, petrov@mipt.ru

Petrov, Dmitry I., Ph.D. (Phys.-Math.), MIPT Laboratory of Applied Computational Geophysics (9, Institutsky Lane, Dolgoprudny, Moscow Region, 141701, RF), Math-Net.ru, eLibrary.ru

Conflict of interest statement

The authors do not have any conflict of interest.

All authors has read and approved the final manuscript.

UDC 004.85 *Original article*

https://doi.org/10.23947/2587-8999-2023-6-1-70-76

Machine learning in the analysis of the electromagnetic field influence on the rate of oilfield equipment's corrosion and salt deposition

Sh. R. Khusnullin[1], K. F. Koledina[1,2], S. R. Alimbekova[3], F. G. Ishmuratov[3]

[1] Ufa State Petroleum Technical University, 1, Kosmonavtov St., Ufa, Russian Federation

[2] Institute of Petrochemistry and Catalysis of Russian Academy of Sciences, 141, October Ave, Ufa, Russian Federation

[3] Ufa University of Science and Technology, 12, Karl Marx St., Ufa, Russian Federation

shamil.khusnullin@gmail.com

Abstract

Introduction. The formation of salt deposits and oilfield equipment's corrosion in most oil fields has become particularly relevant due to the increase in the volume of oil produced and the increase in its water content in recent years. The deposition of salts in the formation and wells leads to a decrease in the permeability of the oil reservoir, the flow rate of wells. The aim of the work is to use machine learning algorithms to simulate the effects of an electromagnetic field on the processes of salt deposition and corrosion. Prediction of experimental results will allow faster and more accurate experiments to establish the influence of electromagnetic fields on the processes of corrosion and salt deposition.

Materials and methods. Three groups of data were used, to train the models, differing in the composition of the studied initial model salt solution: the waters of the Vyngapurovsk's and Priobsk's deposits, as well as tap water. The following machine learning models were used: linear regression with Elastic-Net regularization, the k-nearest neighbors algorithm, the decision tree, the random forest and a fully connected neural network.

Results. It was found that the decision tree and the random forest have the best accuracy of predictions, from the experiments conducted. Python program has been developed to predict the output results of experiments. Modeling with various models and their parameters is carried out.

Discussion and conclusions. From the experiments conducted, it was found that the decision tree and the random forest have the best accuracy of predictions. Neural networks, on the contrary, predict with the least accuracy. This is due to the fact that there is too little data in the training samples. With the increase in the number of observations, it is worth using neural networks of various architectures.

Keywords: salt deposition, electromagnetic impact, oilfield equipment's corrosion, multiple regression methods, machine learning, neural network.

For citation. Machine learning in the analysis of the electromagnetic field influence on the rate of oilfield equipment corrosion and salt deposition / Sh. R. Khusnullin, K. F. Koledina, S. R. Alimbekova, F. G. Ishmuratov // Computational Mathematics and Information Technologies. — 2023. — Vol. 6, no. 1. — P. 70–76.
https://doi.org/10.23947/2587-8999-2023-6-1-70-76

Научная статья

Машинное обучение в анализе влияния электромагнитного поля на скорость коррозии и солеотложения нефтепромыслового оборудования

Ш. Р. Хуснуллин[1], К. Ф. Коледина[1,2], С. Р. Алимбекова[3], Ф. Г. Ишмуратов[3]

[1]Уфимский государственный нефтяной технический университет, Российская Федерация, г. Уфа, ул. Космонавтов, 1

[2]Институт нефтехимии и катализа УФИЦ РАН, Российская Федерация, г. Уфа, пр. Октября, 141

[3]Уфимский университет науки и технологий, Российская Федерация, г. Уфа, ул. Карла Маркса, 12

shamil.khusnullin@gmail.com

Аннотация

Введение. Образование солеотложений и коррозия нефтепромыслового оборудования на большинстве нефтяных месторождений в последние годы получила особую актуальность ввиду роста объемов добываемой нефти и увеличения ее обводненности. Отложение солей в пласте и скважинах приводит к снижению проницаемости нефтеносного пласта, дебита скважин. Целью работы является применение алгоритмов машинного обучения для моделирования воздействия электромагнитного поля на процессы солеотложений и коррозии. Предсказание результатов экспериментов позволит быстрее и точнее проводить опыты, устанавливающие влияние электромагнитных полей на процессы коррозии и отложения солей.

Материалы и методы. Для обучения моделей были использованы три группы данных, различающихся по составу изучаемого исходного модельного солевого раствора: воды Вынгапуровского и Приобского месторождений, а также водопроводная вода. Были рассмотрены следующие модели машинного обучения: линейная регрессия с регуляризацией Elastic-Net, метод *k* ближайших соседей, дерево решений, случайный лес и полносвязная нейросеть.

Результаты исследования. С помощью алгоритмов машинного обучения были смоделированы процессы воздействия электромагнитного поля на образования солеотложений и коррозию нефтепромыслового оборудования. Разработана программа на Python для предсказания выходных результатов экспериментов. Проведено моделирование с различными моделями и их параметрами.

Обсуждение и заключение. Из проведенных экспериментов установлено, что наилучшую точность предсказаний имеют дерево решений и случайный лес. Нейронные сети, напротив, предсказывают с наименьшей точностью. Связано это с тем, что данных в обучающих выборках слишком мало. С увеличением числа наблюдений стоит использовать нейросети различных архитектур.

Ключевые слова: солеотложение, электромагнитное воздействие, коррозия нефтепромыслового оборудования, методы множественной регрессии, машинное обучение, нейронная сеть, случайный лес.

Для цитирования. Машинное обучение в анализе влияния электромагнитного поля на скорость коррозии и солеотложения нефтепромыслового обородувания / Ш. Р. Хуснуллин, К. Ф. Коледина, С. Р. Алимбекова, Ф. Г. Ишмуратов // Computational Mathematics and Information Technologies. — 2023. — Т. 6, № 1. — С. 70–76. https://doi.org/10.23947/2587-8999-2023-6-1-70-76

Introduction. The problem of the salt deposits formation and oilfield equipment's corrosion is particularly acute in most of the actively developed oil fields in recent years. This is due to an increase in oil production and an increase in its water content. The deposition of salts in the formation and wells leads to a decrease in the permeability of the oil-bearing formation, the flow rate of wells, an increase in operating costs and the failure of deep-pumping equipment [1].

Experiments were conducted to study the effect of the electromagnetic field generated by the resonance-wave complex on the corrosion of structural low-carbon steel and on the crystallization of calcium carbonate at the Pilot Research Center. It was found that exposure to EMF reduces the total mass of poorly soluble salts, and also provides protection against corrosion [2, 3].

In this paper, the use of machine learning algorithms is used to simulate the effects of EMF on the crystallization of calcium carbonate and on the corrosion process of structural steel. The object of the study was the influence of electromagnetic fields on the processes of salt deposition and corrosion. The subject of study and analysis is the possibility of using machine learning models to simulate the processes of salt deposition and corrosion under the influence of electromagnetic fields. The purpose of this study is to develop software for modeling experiments on the interaction of electromagnetic fields on salt deposits and corrosion. The forecast of the results will make it easier and faster to conduct such experiments. This will make it possible to more accurately determine the effect of the magnetic field on calcium carbonate deposits and on the oilfield equipment's corrosion rate.

Materials and methods. Experimental studies of the electromagnetic effect on the processes of salt deposition and corrosion were carried out for the water of the Vyngapurovsky and Priobsky deposits, as well as for tap water [4]. To train the algorithms, 3 groups of data were used, differing in the composition of the studied initial model salt solution. The ana-

lyzed data includes information about the composition of solutions, research conditions (flow rate, pressure, temperature), parameters of electromagnetic fields acting on solutions. Output parameters to be predicted: corrosion rate in the flow and static solution, mm/year; distribution of calcium carbonate by morphology (calcite, aragonite, vaterite). Different models were used for each group of reports, since each task has different input and output data [5].

To solve the problem of machine learning in the analysis of the influence of the electromagnetic field on the rate of corrosion and salt deposition of oilfield equipment, the learning algorithms discussed below were applied.

1. Linear regression with Elastic Net regularization.

It is a linear relationship between the target variable and the features:

$$\hat{y} = w_0 + w_1 * x_1 + \ldots + w_D * x_D = < x, w > + w_0$$

for finding optimal weights that minimize the root-mean-square loss function [6]:

$$MSE = \frac{1}{N} * \sum_i^N \left(y^i - \hat{y}^i\right)^2. \tag{1}$$

The gradient descent method is used in practice.

Elastic Net regularization method is used to combat retraining. The 1st and 2nd weight norms are added to the loss function *w:*

$$L(y, \hat{y}, w) = \frac{1}{N} * \sum_i^N \left(y^i - \hat{y}^i\right)^2 + \lambda_1 \|w\|_1 + \lambda_2 \|w\|_1^2, \tag{2}$$

where λ_1 and λ_2 are the regularization coefficients.

2. *k*-nearest neighbors method (*k-NN*).

The essence of the method is as follows: the prediction $\hat{y}$ for object is calculated as the average value of the target variable *y* among its *k* nearest neighbors [7]:

$$\hat{y} = \frac{1}{N} \sum_{i=1}^k y^i. \tag{3}$$

Various metrics (distance functions) are used to find the distance between objects:

– Euclidean distance: $\rho(a,b) = \sqrt[2]{\sum_i (a_i - b_i)}$; (4)

– manhattan metric: $\rho(a,b) = \sum_i |a_i - b_i|$; (5)

– cosine distance: $\rho(a,b) = 1 - \frac{a * b}{|a||b|}$. (6)

3. Decision tree.

The decision tree predicts the value of the target variable by applying a sequence of simple decision rules (which are called predicates). There is a predicate in each node of this tree. If it is correct for the current sample from the selection, the transition is made to the right child, if not, to the left. Often predicates are simply taking a threshold by the value of some attribute. Predictions are recorded in the leaves (for example, the values of the target variable *y*).

4. Random forest.

This is an ensemble of models (a composition of several algorithms), where decision trees are used as the basic algorithm. This method is based on bagging (meta algorithm designed to improve the stability of the solution) [8]. The essence of the method is as follows: from the initial sample, subsamples of the same dimension are obtained by random selection of objects. A decision tree is trained on each sample, and not all features of objects are used, but a random number of them (the method of random subspaces). To get one prediction, the predictions of all models are averaged:

$$\hat{y}(x) = \frac{1}{k}(b_1(x) + \ldots b_k(x)). \tag{7}$$

5. Neural network.

Networks of the following architecture were used in all three tasks: the input layer from D neurons (number of input parameters), a hidden layer and an output layer consisting of m neurons, according to the dimension of the target vector $y = (y_1,..., y_m)$ [9].

The activation function was used to ensure the nonlinearity of transformations, the activation function was used:

$$ReLU(x) = \max(x, 0). \quad (8)$$

6. Model quality assessment.

The following criteria (metrics) are used in regression tasks in order to determine which model best approximates the relationship between features x and dependent variables y:

– RMS error: $MSE = \frac{1}{N}\sum_{i=1}^{N}(y - \hat{y})^2$; (9)

– coefficient of determination: $R^2 = 1 - \frac{\sum_{i=1}^{N}(y_i - \hat{y}_i)^2}{\sum_{i=1}^{N}(y_i - \hat{y}_i)^2}$; (10)

– mean absolute error: $MAE = \frac{1}{N}\sum_{i=1}^{N}|y - \hat{y}|$. (11)

Research results. Tables 1−3 show the results of using models for three groups of experiments.

Table 1

Metric values for the Vyngapurovsk field

Model/ Metric	Linear Regression	*k-NN*	**Decision tree**	Random forest	Neural network
MSE	0.01453	0.0133	**0.0064**	0.0065	20.6408
MAE	0.0839	0.0757	**0.0467**	0.0478	3.2109
R^2	–5.2844	–8.2677	**0.3169**	0.2266	–1.0221

Table 2

Metric values for the Priobsk field

Model/ Metric	Linear Regression	*k-NN*	**Decision tree**	Random forest	Neural network
MSE	0.3073	0.2623	**0.1435**	0.1724	13.9461
MAE	0.2489	0.1972	**0.1314**	0.1724	2.4746
*R*2	–18.8724	–2.1167	**0.5364**	0.1113	–0.9355

Table 3

Metric values for tap water

Model/ Metric	Linear Regression	*k-NN*	**Decision tree**	Random forest	Neural network
MSE	0.3232	0.2525	**0.1799**	0.1845	1.1029
MAE	0.4729	0.4022	**0.3251**	0.3362	0.8847
R^2	–6.9638	–1.7114	**0.0378**	–0.0283	–4.3788

Based on the described algorithms, a Preditct program has been developed — modeling the effects of EMF on the processes of salt deposition and corrosion on oilfield equipment [10] (Fig. 1).

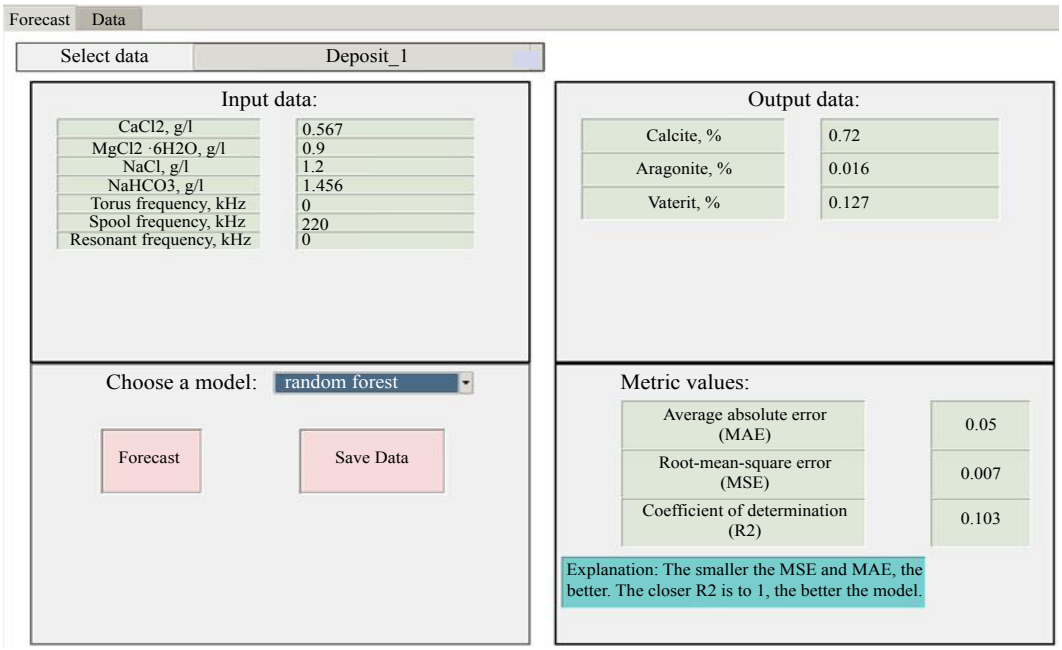

Fig. 1. The interface of the program “Predict” in Russian

The user can enter various input data (the composition of the solution, the frequency of electromagnetic fields, the presence of magnets, etc.) and get output data: the distribution of calcium carbonate by morphology and / or the rate of corrosion. The following machine learning methods can be used for prediction, at the user’s choice: linear regression, the k nearest neighbors method, a decision tree, a random forest and a neural network. To select the best model, the program outputs the readings of quality metrics. Python version 3.10 was chosen as the programming language. Numpy, pandas, and sklearn libraries were used to use machine learning and data processing models. The openpyxl library was used to work with excel files.

Figure 2 shows graphs of the true and predicted values of the output parameters for the Priobsk field obtained by the random forest method. The corrosion rate in the flow (true and predicted value); the distribution of calcium carbonate in the form of calcite (true and predicted value) are considered. As can be seen from the graph above, the random forest algorithm approximates the output data quite well.

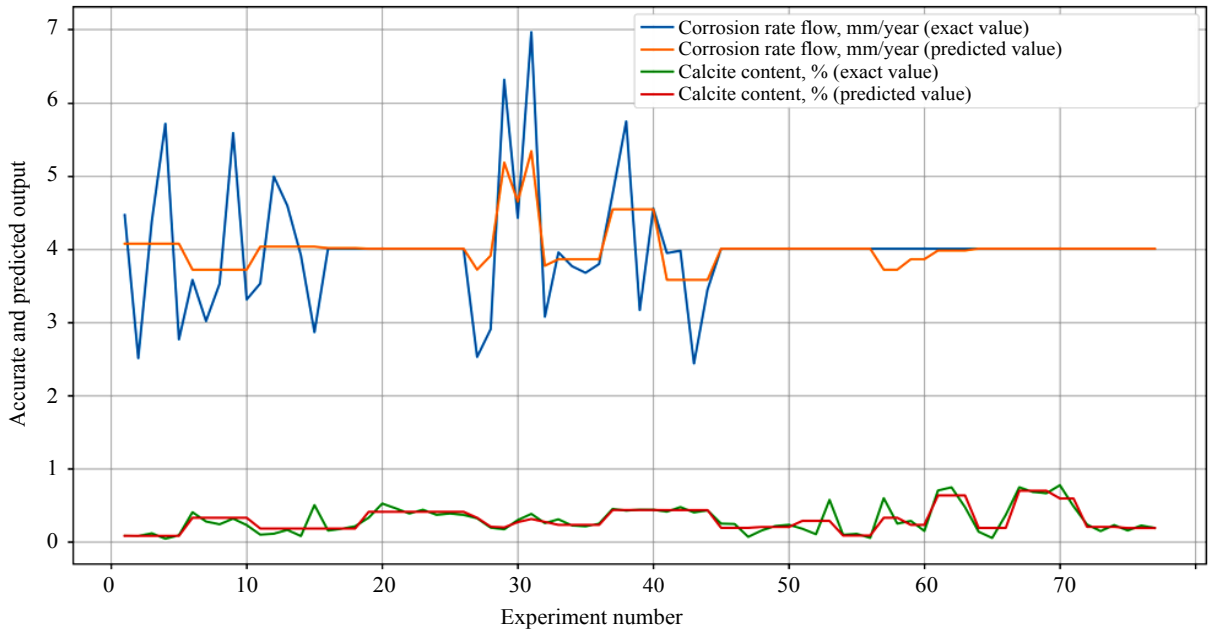

Fig. 2. Graph of true and predicted values by the random forest method

Discussion and conclusions. The decision tree and the random forest have the lowest values of the MSE and MAE metric and the values of R^2 closest to 1 in all three problems, as can be seen from the results (Tables 1−3, Fig. 2). Neural networks, on the contrary, have the worst error rates. This is due to the fact that there is too little data for training.

To analyze such a number of data, it is advisable to use decision trees and a random forest. With an increase in the number of observations, it is worth switching to the use of neural networks, as well as using other architectures (with a large number of hidden layers, recurrent networks, etc.).

References

1. Koledina, K. F. Solving the problem of multi-criteria optimization of the synthesis reaction of benzylalkyl esters by the method of "ideal" point and lexicographic ordering / K. F. Koledina, A. A. Alexandrova // Computational mathematics and information technologies. — 2022. — Vol. 1, no. 1. — P. 12–19. https://doi.org/10.23947/2587-8999-2022-1-1-12-19

2. Shaimardanova, G. F. Genetic algorithm for solving the inverse problem of chemical kinetics / G. F. Shaimardanova, K. F. Koledina // Computational mathematics and information technologies. — 2022. — Vol. 1, no. 1. — P. 41–49. https://doi.org/10.23947/2587-8999-2022-1-1-41-49

3. The influence of the electromagnetic field on the corrosion of low-carbon steel in aqueous mineralized media and on the crystallization of calcium carbonate in the presence of iron(II) ions / S. R. Alimbekova, F. G. Ishmuratov, V. V. Nosov [et al.] // SOCAR Proceedings Special Issue. — 2021. — No. 1. — P. 116−124. http://dx.doi.org/10.5510/OGP2021SI100515

4. Physical methods of preventing salt deposition during oil production / S. R. Alimbekova, R. N. Bakhtizin, A. I. Voloshin [et al.] // Oil and gas business. — 2019. — No. 6. — P. 31–38. http://ngdelo.ru/files/ngdelo/2019/6/ngdelo-6-2019-p31-38.pdf

5. Weisberg, S. Applied linear regression / S. Weisberg — New Jersey: John Wiley & Sons, 2005. — P. 352.

6. Khusnullin, S. R. Machine learning in the analysis of the influence of the electromagnetic field frequency at different solution flow rates on the corrosion rate / S. R. Khusnullin, K. F. Koledina, S. R. Alimbekova // In the collection: Technical and technological systems. Materials of the Thirteenth International Scientific Conference. — Krasnodar, 2022. — P. 462–464.

7. Sun S., Huang R. An adaptive k-nearest neighbor algorithm // 2010 seventh international conference on fuzzy systems and knowledge discovery. — IEEE, 2010. — Vol. 1. — P. 91−94.

8. Chistyakov, S. P. Random forests: an overview // Proceedings of the Karelian Scientific Center of the Russian Academy of Sciences. — 2013. — No. 1. — P. 117−136.

9. Gorbachevskaya, E. N. Classification of neural networks // Bulletin of the Volga State University. VN Tatishcheva. — 2012. — No. 2 (19). — P. 128−134.

10. Program for modeling the effects of electromagnetic field on the processes of salt deposition and corrosion on oilfield equipment (Predict). Khusnullin Sh. R., Koledina K. F., Alimbekova S. R. [et al.] Certificate of registration of computer programs. — No. 2023611354, dated January 19.

Received by the editorial office 08.02.2023.
Received after reviewing 01.02.2023.
Accepted for publication 02.03.2023.

About the Authors:

Khusnullin, Shamil R., student, Ufa State Petroleum Technological University (1, Kosmonavtov St., Ufa, 450064, RF), ORCID, shamil.khusnullin15@gmail.com

Koledina, Kamila F., Dr.Sci. (Phys.-Math.), Associate Professor, Ufa State Petroleum Technological University (1, Kosmonavtov St., Ufa, 450064, RF), researcher, Institute of Petrochemistry and Catalysis, Russian Academy of Sciences (141, Oktyabrya prospect, Ufa, 450075, RF), ORCID, koledinakamila@mail.ru

Alimbekova, Sofya R., Senior Researcher, Pilot Research Center, Ufa University of Science and Technology (12, Karl Marx St., Ufa, 450008, RF), ORCID, ms.sofia.al@gmail.com

Ishmuratov, Farid G., head of the laboratory, Ufa University of Science and Technology (12, Karl Marx St., Ufa, 450008, RF), ORCID, farid_ishmuratov@mail.ru

Claimed contributorship

Shamil Ramilevich Khusnullin: data preparation, machine learning algorithms training. Koledina Kamila Feliksovna: consultation on multiple regression methods. Alimbekova Sofya Robertovna: providing source data. Ishmuratov Farid Gumerovich: providing source data.

Conflict of interest statement

The authors declare that there is no conflict of interest.

All authors have read and approved the final version of the manuscript.

UDC 004.94 *Научная статья*

https://doi.org/10.23947/2587-8999-2023-6-1-77-82

Predicting the kinetics of complex luminescence processes in Python

S. V. Slepnev[1], K. F. Koledina[1,2] ✉

[1]Ufa State Petroleum Technical University, 1, Kosmonavtov St., Ufa, Russian Federation

[2]Institute of Petrochemistry and Catalysis of the Russian Academy of Sciences, 141, October Ave, Ufa, Russian Federation

✉ koledinakamila@mail.ru

Abstract

Introduction. Polyarylene phthalides (PAF) are widely used in optoelectronics today. The reactions occurring during the synthesis of polyarylene phthalides have a complex character, which has not yet been described using mathematical models. In this regard, it is impossible to use PAF in many processes. Polyarylene phthalides have luminescence, good optical and electrophysical properties. The elucidation of the mechanisms of the occurrence of luminescent states of PAF is of both fundamental and practical interest.

The elucidation of the mechanisms of the occurrence of luminescent states of PAF is of both fundamental and practical interest. Due to the complexity of calculating the kinetics of the luminescence intensity of polyarylene phthalides using known mathematical models, the aim of the study was to build a system using machine learning methods that predicts luminescence values depending on temperature and heating time.

Materials and methods. Experimental data have been prepared for calculations, the use of "random forest" and "gradient boosting" methods has been justified, a method for selecting hyperparameters of these models has been selected and the expediency of its use has been justified, optimal models have been constructed and predictions have been obtained.

The results of the study. An algorithm for predicting the luminescence intensity of polyarylene phthalides has been developed. Using machine learning methods based on experimental data, the key hyperparameters of the system were determined and the average accuracy of predicting values was achieved — 80 %.

Discussion and conclusions. High-accuracy forecasts will allow predicting how products containing polyarylene phthalides will react to external influences. The paper presents two methods for solving the problem, as they showed the best results.

Keywords: Python, luminescence, machine learning methods, random forest, gradient boosting.

For citation. Slepnev, S. V. Forecasting the kinetics of complex luminescence processes in Python / S. V. Slepnev, K. F. Koledina // Computational Mathematics and Information Technologies. — 2023. — Vol. 6, no. 1. — P. 77–82. https://doi.org/10.23947/2587-8999-2023-6-1-77-82

Original article

Прогнозирование кинетики сложных процессов люминесценции на Python

С. В. Слепнёв[1], К. Ф. Коледина[1,2] ✉

[1]Уфимский государственный нефтяной технический университет, Российская Федерация, г. Уфа, ул. Космонавтов, 1

[2]Институт нефтехимии и катализа УФИЦ РАН, Российская Федерация, г. Уфа, пр. Октября, 141

✉ koledinakamila@mail.ru

Аннотация

Введение. На сегодняшний день полиариленфталиды (ПАФ) находят широ-кое применение в оптоэлектронике. При этом реакции, протекающие при синтезе полиариленфталидов, имеют сложный характер, который до сих пор не удалось описать с помощью математических моделей. В связи с этим, невозможно использовать ПАФ во многих процессах. При этом ПАФ обладают люминесценцией, хорошими оптическими и электрофизическими свойствами. Выяснение механизмов возникновения люминесцирующих состояний ПАФ представляет как фундаментальный, так и практический интерес. Выяснение механизмов возникновения люминесцирующих состояний ПАФ представляет как фундаментальный, так и практический интерес. В связи со сложностью расчета кинетики интенсивности свечения полиариленфталидов с помощью известных математических моделей была поставлена цель исследования — построить с помощью методов машинного обучения систему, прогнозирующую значения люминесценции в зависимости от температуры и времени нагревания.

Материалы и методы. Подготовлены к вычислениям экспериментальные данные, обосновано использование методов «случайный лес» и «градиентный бустинг», выбран способ подбора гиперпараметров данных моделей и обоснована целесообразность его использования, построены оптимальные модели и получены предсказания.

Результаты исследования**.** Разработан алгоритм предсказания интенсивности свечения полиариленфталидов. Используя методы машинного обучения на экспериментальных данных, были определены ключевые гиперпараметры системы и достигнута средняя точность предсказания значений — 80 %.

Обсуждение и заключения. Прогнозы высокой точности позволят предсказывать, как будут реагировать на внешнее воздействие продукты, включающие в свой состав полиариленфталиды. В работе представлено два метода решения задачи, так как они показали наилучшие результаты.

Ключевые слова: Python, люминесценция, методы машинного обучения, случайный лес, градиентный бустинг.

Для цитирования. Слепнёв, С. В. Прогнозирование кинетики сложных процессов люминесценции на Python / С. В. Слепнёв, К. Ф. Коледина // Computational Mathematics and Information Technologies. — 2023. — Т. 6, № 1. — С. 77–82. https://doi.org/10.23947/2587-8999-2023-6-1-77-82

Introduction. Organic polymer materials are widely used in optoelectronics today. One of the varieties of polymers suitable for these purposes may be polyarylene phthalides (PAF). PAF are characterized by high thermal and chemical resistance, high film-forming properties. PAF have luminescence, good optical and electrophysical properties. The elucidation of the mechanisms of the occurrence of luminescent states of PAF is of both fundamental and practical interest. It is assumed that the luminescence of PAF is due to the formation of active intermediates under energetic action on the polymer, but their chemical nature and properties have not been studied at all [1].

Since the reactions occurring during the synthesis of polyarylene phthalides are complex, the need for detailed research in this practically unexplored area is quite obvious. However, despite the research and experiments carried out [1, 2, 3], a mathematical model describing the behavior of the glow of polyarylene phthalides has not been built.

Due to the complexity of calculating the kinetics of the luminescence intensity of polyarylene phthalides using well–known mathematical models [2, 3], the goal was set to build a system using machine learning methods that predicts luminescence values depending on temperature and heating time.

The following tasks were set to achieve the goal:

– to prepare experimental data for calculations;

– to analyze machine learning algorithms and create a program using the most optimal methods;

– to choose the most successful hyperparameters for models.

Materials and methods. Polyarylene phthalides are a type of aromatic polymers. It is assumed that the luminescence of polyarylene phthalides is due to the formation of active intermediates under energetic action on the polymer. In experimental studies, the heating temperature of the polyarylene phthalide membrane was changed in the range

from 298 to 460 K for several hours, using different rates of controlled heating and cooling of the polyarylene phthalide membrane. They found that the temperature effect on the membrane leads to the appearance of a long-fading glow of recombination luminescence [1].

PAF membrane was irradiated with unfiltered light for 10 minutes (100 W lamp), after which it was left at a temperature of 298 K for 8 hours to accumulate stable radical ions. The temperature of the PAF film was changed in the range from 298 to 460 K for several hours, using different speeds of controlled heating and cooling of the PAF membrane.

Data on the characteristics of individual polyarylene phthalides are presented in the following categories: time, temperature, luminescence intensity. There are 20 experiments in total, 200 values for each characteristic.

Various machine learning methods were tested on the obtained data and the most suitable models were selected for subsequent improvement. The selection of hyperparameters is implemented through a randomized search for parameters, each of which is selected from a distribution of possible values.

Random forest. The Random Forest algorithm is a universal machine learning algorithm, the essence of which is to use an ensemble of decision trees. The decision tree itself provides an extremely low quality of classification, but due to the large number of them, the result is significantly improved [4].

Compared to other machine learning methods, the theoretical part of the Random Forest algorithm is simple. There is no large amount of theory, only the formula of the final classifier is needed $a(x)$:

$$a(x) = \frac{1}{N}\sum_{i=1}^{N} b_i(x), \tag{1}$$

where N is the number of trees; i is the counter for trees; b is the decision tree; $a(x)$ is the sample generated from the data.

However, despite its universality, this method has a number of significant drawbacks [5]:

– complexity of interpretation;

– random forest can't extrapolate;

– the algorithm is prone to retraining on highly noisy data;

– for data involving categorical variables with a different number of levels, random forests are biased in favor of features with a large number of levels;

– larger size of the resulting models. Requires $O(N \cdot C)$ memory to store the model, where C is the number of trees.

Gradient boosting. It is a machine learning method that creates a crucial prediction model in the form of an ensemble of weak prediction models, usually decision trees. He builds the model in stages, allowing to optimize an arbitrary differentiable loss function [6].

Let L be a differentiable loss function, and algorithm $a(x)$ is a composition of basic algorithms:

$$a(x) = a_k(x) = b_1(x) + ... + b_k(x), \tag{2}$$

where the basic algorithm b_k is trained so as to improve the predictions of the current composition:

$$b_k = \arg\min \sum_{i=1}^{N} L(y_i, a_{k-1}(x_i) + b(x_i)). \tag{3}$$

The b_0 model is chosen in such a way as to minimize losses on the training sample:

$$b_0 = \arg\min \sum_{i=1}^{N} L(y_i, b(x_i)). \tag{4}$$

Consider the Taylor decomposition of the loss function L to build basic algorithms in the following steps up to the first term in the neighborhood of the point$(y_i, a_{k-1}(x_i))$:

$$L(y_i, a_{k-1}(x_i)) := L(y_i, a_{k-1}(x_i)) + b(x_i)\, g_i^{k-1}. \tag{5}$$

Let's get an optimization problem by getting rid of the permanent members:

$$b_k \approx \arg\min \sum_{i=1}^{N} b(x_i) g_i^{k-1}. \tag{6}$$

The basic algorithms b_k are trained to predict the values of the anti-gradient of the loss function from the current predictions of the composition at each iteration.

The main disadvantages of this method include the susceptibility to retraining and the voting system of appraisers. The vote of appraisers in gradient boosting is unequal. Some appraisers have a higher weight than others. As a rule, the vote of the very first trained appraiser has the lowest weight, and the last appraiser has the highest weight when voting.

Research results. The regression problem was solved using the Python programming language, and the accuracy of the solution was estimated through the coefficient of determination, which is calculated by the formula:

$$R^2 = 1 - \frac{S_{res}}{S_{tot}}, \tag{7}$$

where S_{res} is the sum of squares of residual errors, and S_{tot} is the total sum of errors.

Fig. 1, 2 shows the results of modeling the kinetics of the intensity of the PAF glow depending on the temperature change. The red curve shows experimental data on the intensity of the glow after exposure to temperature (the blue dotted curve along the auxiliary vertical axis).

Figure 1 shows intensity modeling by gradient boosting (green curve). Figure 2 shows the intensity simulation by the random forest method (green curve).

The coefficient of determination, when using gradient boosting, is 83 %, and in the case of using a random forest — 88 %.

The results turned out to be slightly different from each other due to the difference in methods, as expected. When using the gradient boosting method, the prediction turns out to be less accurate, and peaks are predicted at those times when they did not exist. In the case of a random forest, there are predictions that lie closer to the experimental data. Since gradient boosting copes with temperature prediction worse, this affects the predictive ability of the entire model. Such a result can be justified by an imperfect selection of hyperparameters and an abrupt change in the intensity of the glow, which makes it difficult to determine the direction of the gradient of the function.

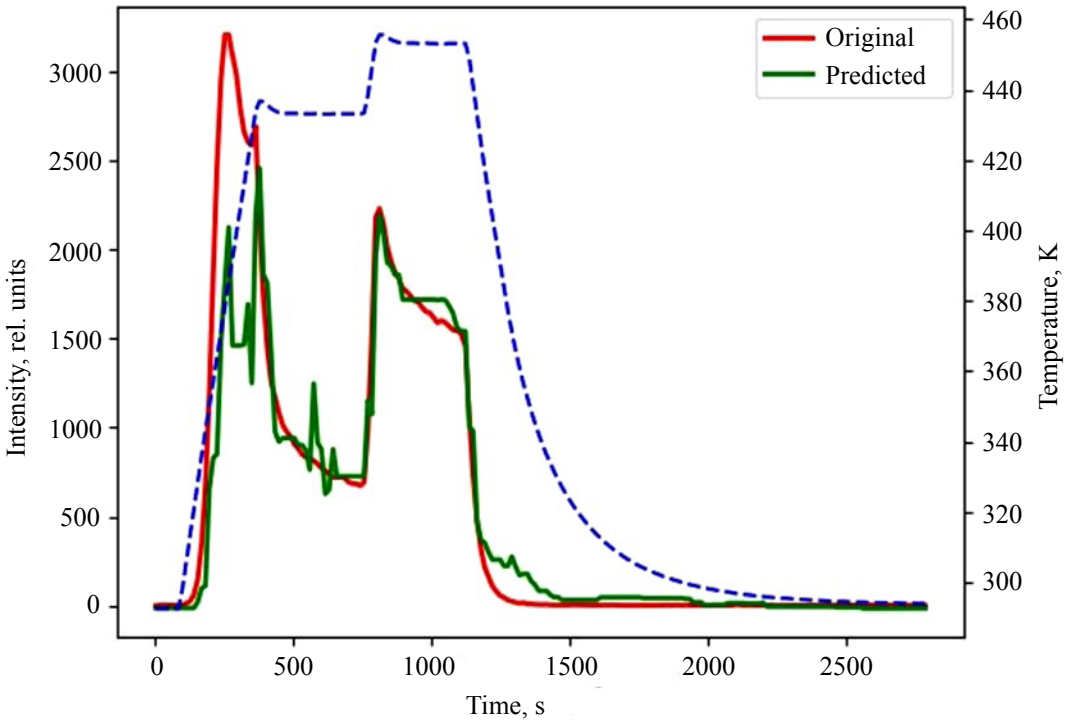

Fig. 1. Modeling of the kinetics of the intensity of the PAF glow by the Gradient boosting method

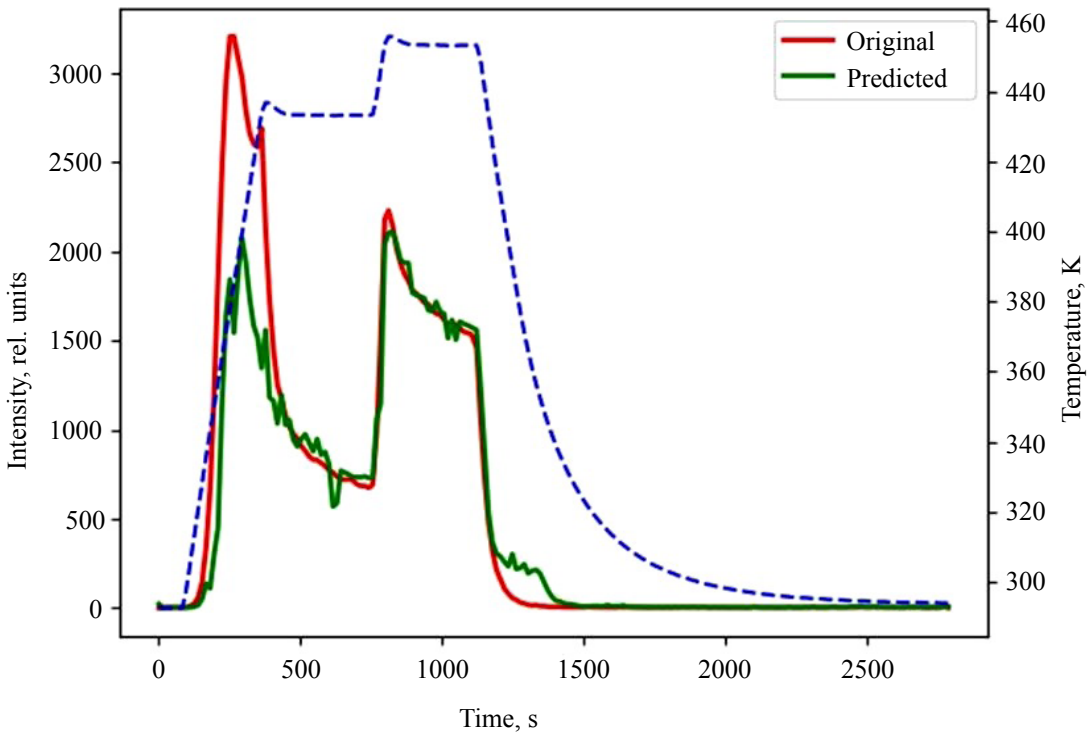

Fig. 2. Modeling of the kinetics of the intensity of the PAF glow by the Random forest method

Discussion and conclusions. The result obtained in the course of solving the problem of predicting the luminescence intensity of polyarylene phthalides is relevant for use in industrial and laboratory processes. Despite the high predictive power of this model, it tends to often make mistakes when predicting peaks, which requires further refinement. To reduce the modeling error, it is possible to resort to combining approaches and using other methods to obtain greater accuracy. An additional way to improve the model is also a more accurate selection of hyperparameters. It, in turn, requires high computing power, since it uses a search of all possible combinations and can be carried out for weeks for the current task. A potential solution to the problem may be the preliminary analysis of data using genetic algorithms to search for extremes and the subsequent transfer of data for training machine learning algorithms.

References

1. Ovchinnikova, M. Yu. Kinetic model of thermally stimulated luminescence of polydiphenylene phthalide films / M. Yu. Ovchinnikova,V. A. Antipin, S. L. Khursan // Kinetics and catalysis. — 2019. — Vol. 60, no. 5. — P. 547–554.

2. Koledina, K. F. Solving the problem of multi-criteria optimization of the synthesis reaction of benzylalkyl esters by the method of “ideal” point and lexicographic ordering / K. F. Koledina, A. A. Alexandrova // Computational mathematics and information technologies. — 2022. — Vol. 1, no. 1. — P. 12–19 Doi 10.23947/2587-8999-2022-1-1-12-19

3. Shaimardanova, G. F. Genetic algorithm for solving the inverse problem of chemical kinetics / G. F. Shaimardanova, K. F. Koledina // Computational mathematics and information technologies. — 2022. — Vol. 1, no. 1. — P. 41–49. Doi 10.23947/2587-8999-2022-1-1-41-49

4. Chistyakov, S. P. Random forests: an overview // Proceedings of the Karelian Scientific Center of the Russian Academy of Sciences. — 2013. — No. 1. — P. 117–136.

5. Brunton S. L., Kutz J. N. Data analysis in science and technology / translated from English by A. A. Slinkin. — Moscow : DMK Press, 2021. — 574 p.

6. Andreas Muller, Sarah Guido Introduction to Machine Learning using Python. O’Reilly. — 2016. — 340 p.

7. Sun S., Huang R. An adaptive k-nearest neighbor algorithm // 2010 seventh international conference on fuzzy systems and knowledge discovery. — IEEE, 2010. — Vol. 1. — P. 91–94.

8. Aurelien Geron Applied machine learning using Scikit-Learn and TensorFlow. — Moscow : Dialectics, 2018. — 690 p.

Received by the editorial office 10.02.2023.
Received after reviewing 02.03.2023.
Accepted for publication 03.03.2023.

About the Authors:

Slepnev, Sergey V., student, Ufa State Petroleum Technological University (1, Kosmonavtov St., Ufa, 450064, RF), ORCID, 14b59b59@gmail.com

Koledina, Kamila F., Dr.Sci. (Phys.-Math.), Associate Professor, Ufa State Petroleum Technological University (1, Kosmonavtov St., Ufa, 450064, RF), researcher, Institute of Petrochemistry and Catalysis, Russian Academy of Sciences (141, Oktyabrya prospect, Ufa, 450075, RF), ORCID, koledinakamila@mail.ru

Claimed contributorship

Slepnev Sergey Vyacheslavovich: program development and algorithm implementation. Koledina Kamila Feliksovna: task formalization, testing, specification development.

Conflict of interest statement

The authors declare that there is no conflict of interest.

All authors have read and approved the final version of the manuscript.

UDC 519.25 *Original article*

https://doi.org/10.23947/2587-8999-2023-6-1-83-89

Forecasting trends in the development of time series by estimating the Hodges-Lehman median

V. V. Misyura[1], E. V. Misyura[2]

[1]Don State Technical University, 1, Gagarin Sq., Rostov-on-Don, Russian Federation

[2]Russian University of Economics named after Plekhanova, Institute of Digital Economy and Information Technologies, 36, Stremyanny Lane, Moscow, Russian Federation

vvmisyura2011@gmail.com

Abstract

Introduction. The lack of stationarity in the time series' development, small samples, the outliers presence, jumps do not allow to find estimates of model parameters that have good properties of statistical estimates and, as a result, to find reliable forecasts, both in the development trend of the process and in its numerical expression. The means to solve these problems is the use of ordinal or robust statistics. Scientific monographs and special chapters in books on mathematical statistics contain a deep and extensive theory on the study of the properties of ordinal statistics, which are the justification for their application in forecasting methods. The aim of the work is to develop and verify method for obtaining one-step forecasts of trends in the development of time series based on stable statistical estimates.

Materials and methods. The article presents the results of the development of a method for obtaining one-step forecasts of trends in the development of time series based on the construction of confidence intervals of a selective stable Hodges-Lehman estimate based on Walsh averages. In particular, the Hodges-Lehman median is used to solve the problem of small samples obtained during the procedure of shifting the time series window. The proposed method is considered in detail in the article: the basic definitions, the theoretical justification of the method, calculation formulas, a detailed description of the algorithm, formulas for calculating the quality metric of forecasts are given.

The results of the study. The method was implemented in computational experiment using the example of forecasting the Urals crude oil's spot price. The article presents the computational experiment's results. The parameters of the proposed method can be configured to obtain reliable one-step forecasts.

Discussion and conclusions. The method proposed in the article has shown its effectiveness on experimental data and can be used as an independent method for constructing one-step forecasts of trends in the development of time series. Further development of the method involves the improvement of computational procedures, verification of the method in case of jumps in the dynamics of the time series.

Keywords: ordinal statistics, random variable, random process, median, Hodges-Lehman medians, forecasting, trend, average absolute error.

For citation. Misyura, V. V. Forecasting trends in the development of time series by estimating the Hodges-Lehman median / V. V. Misyura, E. V. Misyura. // Computational Mathematics and Information Technologies. — 2023. — Vol. 6, no. 1. — P. 83–89. https://doi.org/10.23947/2587-8999-2023-6-1-83-89

Научная статья

Прогнозирование тенденций развития временных рядов с помощью оценки медианы Ходжеса-Лемана

В. В. Мисюра[1], Е. В. Мисюра[2]

[1]Донской государственный технический университет, Российская Федерация, г. Ростов-на-Дону, пл. Гагарина, 1

[2]Российский экономический университет им. Плеханова, Институт цифровой экономики и информационных технологий, Российская Федерация, г. Москва, Стремянный переулок, 36

vvmisyura2011@gmail.com

Аннотация

Введение. Получение достоверных прогнозов, как в тенденции развития процесса, так и в его численном выражении является актуальной научной проблемой. Отсутствие стационарности в развитии временных рядов, малые выборки, наличие выбросов, скачков не позволяют найти оценки параметров модели, обладающих хорошими свойствами статистических оценок. Одним из средств, позволяющим решить указанные проблемы, является применение порядковых или робастных статистик. Научные монографии и специальные главы в книгах по математической статистике содержат глубокую и обширную теорию по исследованию свойств порядковых статистик, которые являются обоснованием их применения в методах прогнозирования. Целью настоящей работы является разработка и верификация метода получения одношаговых прогнозов тенденций развития временных рядов, основанного на устойчивых статистических оценках.

Материалы и методы. Разрабатывается метод получения одношаговых прогнозов тенденций развития временных рядов, основанных на построении доверительных интервалов выборочной устойчивой оценки Ходжеса-Лемана по средним Уолша. В частности, с помощью медианы Ходжеса-Лемана решается проблема малых выборок, полученных при выполнении процедуры сдвига окна временного ряда. Подробно рассматривается предложенный метод: даются основные определения, теоретическое обоснование метода, формулы расчета, подробное описание алгоритма, приводятся формулы расчета метрики качества прогнозов.

Результаты исследования. Метод получил реализацию в вычислительном эксперименте на примере прогнозирования спотовой цены на нефть марки Urals. Приведены результаты вычислительного эксперимента. Параметры предложенного метода могут быть настроены так, чтобы получать достоверные одношаговые прогнозы.

Обсуждение и заключения. Предложенный метод показал свою эффективность на экспериментальных данных и может быть использован как самостоятельный способ построения одношаговых прогнозов тенденций развития временных рядов. Дальнейшее развитие метода предполагает усовершенствование вычислительных процедур и верификацию в случае наличия скачков в динамике временного ряда.

Ключевые слова: порядковая статистика, случайная величина, случайный процесс, медиана, медиана Ходжеса-Лемана, прогнозирование, тренд, средняя абсолютная ошибка.

Для цитирования. Мисюра, В. В. Прогнозирование тенденций развития временных рядов с помощью оценки медианы Ходжеса-Лемана / В. В. Мисюра, Е. В. Мисюра // Computational Mathematics and Information Technologies. — 2023. — Т. 6, № 1. — С. 83–89. https://doi.org/10.23947/2587-8999-2023-6-1-83-89

Introduction. There are a large number of methods and methods of forecasting, which use mathematical models of a random process, and statistical estimates of model parameters, with the help of which the model is configured for a specific implementation. However, the lack of stationarity in the development of the process makes it impossible to use one model throughout the entire forecasting period. Small samples, the presence of outliers, and the lack of a priori information should be added to the non-stationarity. All this does not allow us to find estimates of model parameters that have good properties of statistical estimates. Such models in which the parameters are not well defined are called models with undefined parameters. Robust statistics are one of the means that allows to remove uncertainty to some extent in cases of using small and clogged samples when setting model parameters. Robust statistics are usually understood as ordinal and sign statistics.

Ordinal statistics are widely used in statistical practice. A deep and extensive theory has been developed for them, both with finite sample sizes and in asymptotics. Many statistical procedures for estimating parameters and testing statistical hypotheses are based on the use of ordinal statistics. Scientific monographs and special chapters in books on mathematical statistics are devoted to ordinal statistics (see, for example, [1, 2, 3]. The proposed approach to predicting trends in the development of random processes over time is justified by the properties of ordinal statistics.

The study is devoted to the analysis of time series in order to predict the trend of their development over time. The article develops the idea of forecasting trends in the development of time series proposed in [4] and based on the use of estimates of ordinal statistics. In [4], a successful attempt was made to predict the behavior trends of financial indices

using robust statistics, namely the use of median estimates to calculate the measure of dispersion around the sample center. The article proposes to solve the problems of selecting weighting coefficients and small samples when performing the procedure for shifting the window of a time series by constructing confidence intervals of a sample stable Hodges-Lehman estimate based on Walsh averages.

Materials and methods.

A method for predicting the trend of the development of a random process over time.

Consider a time series as an implementation of a random process $\{X\tau,\ 0 \le \tau \le T\}$. A random sequence $\{h_t \le T\}$ will be obtained using the formula $h_t = \ln(X_t/X_{t-1})$, where X_t is the observed level of the time series. Let's assume that X_{i+1}, i=1,2,…,T can be three types of direction of change of a numerical value: falling (−1); maintaining (0); trend growth (1).

The function that will allow you to predict the trend of the behavior of a time series for one time period is based on the following formula:

$$\mathrm{Trend}_i = \begin{cases} -1, \theta_+^- < 0, \\ 0, \left(\theta_+^- >\right) \& \left(\theta_-^i < 0\right), \\ 1, \theta_-^i > 0, \end{cases} \tag{1}$$

where θ_-^i and θ_+^i are the threshold variables of the function.

Threshold variables $\theta_-^{i+\tau}$ and $\theta_+^{i+\tau}$ for calculating a one-step forecast of the trend in the development of a time series are proposed to be calculated as the boundaries of the confidence interval of the sample ordinal statistics of random sequences $\{h_i, h_{i+1}\ldots h_{i+\tau-1}\}$, i=1,…,T–τ+1, where a certain number 1<τ<T determines the width of the window of the time series shift procedureh_k, k=1,…,T.

The values of random variables $H_{(1)}, H_{(2)},\ldots,H_{(n)}$ are called ordinal statistics if they correspond to random variables included in the sample $H_1, H_2,\ldots,H_n$, arranged in ascending order of their values $h_{(1)} \le h_{(2)} \le \ldots \le h_{(n)}$. The statistical properties of ordinal statistics, both for finite and small sample sizes, and for large sample sizes (that is, in asymptotics), have been studied in detail and described in the literature [3]. The justification for the use of confidence bounds of ordinal statistics is the following Statement 1, the proof of which follows from [4, 94].

Consider the general case. Let $\{H_{(1)}, H_{(2)},\ldots,H_{(\tau)}\}$ be ordinal statistics for the sample $\{H_1, H_2,\ldots,H_\tau\}$. We denote the quantile of the level p by $h_p = F^{-1}(p)$, $0 < p < 1$, where $F_H(h)$ is the unknown distribution function of the observed random variable. The following theorem is valid.

Statement 1. Let two numbers r and s be such that, $P(H_{(r)} < h_p < H_{(s)}) = 1-2\alpha$ given confidence probability and an interval $(H_{(r)}, H_{(s)})$ with random boundaries $H_{(r)}$ and $H_{(s)}$ includes an unknown quantile $h_p = F^{-1}(p)$, $0 < p < 1$. Then the probability $P(H_{(r)} < h_p < H_{(s)})$ does not depend on the unknown distribution function $F_H(h)$.

Let's choose the sample median as the ordinal statistic for the sample $(h)_i^{i+\tau-1} = \{h_i,\ \ h_{i+1}\ldots h_{i+\tau-1}\}$. Then, as an interval estimate for $Me(h)_i^{i+\tau-1}$ can choose a two-dimensional statistic of the form (h_l, h_k), $i \le l < k \le i+\tau-1$, i=1,…, N–τ+1, that defines a symmetric interval with a confidence level 1–2α, assuming $k = \tau-l-1+i$.

Because

$$P(h_l < Me(h)_i^{i+\tau-1} < h_k) = (1/2)^\tau \sum_{t=l}^{\tau-l} C_\tau^t = 1-2\alpha, \tag{2}$$

the value of l, according to the Moivre-Laplace theorem, can be calculated by the formula:

$$l = \left[0{,}5\left\{\tau+1-\sqrt{\tau}\Psi(1-\alpha)\right\}+1\right]+i,\ i=1,\ldots,N-\tau+1\ . \tag{3}$$

Note that the sample median is calculated by the formula:

$$\mathrm{med}\,(H_1,H_2,\ldots,H_n) = \begin{cases} \frac{1}{2}\left(H_{(\frac{n}{2})} + H_{(\frac{n}{2}+1)}\right), \text{если } n/2 \text{ — целое}, \\ H_{(\frac{n+1}{2})}, \text{если } (n+1)/2 \text{ — целое}, \end{cases} \tag{4}$$

where $H_{(i)}$ is the i-th ordinal statistic equal to the i-th value of the sample series $h_1 \le h_2 \le \ldots \le h_n$, ranked in ascending order.

The procedure of shifting a time series with a window width $1<\tau<T$ can lead to the problem of calculating a robust median estimate, since estimates are calculated from small samples. In this case, the median estimate may be unstable and not very accurate.

It is proposed to construct a confidence interval of the median of samples using a stable Hodges-Lehman estimate based on Walsh averages.

The Hodges-Lehman ordinal statistics on Walsh averages are calculated using the formula [2, p. 103]:

$$H_{H-L} = \text{med}[(H_{(i)} + H_{(j)})/2],\ \ 1 \le i \le j \le \tau. \tag{5}$$

In formula (5), the median is calculated by formula (4) from the set $n(n-1)/2$ of Walsh averages $(H_{(i)}+H_{(j)})/2$, $1 \le i \le j \le \tau$. The properties of the Hodges-Lehman median H_{H-L} are well studied and described in detail in the literature [2, 5, 6]. It should be noted that this estimate is highly resistant to deviations from the normality of the distribution and the clogging of the sample.

Thus, the application of the Hodges-Lehman estimate leads to the calculation of the sample median on samples whose volume exceeds 30 if the window width $\tau \ge 9$.

To solve the problem of predicting the trend of development of random processes in time, the following algorithm is proposed.

1. Initialization.

A random sequence $\{ht \le T\}$, is obtained using the formula $h_t = \ln(X_t / X_{t-1})$, where X_t, $t = 1,...,T$ is the level of the observed time series.

2. Iteration.

Let some even number $1<\tau<T$ determine the width of the window of the time series shift procedure h_k, $k=1,...,T$. Random sequences $(h)_i^{i+\tau-1} = \{h_i,\ \ h_{i+1}...h_{i+\tau-1}\}$, with a one-step shift $\{h_k\}$ at $i=1,...,T-\tau+1$ are ordered in ascending order. For a sequence $(h)_i^{i+\tau-1}$ by formulas (2), (3), (4), (5) we construct a confidence interval of the Hodges-Lehman estimate with a given level of significance α. Threshold variables θ^i_- and θ^i_+ get the value of the left and right bounds of confidence intervals, respectively.

We calculate the trend indicators using the formula (1).

To calculate the forecast error of the proposed method for $i=1,...,T-\tau+1$ we obtain the actual trend values of the dynamics of the time series $X_t, t = 1,...,T$ using the following formulas:

$$\text{Trend}_i^{fk} = \begin{cases} -1, X_i - X_{i-1} < -\sigma_i \\ 0, (X_i - X_{i-1} \ge -\sigma_i)\ \&\ (X_i - X_{i-1} \le \sigma_i), \\ 1, X_i - X_{i-1} > -\sigma_i \end{cases} \tag{6}$$

where $\sigma_i = \sqrt{Me(\sigma^2)_i^{i+\tau-1}}$, $Me(\sigma^2)_i^{i+\tau-1}$ is the median of a random sequence

$$(\sigma^2)_i^{i+\tau-1} = \left\{ \left(X_i - Me(X)_i^{i+\tau-1}\right)^2, ..., \left(X_{i+\tau-1} - Me(X)_i^{i+\tau-1}\right)^2 \right\},\ i=1,...,T-\tau+1.$$

3. Stop.

Thus, after implementing the algorithm described above, we obtain two sequences $\{\text{Trend}_i\}, \{\text{Trend}_i^{fk}\}$, of dimensions $1,...,N-\tau+1$, consisting of elements of the set: $\{-1,0,1\}$.

Now we can build an error matrix that shows how well the algorithm determines the trend of the dynamics of the time series levels. The error matrix is used to evaluate the quality of the algorithm.

		−1	1	0
Forecast	−1	TP(−1,−1)	FN(−1,0)	FN(−1,1)
	0	FN(0,−1)	TP(0,0)	FN(0,1)
	1	FN(1,−1)	FN(1,0)	TP(1,1)

Here TP $(\hat{\xi}, \xi)$ is the number of forecasts that correctly determined the trend estimate ξ, FN $(\hat{\xi}, \xi)$ is the number of forecasts that incorrectly determined the direction of the dynamics of the time series.

The quality of the forecasts obtained can be determined by the ratio:

$$\text{accuracy} = \sum_{\xi=-1}^{1} TP(\xi,\xi) \Big/ (T - \tau + 1). \tag{7}$$

It is also possible to calculate the quality metrics of the proposed method for each of the function values $\{\text{Trend}_i^{fk}\}$. For example, the accuracy for predicting falls and growth can be calculated using the formulas:

$$\text{accuracy}(1) = TP(1,1) \ / \ (TP(1,1) + FN(1,0) + FN(1,-1)). \tag{8}$$

$$\text{accuracy}(-1) = TP(-1,-1) \ / \ (TP(-1,-1) + FN(-1,0) + FN(-1,1)). \tag{9}$$

The mean Absolute error (MAE) of the forecast can also be an indicator of the quality of the proposed method for obtaining one-step forecasts of the trend in the development of a time series.

$$\text{MAE} = \frac{1}{T - \tau + 1} \sum_{i=1}^{T-\tau+1} \left| \text{Trend}_i - \text{Trend}_i^{fk} \right|. \tag{10}$$

Research results. For the analysis and testing of the described method, the logarithm of the change in the spot price of Urals crude oil was selected. For the study, the closing prices of trades on the Moscow Stock Exchange for the period from 12.07.2018 to 23.02.2022 were taken. The sample size was 946 values. The computational experiment was carried out using the *R* statistical programming environment and MS Excel data forecasting and analysis tools.

Omissions in the data on days when trading is not conducted (holidays and weekends) have been restored subject to the following rules:

− if one day was missed, then the previous day's closing indicator is assigned to it;

− if two days are missed, then the first day is restored according to the previous paragraph, the second according to the value of the next day;

− if three days are skipped, the first two days are assigned the value of the previous one, and the third day is restored according to the value of the next day's trading closing;

− if 4 days are skipped, the first two days are filled with the value for the previous day, the third and fourth with the value for the next day;

− if more than 4 days were missed (there are no such long gaps in this study), the data would be restored using linear (or nonlinear) regression from time.

The resulting series contains 1323 values. Figure 1 shows the graph of the time series.

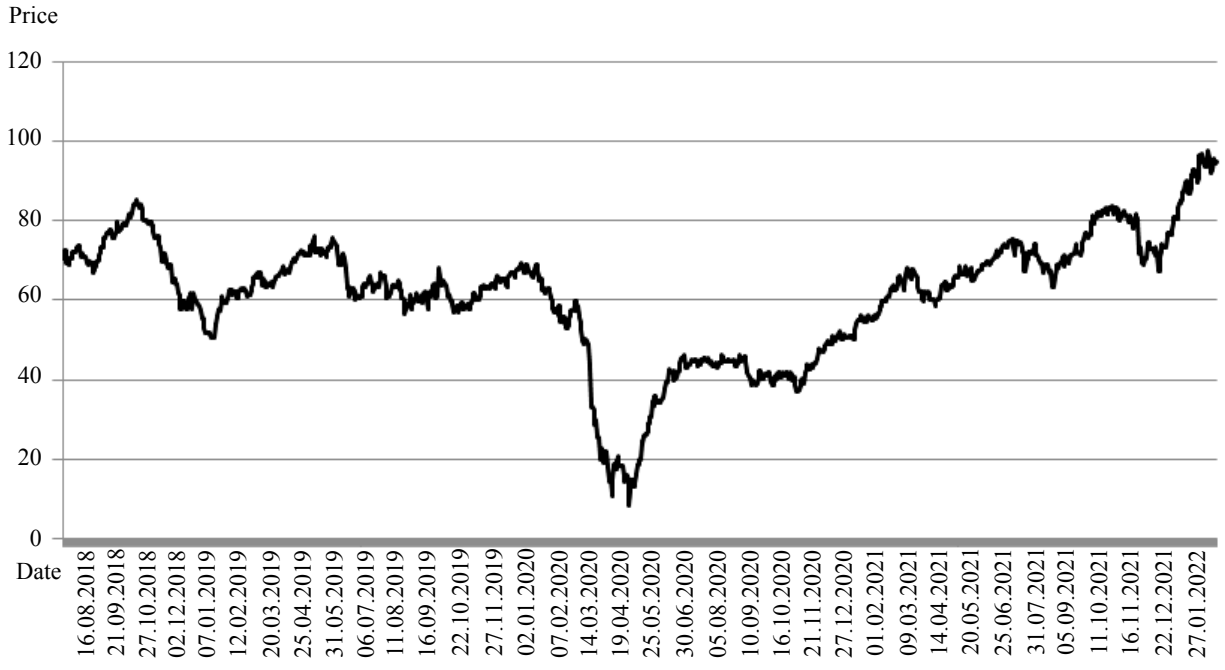

Fig. 1. Dynamics of the spot price of Urals crude oil from 12.07.2018 to 23.02.2022 (the price is indicated on the vertical axis)

Figure 2 shows the logarithm of the change in the spot price of Urals crude oil.

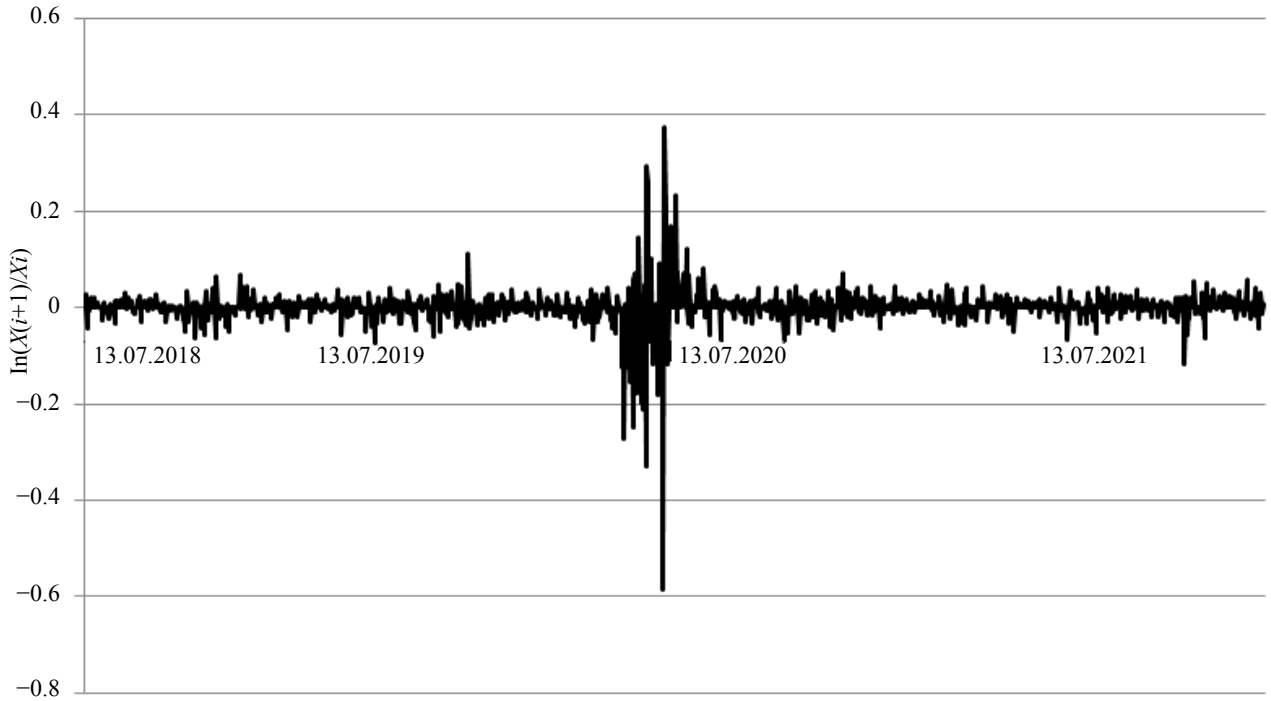

Fig. 2. Logarithm of the change in the spot price of Urals crude oil from 13.07.2018 to 23.02.2022

To implement the described method of obtaining a one-step forecast of the trend in the development of a time series, we will allocate a time period from 05/23/2020 to 02/23/2022 corresponding to a stationary random process h_k, k=1,...,643.

The algorithm was implemented for various values $\tau \geq 9$. Figure 3 shows a graph of the dependence of the MAE error on the width of the window.

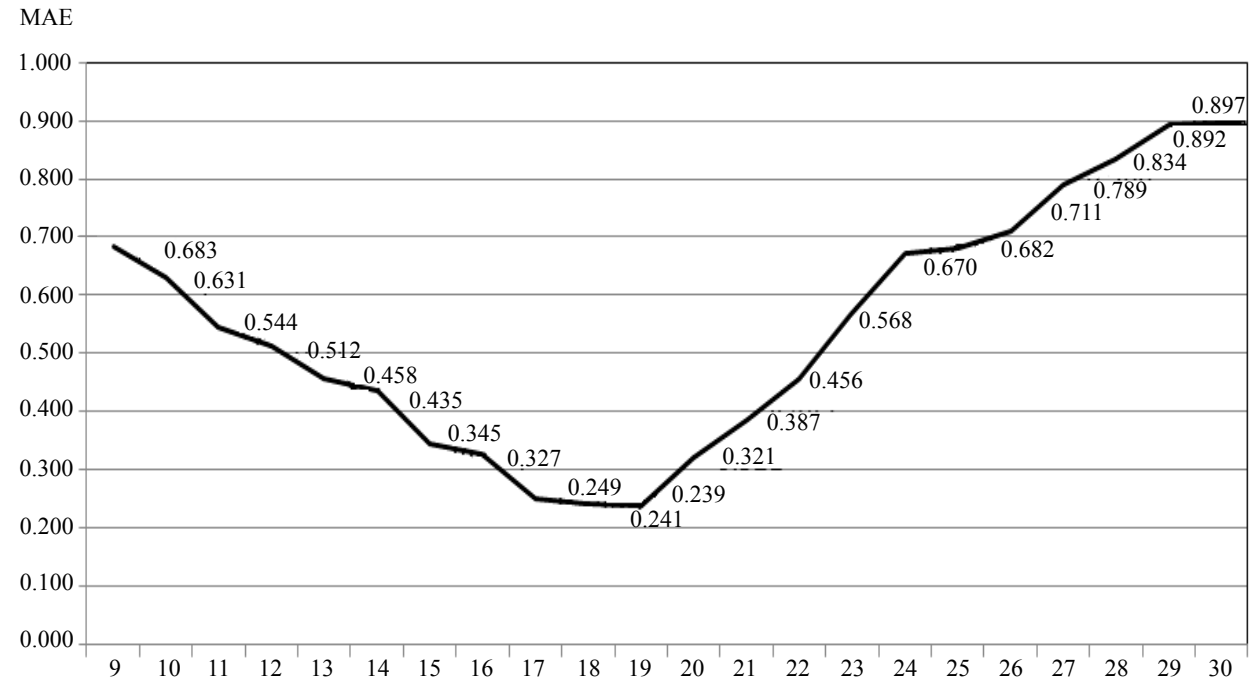

Fig. 3. Graph of the dependence of the average absolute error of the forecast on the width of the window

The error matrix for $\tau = 9$ looks like this.

		−1	0	1
Forecast	−1	71	35	46
	0	50	97	56
	1	70	60	149

Then it is not difficult to calculate the accuracy of the constructed forecast accuraccy = 317/634=0.5, and the accuracy for forecasts of various directions of oil price dynamics: accuraccy(−1)=71/152=0.467, accuraccy(0)= 97/203=0.478, accuraccy(1)=149/279=0.53. The highest accuracy of the algorithm for the selected data set corresponds to the forecast of oil price growth, although there is no significant difference for falling and maintaining the trend.

Discussion and conclusions. The parameters of the proposed method can be configured so as to obtain reliable one-step forecasts of the direction of development of time series. With the passage of the window width of a certain threshold value, the forecast error begins to grow. The main computational complexity of the algorithm consisted both in obtaining direct Hodges-Lehman estimates and determining the boundaries of confidence intervals. The forecast method proposed in the article based on stable ordinal statistics has shown its effectiveness on experimental data and can be used as an independent method of constructing one-step forecasts. Further development of the proposed method involves improvements in computational procedures, verification of the method in the case of outliers and jumps in a random sequence.

References

1. David, G. Ordinal statistics / G. David. — Moscow : Nauka. The main edition of the physical and mathematical literature, 1979. — 336 p.

2. Kobzar, A. I. Applied mathematical statistics. For engineers and scientists / A. I. Kobzar. — Moscow : FIZMATLIT, 2006 — 816 p.

3. Sarkhan, A. E. Introduction to the theory of ordinal statistics / A. E. Sarkhan, V. Grinberg / trans. from English. edited by F. Ya. Boyarsky. — Moscow : Statistics, 1970. — 414 p.

4. Misyura, V. V. Forecasting trends in the development of random processes using ordinal statistics/ V. V. Misyura // Don's Engineering journal. — 2018. — № 4 (51). — P. 115

5. Shulenin, V. P. Mathematical statistics: Nonparametric statistics / V. P. Shulenin / Part 2. — Tomsk : Publishing house of NTL, 2012.

6. Hodjes, J. L. Estimation of location based on rank tests / J. L. Hodjes, E. L. Lehmann // The Annals of Mathematical Statistics.— 1963. — No. 4. — P. 598−611.

Submitted for publication 14.02.2023.
Submitted after peer review 07.03.2023.
Accepted for publication 09.03.2023.

About the Authors:

Misyura, Valentina V., Candidate of Physical and Mathematical Sciences, Associate Professor, Department of Mathematics and Computer Science, Don State Technical University (1, Gagarin Sq., Rostov-on-Don, 344003, RF), ORCID, vvmisyura2011@gmail.com

Misyura, Elena V., Russian University of Economics named after Plekhanova, Institute of Digital Economy and Information Technologies (36, Stremyanny Lane, Moscow, 117997, RF), ORCID, misurahelen@gmail.com

Conflict of interest statement

The author does not have any conflict of interest.

All authors has read and approved the final manuscript.